GEOMETRIC CONTROL OF A QUADROTOR IN PRESENCE OF DISTURBANCES AND TIME-DELAYS

A

Thesis Submitted

in Partial Fulfilment of the Requirements

for the Degree of

DOCTOR OF PHILOSOPHY

By

MANMOHAN SHARMA

Department of Electronics and Electrical Engineering

Indian Institute of Technology Guwahati

Guwahati - 781039, Assam, India

Feb 2021

GEOMETRIC CONTROL OF A QUADROTOR IN PRESENCE OF DISTURBANCES AND TIME-DELAYS

MANMOHAN SHARMA

Certificate

This is to certify that the thesis entitled **"GEOMETRIC CONTROL OF A QUADROTOR IN PRESENCE OF DISTURBANCES AND TIME-DELAYS"**, submitted by **Manmohan Sharma (166102009)**, a research scholar in the *Department of Electronics and Electrical Engineering, Indian Institute of Technology, Guwahati,* for the award of the degree of **Doctor of Philosophy**, is a record of an original research work carried out by him under my supervision and guidance. The thesis has fulfilled all requirements as per the institute's regulations and, in my opinion, has reached the standard needed for submission. The results embodied in this thesis have not been submitted to any other University or Institute for the award of any degree or diploma.

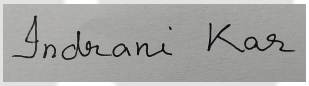

Dated : 29/04/2021
Guwahati.

Dr. Indrani Kar
Dept. of Electronics and Electrical Engg.
Indian Institute of Technology Guwahati
Guwahati - 781039, Assam, India.

Acknowledgments

I want to express my wholehearted gratitude to my supervisor Dr. Indrani Kar for her excellent guidance and support throughout the course of thesis work. I am very thankful for her patience in correcting my mistakes in the thesis work as well as in my manuscripts. I must mention that there were situations in the beginning when it felt that the research work I have undertaken is impossible. But because of her constant mental support, I kept persevering and successfully completed my thesis work in due time. I am grateful to her for procuring the hardware set up for my research, which helped immensely improve my research work quality.

I want to thank my doctoral committee members Prof. Chitralekha Mahanta, Dr. Hanumant Singh Shekhawat, and Dr. Prithwijit Guha, for evaluating the progress of my work. Their valuable suggestions were very helpful in improving the quality of my research work. I want to thank Dr. Srinivasan Krishnaswamy for fruitful discussions in my research work's early days. I want to thank all the members responsible for establishing and maintaining Control and Instrumentation Laboratory, which served as a platform to perform my work.

I want to express my sincerest gratitude to members of the Aeromodelling Club of IIT Guwahati for their patience in explaining and setting up the experimental setup to perform my research work. My special thanks to Pravardhan Reddy, a member of the Aeromodelling Club of IIT Guwahati, for his help while developing the hardware setup. I would also like to express my gratitude to Kuldeep Dhiman of IIT Kanpur for explaining to me the workings of Pixhawk controller boards, without which the experimental results would not have been possible. During my experimental work, a lot of assistance was provided by Afzal Ahmad, a B.Tech student of IIT Guwahati. For his assistance, I would like to express my gratitude to him. Most importantly, I would like to thank my seniors Arghya Chakravarty, Sourav Pandey, and YV Karteek for giving me an early start in my research work. My thanks to other lab members (but not limited to) Raju Dahal, Kasturi Das, Sami AL Issa and Tamen Thapa Sarkar.

I am grateful and indebted to IIT Guwahati and MHRD for providing all the facilities and financial assistance. I want to thank my parents for their constant support

and patience during my thesis work. Finally, I would like to thank God for giving me this opportunity.

(Manmohan Sharma)

Abstract

Quadrotors have gained immense popularity among aerial vehicles in recent years due to their diverse applications. Owing to their vertical take-off and landing (VTOL) capabilities in limited spaces and hovering abilities over a specified target, quadrotors find wide utility in surveillance, search and inspection, and several other social and military applications. Recent advances in miniaturized sensors and high computational efficiency have played a major role in the development of aerial vehicles, especially quadrotors.

Control of unmanned aerial vehicles is very challenging due to their highly nonlinear dynamics and parameter variations with flight conditions. Several linear and nonlinear control techniques have been proposed in the literature for stabilization and tracking control of quadrotors. Most of the literature design the control laws using Euler angles or quaternions. It is well known that Euler angles have singularity while quaternions have ambiguities while representing the attitude of a quadrotor. To remove the singularities associated with Euler angles and ambiguities with quaternions, rotation matrices have been used to develop controllers in recent literature. Building upon these developments, the thesis attempts to develop globally valid control laws in the presence of disturbances. The effect of external disturbances considered in the literature assumes that the bound on the disturbances is known a priori. This is a limitation of controllers present in the literature since it is very difficult to know such bounds in practice. The thesis aims to remove this limitation.

Most of the literature does not consider offset between the center of gravity and the body-fixed frame's origin. The offset between the center of gravity and geometric center was explicitly compensated in some literature where 6-DOF rigid body dynamic model was considered while designing the adaptive controller. This offset may be compensated through integral actions, but if the nonlinear dynamic model is not properly considered, additional disturbances may result. The assumption of zero offset is not practical, and therefore the thesis attempts to remove this shortcoming of present literature. An adaptive control law is proposed to estimate this offset and estimate the mass and moment of inertia of the quadrotor.

Time delays are widespread in the physical systems and engineering domain. The

literature on the control of quadrotors with input delay is very limited. Teleoperation is the next big thing in the robotics industry. But such a task is not without its own set of challenges. The main challenge is packet loss, distortion, and time delay. It is quite desirable to be able to control a robotic device over a network with remote access. Almost all the literature on quadrotors does not consider communication time delay. The presence of communication time delay may result in instability in the system. Motivated by the current state of the literature, we propose to design a controller considering both inputs as well as state delay experienced while operating the device over a network.

A trajectory tracking control law with finite-time convergence on the nonlinear manifold $SE(3)$ is more desirable since most of the existing finite-time control laws only stabilize the attitude. Closed-loop systems under finite-time control usually demonstrate a faster convergence rate, higher tracking precision, better disturbance rejection properties, and robustness against uncertainties. Because of above mentioned attractive features and better practical implementation in actuators, the continuous feedback finite-time control method has gained more attention in recent years. Moreover, the continuous feedback stabilization in finite-time does not excite unmodeled high-frequency dynamics as compared to discontinuous feedback. Motivated by these advantages of finite-time convergence property, a finite-time stable geometric controller is designed for a quadrotor. The proposed control law is not only globally valid but also robust to external disturbances.

Contents

List of Figures

List of Tables

Mathematical Notations

$\mathbb{R}$	set of real numbers
$\mathbb{R}^{3\times3}$	set of 3×3 matrices with real entries
$SO(3)$	Special Orthogonal Group of dimension 3
$SE(3)$	Special Euclidean Group of dimension 3
$\mathfrak{so}(3)$	Lie Algebra of $SO(3)$
$\mathfrak{se}(3)$	Lie Algebra of $SE(3)$
Ω	Angular Velocity expressed in body-fixed frame
ω	Angular Velocity expressed in inertial frame
$R(t)$	Rotation Matrix
τ	Torque in body frame
f_b	Force in body frame

Chapter 1

Introduction

1.1 Background

A mechanical system is a physical system having moving parts. For example, a car with wheels that can rotate is a mechanical system. A mechanical system comprises actuators, power supplies, sensors, etc. The degree of freedom of a mechanical system is defined to be the number of the independent direction of motions it can perform. For example, a mobile robot can move in a plane as well as rotate about a vertical axis, and hence it has 3 degrees of freedom. A mechanical system has a number of inputs to control its degree of freedom. If the degree of freedom is the same as the number of control inputs, then the mechanical system is called a fully actuated mechanical system. Examples of such systems include spacecraft and simple pendulum. Underactuated mechanical systems belong to a class of mechanical systems where the number of control inputs is less than the number of degrees of freedom to be controlled. This class of systems has been the subject of active scientific research fueled by their broad applications in different disciplines. Examples of such systems include underwater vehicles, wheeled mobile robots, quadrotors, spacecraft, helicopters, etc.

Quadrotors are underactuated since they have four control inputs but six degrees of freedom, three rotational and three translational. Recently quadrotors are becoming increasingly popular aerial vehicles due to their multifaceted applications. Several quadrotors applications include but are not limited to building surveillance, search and inspection, and research applications. These critical applications of quadrotors are possible mainly due to their vertical take-off and landing (VTOL) capabilities in limited spaces and hovering capabilities over the target. The first reported quadrotor helicopter was built by Breguet Brothers in 1907 and is reported to have lifted into flight. But the development of quadrotors was stalled for many years due to design and control issues. The recent advances in miniaturized sensors (MEMS) and high computational efficiency

have made possible aerial vehicles' development, especially quadrotors. Due to its critical applications several academic institutions and industry [1] [2] [3] [4] [5] [6] are trying to develop quadrotors suitable to their specific requirements.

A quadrotor is made of four rotors placed perpendicular to each other, as shown in Fig. 1.1. One pair of opposite rotors rotate in the same direction while the other pair rotate in the opposite direction. Due to the opposite sense of rotation of the rotors, the gyroscopic and aerodynamic torques tend to cancel in trimmed flight. One of the advantages of a quadrotor over conventional helicopters is its mechanical simplicity and hence is very easy to build. Another advantage is payload enhancement since four rotors are used, and hence more lift thrust can be generated. Unlike helicopters, a swashplate mechanism is not required to control the movement of the quadrotors, which simplifies the design of the quadrotors. A disadvantage of a quadrotor is the high energy requirement to control the four rotors.

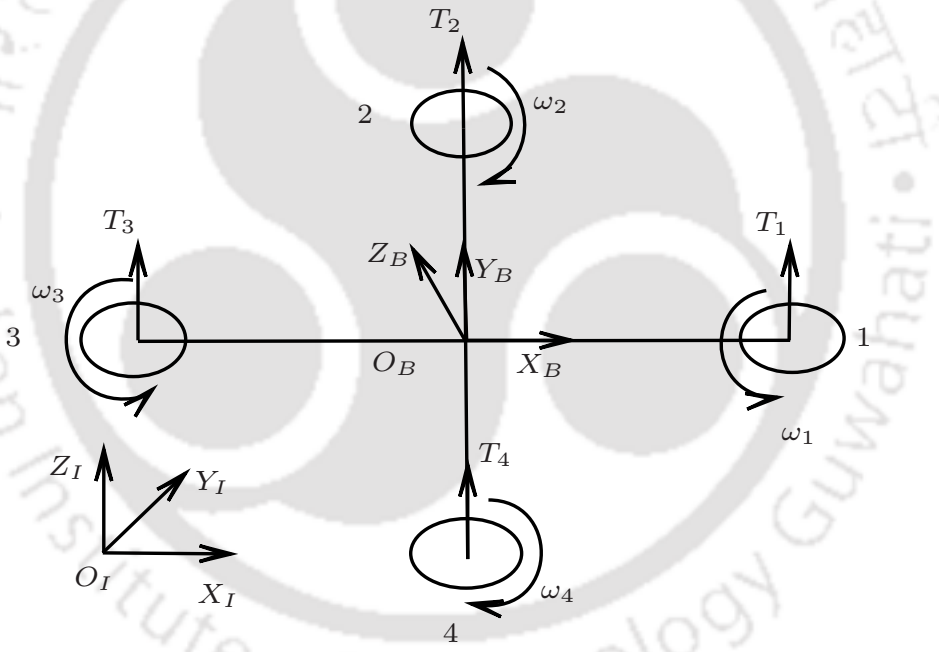

Figure 1.1: Quadrotor Configuration

Control of unmanned aerial vehicles are very challenging mainly due to the following reasons:

• The dynamics of a quadrotor are highly nonlinear and coupled. For example, roll motion results in motion in the $Y-$direction, and pitch motion results in motion in the $X-$direction.

• There are only four control inputs but six degrees of freedom to manipulate. This is known as underactuation, due to which the control design becomes non-trivial.

• The parameters of a quadrotor, such as mass, the moment of inertia, moment arm, etc., may vary with flight conditions if load is being transported or a gimbal is attached. Therefore, it is challenging to design an accurate trajectory tracking control law since it will depend on these parameters.
• For outdoor operation, the effect of wind should be taken into account for stability and better tracking performance.
• The aerodynamic effects comes into play at the high speed of operation. Therefore, at a high speed of operation, one should consider these effects for accurate tracking operation.

Several linear and nonlinear control techniques have been reported in the literature for the stabilization and tracking control of a quadrotor.

1.2 Dynamic Modeling of Quadrotors

This section introduces the dynamic model of a quadrotor using Newton's second law of motion. This modeling approach is predominantly available in the literature. An approach to modeling using variational principles which results in singularity free model is presented in chapter 2. The dynamic equation of a quadrotor is obtained by considering two frames of reference. The inertial frame of reference is denoted by $\{O_I, X_I, Y_I, Z_I\}$ with the origin as O_I as shown in Fig. 1.1. The body-fixed frame of reference is denoted by $\{O_B, X_B, Y_B, Z_B\}$ with the origin as O_B. To define a rigid body's configuration with respect to an inertial frame, we need to specify both position and orientation of the rigid body with respect to the inertial frame. Various forces acting on a quadrotor can be modeled as

- Gravitational force acting at the center of mass of the body O_B.
- Gyroscopic effects due to the rotation of the propeller plane.
- Aerodynamic effects due to blade flapping and rotation of the propeller.
- Drag forces due to motion in a fluid which is air in this case.

The complete dynamic equations should take all these forces into account. However, in literature, control has been developed mainly with a simplified model neglecting some of the effects, such as aerodynamic effects. Let us define some symbols before writing the dynamic equations of motion.

$x \in \mathbb{R}^3$: position of origin of body fixed frame with respect to earth fixed frame. $R \in SO(3) := \{R \in \mathbb{R}^{3\times3} | R^T R = I_3,\ \det(R) = 1\}$: rotation matrix to specify the orientation of body fixed frame with respect to earth fixed frame, v : velocity of O_B with respect to inertial frame, ϕ : roll angle, θ : pitch angle, ψ : yaw angle, ω_i : angular velocity of rotor i, I=diag$\{I_x,I_y,I_z\}$: inertia matrix in body fixed frame, I_r : rotor Inertia, $\hat{\cdot}$:

map from $\mathbb{R}^3$ to $\mathfrak{so}(3)$(the set of skew-symmetric matrices), T_i=thrust produced by rotor i, Ω= body angular velocity, f_b : Forces expressed in the body fixed frame, τ_a : External control input, l : distance from COM to propeller center.

The dynamic equation of motion of the vehicle from Newton-Euler approach neglecting aerodynamic effects but including gyroscopic effects is given by:

$$\begin{aligned} \dot{x} &= v \\ \dot{v} &= -ge_3 + \frac{1}{m} R f_b \\ \dot{R} &= R\hat{\Omega} \\ I\dot{\Omega} &= -\Omega \times I\Omega - \sum_{i=1}^{4} I_r(\Omega \times e_3)\omega_i + \tau_a \end{aligned} \tag{1.1}$$

The first two equations are the translational dynamics whereas the last two are the rotational dynamics. In comparison to the other moments, the gyroscopic terms have very insignificant roles in the overall attitude of the craft. They are presented to provide a more accurate model, but will not be used in the simulation or implementation of the control system in order to reduce the overall complexity of the system. This set of equations will be derived in chapter 2 using variational principles. If ZYX set of Euler angles are used to specify orientation [7], then rotation matrix R is given by:

$$R = \begin{bmatrix} c_\psi c_\theta & c_\psi s_\theta s_\phi - s_\psi c_\phi & c_\psi s_\theta c_\phi + s_\psi s_\phi \\ s_\psi c_\theta & s_\phi s_\theta s_\psi + c_\phi c_\psi & s_\psi s_\theta c_\phi - c_\psi s_\phi \\ -s_\theta & c_\theta s_\phi & c_\theta c_\phi \end{bmatrix}$$

where c_θ and s_θ represent $\cos\theta$ and $\sin\theta$ respectively. The ranges for the angles are $-\pi < \phi \leq \pi$, $-\frac{\pi}{2} < \theta < \frac{\pi}{2}$ and $-\pi < \psi \leq \pi$.

The control input torque τ_a is generated by the thrust produced from the rotors. Since $T_i \propto \omega_i^2$, increasing angular velocity of rotor 2 and decreasing that of 4 produces roll motion. Similarly, increasing the angular velocity of rotor 3 and decreasing that of 1 produces pitch motion. The yaw motion is produced due to the reactive torque exerted on the frame of the body by the propeller in accordance with Newton's third law of motion. Since reactive torque $T_d \propto \omega_i^2$, yaw motion is produced if we increase angular velocity of 2, 4 and decrease that of 1, 3 by the same amount. Let us define the following notations for thrust generated by propellers and reactive torque produced

$$\begin{aligned} T_i &= k_t \omega_i^2 \\ T_d &= k_d \omega_i^2 \end{aligned} \tag{1.2}$$

where k_t and k_d are constants of proportionality.

Putting together above equations, torque input in the body frame is given by

$$\tau_a = \begin{bmatrix} l k_t ({\omega_2}^2 - {\omega_4}^2) \\ l k_t ({\omega_3}^2 - {\omega_1}^2) \\ k_d ({\omega_2}^2 + {\omega_4}^2 - {\omega_1}^2 - {\omega_3}^2) \end{bmatrix}$$

The body force F_b can be written as:

$$f_b = \begin{bmatrix} 0 \\ 0 \\ k_t ({\omega_1}^2 + {\omega_2}^2 + {\omega_3}^2 + {\omega_4}^2) \end{bmatrix}$$

Finally the dynamic equations of motion can be written as:

$$\begin{aligned} \ddot{x} &= \frac{(\cos\phi \sin\theta \cos\psi + \sin\phi \sin\psi)}{m} U_1 \\ \ddot{y} &= \frac{(\cos\phi \sin\theta \sin\psi - \sin\phi \cos\psi)}{m} U_1 \\ \ddot{z} &= -g + \frac{(\cos\phi \cos\theta)}{m} U_1 \\ \ddot{\phi} &= \dot{\theta}\dot{\psi}\left(\frac{I_y - I_z}{I_x}\right) - \frac{I_r}{I_x}\dot{\theta}\Omega + \frac{l}{I_x} U_2 \\ \ddot{\theta} &= \dot{\phi}\dot{\psi}\left(\frac{I_z - I_x}{I_y}\right) + \frac{I_r}{I_y}\dot{\phi}\Omega + \frac{l}{I_y} U_3 \\ \ddot{\psi} &= \dot{\theta}\dot{\phi}\left(\frac{I_x - I_y}{I_z}\right) + \frac{1}{I_z} U_4 \end{aligned} \tag{1.3}$$

where

$$\begin{aligned} U_1 &= k_t ({\omega_1}^2 + {\omega_2}^2 + {\omega_3}^2 + {\omega_4}^2) \\ U_2 &= k_t ({\omega_2}^2 - {\omega_4}^2) \\ U_3 &= k_t ({\omega_3}^2 - {\omega_1}^2) \\ U_4 &= k_d ({\omega_2}^2 + {\omega_4}^2 - {\omega_1}^2 - {\omega_3}^2) \\ \Omega &= \omega_2 + \omega_4 - \omega_1 - \omega_3 \end{aligned} \tag{1.4}$$

1.3 Attitude Representations

A rigid body's attitude is the orientation of its body-fixed frame with respect to the inertial frame. A rigid body's attitude evolves on a non-Euclidean manifold called the Special Orthogonal Group of dimension three or $SO(3)$. There are various ways to represent the attitude [8] of a rigid body in non-Euclidean and Euclidean space. The different representations are rotation matrix representation, Euler axis, principal angle, Euler angles, quaternions, Rodrigues parameters, modified Rodrigues parameters etc. A summary of each of these representations is given in the following subsections.

1.3.1 Rotation matrix

Let R denote the rotation matrix from the body-fixed frame to the inertial frame of reference. The columns of the rotation matrix represent the components of the body-fixed basis unit vectors expressed in the inertial frame. The rotation matrix has the property that

$$R^T R = RR^T = I \tag{1.5}$$

from which it follows that $R^{-1} = R^T$. Hence the determinant of $R = \pm 1$. A rigid-body transformation for which $\det(R) = 1$ is called a rotation matrix. Two successive rotations can be represented by:

$$R'' = R'R \tag{1.6}$$

where R'' is obtained by first undergoing rotation about R followed by rotation R'.

1.3.2 Euler axis and Principal Angle

The rotation of a coordinate frame about another can also be expressed by an angle Φ about an axis passing through the common origin. The Euler axis is obtained by finding the rotation matrix's eigenvector corresponding to the eigenvalue of 1. The principal angle is obtained by finding the trace of R and using the following:

$$\cos\Phi = \frac{1}{2}(\text{trace}(R) - 1) \tag{1.7}$$

1.3.3 Euler Angles

The minimum number of rotations required to represent the attitude of a rigid body is 3. The three-angle representation of attitude is called Euler angles representation, and the angles are called Euler angles. The final rotation matrix is obtained by multiplying three elementary rotations. For example, rotation matrix for $(\psi)_3$, $(\theta)_2$ and $(\phi)_1$ is ob-

tained by multiplying successive rotations by $Z-$axis, followed by successive rotations about rotated Y and $X-$axis. The final rotation matrix is given by:

$$R = R(\phi)R(\theta)R(\psi) = \begin{bmatrix} c_\theta c_\psi & c_\theta s_\psi & -s_\theta \\ s_\phi s_\theta c_\psi - c_\phi s_\psi & s_\phi s_\theta s_\psi + c_\phi c_\psi & s_\phi c_\theta \\ c_\phi s_\theta c_\psi + s_\phi s_\psi & c_\phi s_\theta s_\psi - s_\phi c_\psi & c_\phi c_\theta \end{bmatrix}$$

where c_θ and s_θ represent $\cos\theta$ and $\sin\theta$ respectively.
The Euler angles for the above representation can be found as:

$$\begin{aligned} \phi &= \tan^{-1}(\frac{c_{23}}{c_{33}}) \\ \theta &= -\sin^{-1} c_{13} \\ \psi &= \tan^{-1}(\frac{c_{12}}{c_{11}}) \end{aligned} \tag{1.8}$$

where c_{ij} is the element corresponding to i^{th} row and j^{th} column of the matrix R. One of the problems with Euler angle representation is that at a specific orientation, it is not possible to determine all angles from the rotation matrix. For example, for the above representation, there is a singularity at $\theta = \pm 90°$. At this orientation, ϕ and ψ cannot be determined uniquely. This is referred to as singularity.

1.3.4 Quaternions

Quaternions are four parameters representation of attitude derived from Euler axis and principal angle. This is a singularity free representation of attitude. A quaternion has four parameters, the first three of which form a vector $q = [q_1, q_2, q_3]^T$ while the last one, q_4 is a scalar. The quaternions are represented as :

$$\begin{aligned} q_i &= e_i \sin\frac{\Phi}{2} \\ q_4 &= \cos\frac{\Phi}{2} \end{aligned} \tag{1.9}$$

where $\mathbf{e}= [e_1, e_2, e_3]$ is the Euler axis and Φ is the principal angle. From above equation it is observed that following constraints are satisfied:

$$q_1{}^2 + q_2{}^2 + q_3{}^2 + q_4{}^2 = 1 \tag{1.10}$$

This equation implies that the attitude representations using quaternions evolve on a four- dimensional unit sphere. The rotation matrix in terms of quaternions is written as:

$$R = \begin{bmatrix} {q_1}^2 - {q_2}^2 - {q_3}^2 + {q_4}^2 & 2(q_1q_2 + q_3q_4) & 2(q_1q_3 - q_2q_4) \\ 2(q_1q_2 - q_3q_4) & -{q_1}^2 + {q_2}^2 - {q_3}^2 + {q_4}^2 & 2(q_2q_3 + q_1q_4) \\ 2(q_1q_3 + q_2q_4) & 2(q_2q_3 - q_1q_4)c_\psi & -{q_1}^2 - {q_2}^2 + {q_3}^2 + {q_4}^2 \end{bmatrix}$$

The quaternions elements can be computed as:

$$\begin{aligned} q_1 &= \frac{c_{23} - c_{32}}{4q_4} \\ q_2 &= \frac{c_{31} - c_{13}}{4q_4} \\ q_3 &= \frac{c_{12} - c_{21}}{4q_4} \\ q_4 &= \pm\frac{1}{2}\sqrt{1 + c_{11} + c_{22} + c_{33}} = \pm\frac{1}{2}\sqrt{1 + \text{trace}(R)} \end{aligned} \tag{1.11}$$

The rotation matrix derived from quaternions is computationally efficient than derived from Euler angles since the former does not have trigonometric functions in them. The successive rotations in quaternion space can be written as:

$$R(q'', q_4'') = R(q', q_4')R(q, q_4) \tag{1.12}$$

One of the problems of using quaternions is sign ambiguity. The quaternion (q, q_4) and $(-q, -q_4)$ represent same rotation matrix. This results in unwinding phenomenon [9]. In quaternion space, (q, q_4) and $(-q, -q_4)$ represent the same rotation matrix $R \in SO(3)$, but $(-q, -q_4)$ is unstable hence attitude starting near it travels to the antipodal point (q, q_4). This results in wastage of control effort and unnecessary rotation in $SO(3)$.

1.3.5 Rodrigues Parameters

A set of 3 parameters of attitude representation, $\rho = (\rho_1, \rho_2, \rho_3)^T$ derived from quaternions is called Rodrigues parameters. It is derived as :

$$\rho = \frac{q}{q_4} = \mathbf{e}\tan\frac{\Phi}{2} \tag{1.13}$$

The advantage of Rodrigues parameters is that only three parameters are needed and are less computationally intensive than Euler angle representation. But like Euler angles, they have a singularity at $\Phi = n\pi$, and their use is limited to $\Phi < 180°$.

1.3.6 Modified Rodrigues Parameters

A modified 3 parameter set derived from Rodrigues parameters in order to extend its use for $\Phi > 180°$ is defined as :

$$p = \frac{q}{1+q_4} = \mathbf{e}\tan\frac{\Phi}{4} \tag{1.14}$$

This set $p = (p_1, p_2, p_3)^T$ is nonsingular for $\Phi < 360°$. However, it has a singularity at $\Phi = 360°$.

1.4 Literature Review of Control Strategies

Several linear and nonlinear control techniques have been proposed in the literature for the stabilization and tracking control of quadrotors. The most common linear methods have been PID and LQR. Nonlinear strategies employed for the stabilization of quadrotor dynamics have been the Lyapunov function approach, feedback linearization, backstepping, sliding mode control, and more recently, geometric control techniques.

• Linear Control Approach:

In [10], PID and LQR control techniques were compared to stabilize the attitude dynamics of a micro quadrotor. PID controller was implemented on a simplified model, while the LQR controller was developed on a complete model. But since the PID controller was tuned on a complete model with actuator dynamics taken into consideration, it performed better than the LQR controller, which was developed without taking actuator dynamics into consideration. The PID control strategy is also employed in [11] in which attitude, altitude, and position control tests are presented on Stanford Testbed of Autonomous Rotorcraft for Multi-Agent Control(STARMAC) using PID controllers. The aerodynamic effects present at high velocity have been treated as external disturbances, and only PID controllers are used to show good performance. The effect of wind and external disturbances has been neglected.

• Feedback Linearization Approach:

The initial approach to quadrotor control has been through feedback linearization. Since the dynamics are underactuated and any combination of outputs for input-output feedback linearization results in unstable zero dynamics, dynamic extension to feedback linearization has been attempted in literature. In [12], it was shown that control using input-output feedback linearization is not possible since the decoupling matrix is singular. Hence dynamic feedback extension of the control input is employed to develop the

controller. In [13], coupling effects between rolling and transverse motions and between pitching and forward motions are neglected. This resulted in an approximately linear system. Input-output feedback linearization with dynamic extension was applied to this system, and it was shown to have stable zero dynamics. In both the above cases, higher-order derivatives of the states were required, and hence these are sensitive to external disturbances and sensor noise. Model uncertainty can result in degradation of the performance and may also cause instability because of inversion. In[14], an outer loop approach to stabilize the zero dynamics is proposed. The method avoids the use of dynamic extension, and hence higher-order derivatives are not required. The desired values for pitch and roll are chosen depending on the desired value of position such that the zero dynamics are rendered stable. In [15], two control approaches were presented, namely feedback linearization and backstepping. The estimates of position and orientation were obtained using a single camera. The y and yaw motion was controlled using a PD controller, while a feedback linearization controller was developed for x and z motion. In [16], estimates were obtained using two cameras resulting in better controller performance even in the presence of pose estimation errors.

Since rotational dynamics are independent of translational dynamics, the rotational dynamics can be controlled independently of the translational dynamics. This approach has been applied in [17] where control for the angular subsystem is developed using a Lyapunov function while a PD control was used for z dynamics. A novel feedback controller based on compensating the gyroscopic and Coriolis effects is proposed in [18]. The controller avoids the singularity inherent with Euler angle representation. It was shown that the controller was exponentially stable when Coriolis and gyroscopic effects were compensated, while a PD controller without the compensation of these effects resulted in asymptotic stability only. A controller based on nested saturation algorithm[19] is proposed in [20] on a model developed using the Lagrangian approach. A separate nested saturation algorithm is developed for (y, roll) and (x, pitch) motion. A PD controller was developed for z and yaw motion. In [21], separate Lyapunov functions were used for tracking and attitude stabilization. The effect of virtual control error is taken into consideration, and a separate Lyapunov function for motor dynamics is used to bound these errors.

In [22], a path following controller is presented for a quadrotor helicopter model. The controller relies on input dynamic extension and feedback linearization. Besides solving the path following problem, the control design allows one to specify the quadrotor's speed profile and yaw angle along the path.

• **Backstepping and sliding mode techniques:**

In [23], backstepping and sliding mode techniques were applied for the stabilization of attitude dynamics of a micro quadrotor. Control was first developed for the angular subsystem since it is independent of the translational subsystem. In [24], a backstepping technique was applied to develop the control by dividing the system into fully actuated, underactuated, and propeller subsystems. Control law was developed for each subsystem to follow the desired trajectory. In [25], the model was divided into fully actuated and underactuated subsystems. A rate bounded PID controller was used for z dynamics and a sliding mode controller for yaw dynamics. Sliding mode control was also developed to stabilize the underactuated subsystem consisting of x, y, roll, and pitch motion.

One of the practical limitations of the backstepping technique is that the virtual control input's analytic derivative form is very difficult to get in many situations. Overcoming this difficulty, a command filtered backstepping technique has been proposed in [26] for stabilizing the quadrotor attitude where a linear tracking differentiator is employed to extract the attitude command derivative avoiding tedious computations. This subverted the virtual control input derivative calculation analytically and resulted in less dependence on the dynamic model. A command-filtered adaptive backstepping technique to control VTOL vehicles has been applied in [27] where the problem of input saturation, as well as mass uncertainty, has been dealt with. An adaptive law based on immersion and inversion technique [28] has been proposed to estimate mass, which is further utilized in developing a nested saturation-based tracking law. The immersion and invariance [28] based adaptive law guarantees the parameter convergence to its true value as opposed to conventional adaptive laws, which is a major shortcoming of the conventional adaptive laws. Similar to [26] command filter has been used to avoid tedious virtual control input derivative calculations.

Backstepping technique along with nonlinear $\mathcal{H}_\infty$ control was applied in [29]. The nonlinear $\mathcal{H}_\infty$ control was applied for robust attitude stabilization while backstepping was applied in cascade for trajectory tracking of the unmanned aerial vehicle.

• **$\mathcal{H}_\infty$ and Model Predictive Control:**

The goal of the nonlinear $\mathcal{H}_\infty$ control strategy, introduced by Van der Schaft in the article [30], is to achieve a bounded ratio between the energy of the so-called error signals and the energy of the disturbance signals. In general, this theory's nonlinear approach considers two Hamilton-Jacobi-Bellman-Isaacs partial differential equations (HJBI PDEs), which replace the Riccati equations in the case of the linear $\mathcal{H}_\infty$ control formulation. The nonlinear case's main problem is the absence of a general method to solve these HJBI PDEs.

The basic strategy of MBPC is the repeated optimization of a performance objective

over a finite horizon. After its introduction in the late 1960s, it has received much interest and has been proven to be very successful in industrial applications. The main advantage of MBPC is that the constraints can be easily handled, and therefore complex processes can be controlled without special precautions. Same as the $\mathcal{H}_\infty$ flight controller, the MBPC controller can handle multivariable control problems naturally. It can also take into account actuator constraints and ensure stability even if the constraints are exceeded.

A combined 2-DOF $\mathcal{H}_\infty$ and Model-Based Predictive Control (MBPC) was applied in [31]. The control was implemented in two loops. In the inner loop, the $\mathcal{H}_\infty$ controller provided robust stabilization and disturbance rejection. The speed, throttle, and yaw were controlled in the first outer loop with $\mathcal{H}_\infty$ controllers. To handle the longitudinal and lateral motion even in the large maneuvers, which exceeds the actuators' constraints, the model-based predictive control (MBPC) is implemented in the second outer loop.

A path tracking underactuated $\mathcal{H}_\infty$ control strategy was proposed in [32]. An inner loop $\mathcal{H}_\infty$ controller was designed to control the quadrotor's attitude and altitude. The outer-loop control is performed using a model-based predictive controller (MPC) to track the reference trajectory. An integral predictive and nonlinear robust control strategy was presented in [33] to solve the path following problem for a quadrotor helicopter. The proposed control structure is a hierarchical scheme consisting of a model predictive controller (MPC) to track the reference trajectory together with a nonlinear $\mathcal{H}_\infty$ controller to stabilize the rotational movements. In both controllers, the integral of the position error is considered, allowing the achievement of a steady-state null error when sustained disturbances are acting on the system.

• **Observer Based Control:**

In all the above works, it was assumed that the vehicle's full state information was available, and no external disturbance was present in the system. Several observer-based control [34, 35] has been proposed in the literature to deal with such issues. In [36], sliding mode observer with backstepping control has been proposed, while in [37], a higher-order sliding mode observer has been proposed to not only observe the unmeasurable states but also to estimate the external disturbances such as wind and parameter uncertainties. In [38], a Lyapunov function approach is used to estimate the moments due to wind, while in [39], wind effects are modeled based on the Dryden wind-gust model from which wind forces are estimated. These estimates are then used to reject the external disturbance due to wind. In [40] and [11], aerodynamic effects at high velocities such as blade flapping and total thrust variation with angle of attack have been modeled and compensated using feedback linearization.

• **Intelligent Control:**

Intelligent control algorithms apply several artificial intelligence approaches, some biologically-inspired, to control a system. Examples include fuzzy logic, neural networks, machine learning, and genetic algorithm. They typically involve considerable uncertainty and mathematical complexity. This complexity and abundant computational resources required are limitations to the use of intelligent systems. Intelligent control is not limited to fuzzy logic and neural networks, but the two are the most widely used. Fuzzy logic algorithms deal with many-valued logic, not discrete levels of truth.

The central nervous system and brain biologically inspired artificial neural networks. A robust neural networks algorithm was applied to a quadrotor in [41] to stabilize against modeling error and considerable wind disturbance. The method showed improvements with respect to achieving the desired attitude and reducing weight drift. An intelligent fuzzy controller was applied in [42] to control the position and orientation of a quadrotor with good response in simulation. However, a significant limitation of this work was the trial and error approach for tuning input variables.

Output feedback control was implemented on a quadrotor using neural networks [43] for leader-follower quadrotor formation to learn the full dynamics of the UAV, including unmodeled dynamics. A virtual neural network control was implemented to control all six degrees of freedom from four control inputs. The Lyapunov stability theory showed that the position, orientation, velocity tracking errors, observer estimation errors, and virtual control were semi-globally uniformly ultimately bounded.

An adaptive neural network scheme was applied in [44]. The proposed solution of two parallel single hidden layers proved fruitful as this reduced tracking error, and no weight drift was achieved. Neural nets were utilized in [45] to estimate the aerodynamic components. One was utilized for aerodynamic components and one for aerodynamic moments. The inner-outer loop structure was used. The outer loop was used for position control, whereas the inner loop was used for attitude control. The backstepping technique was directly applied to the Lagrangian form of the dynamics. The control structure developed was inherently robust to unmodeled disturbances.

• **Geometric Control:**

The attitude representation using Euler angles suffers from singularity while there is sign ambiguity with the quaternion approach. The use of Euler angles also restricts the ability of aerial vehicles to track nontrivial trajectories. A geometric control approach is a coordinate-free approach, and hence the singularities and complexities when using local coordinates can be avoided. In [46], a nonlinear tracking controller has been developed directly on $SE(3)$, which is almost global. The controller was developed to track a three-

dimensional translational position and a one-dimensional heading direction. Robust [47] and robust adaptive [48] variants of this controller have also been proposed in the literature. The controller has been developed for two modes: attitude-controlled flight mode and position-controlled flight mode. In [48], first, an adaptive tracking controller was developed assuming inertia matrix was unknown, but the bounds on the inertia matrix were known. The controller was developed assuming no disturbance. Then another robust controller was developed assuming bounded disturbance in the attitude dynamics. In [49], geometric nonlinear PID is developed for a quadrotor UAV on $SO(3)$. Since a quadrotor has only four inputs, asymptotic stability for only four outputs can be achieved. Hence two fight modes are proposed, namely attitude-controlled flight mode and position-controlled flight mode. The controller is developed assuming some bounded disturbances in the dynamics.

A feedback trajectory tracking scheme has been proposed in [50] where angular velocity along the thrust direction is regulated to be zero. The other components of angular velocity are used for tracking the desired trajectory. The developed scheme promises exponential stability of the desired position tracking while the angular velocity tracking control is finite-time stable. Since a finite time-stable closed-loop system have better robustness and disturbance rejection properties [51], a finite time stable tracking control scheme was developed for underactuated aerial vehicles and simulated on a quadrotor dynamics in [52]. The control law was simulated on a discrete dynamics derived using Lie Group Variational Integrators (LGVI) [53]. First, the desired control was developed to stabilize the translational dynamics in finite-time. Based on this control force, the desired attitude trajectory is generated. To track this generated attitude trajectory, a finite-time stable attitude tracking control scheme is developed. In [54], a geometric controller was developed for a tilt rotor UAV. The paper utilized left tracking error on $SE(3)$ unlike [46], where right tracking error was used because left tracking error function results in simpler control law design.

Due to topological restriction [9] on $SO(3)$, it is not possible to design continuous-time controllers on $SO(3)$ having global exponential convergence. This is because any configuration error function, defined on $SO(3)$, results in more than one critical point. Hence, one cannot achieve global convergence with only one configuration function. Hence multiple configuration error functions have been used in the literature to overcome this restriction. The idea is to switch between these error functions according to hybrid system framework [55]. Another novel strategy to overcome this restriction has been proposed in [56], where the authors achieve global attractivity with their approach and avoid discontinuities in time. The main idea is to shift the desired attitude temporarily based on the initial condition. The proposed controller is discontinuous in the initial condition

but is continuous in time. The shifted desired trajectory converges to the true attitude trajectory in due time and hence guarantees asymptotic convergence.

• **Control with input and state constraints:**

Due to physical constraints on actuators, e.g., rotor speed, many researchers design controllers with input saturation. In addition, constraints on states should also be considered for practical reasons. An attitude stabilization technique, considering the bounds on the input signal, is developed in [57]. A backstepping controller was developed using the saturation function for the control input. In [58], an inner-outer loop approach was developed for trajectory tracking control of a quadrotor UAV. The outer loop generated the saturated thrust, reference roll, and pitch angles, while the inner loop was designed to follow these reference angles using a PID controller. In [59], a robust attitude controller was designed for multiple input multiple output uncertain quadrotors considering parametric uncertainties, external disturbances, and input time delays. A nominal input was designed for the nominal system with input time delay. To deal with parametric uncertainties and external disturbances, a robust compensating input is added with the nominal input. Compared to [60], singularity free quaternion based robust controller has been proposed in [61]. Similar to [60], a robust attitude controller is designed in [61] for uncertain quadrotors considering various uncertainties, external disturbances, coupling, and nonlinearities. In [59], a robust attitude controller was designed for multiple input multiple outputs uncertain quadrotors considering parametric uncertainties, external disturbances, and input time delays. A nominal input was designed for the nominal system with input time delay. To deal with parametric uncertainties and external disturbances, a robust compensating input is added with the nominal input. A similar robust controller considering parametric uncertainties, unmodeled uncertainties, and input as well as state delays is designed in [62, 63]. The external disturbances and multiple time-varying states, and input time delays are taken into consideration. As an improvement over [59], a nominal input was designed for an uncertain and delay-free model, and then a robust compensator was added to take into account the effects of multiple uncertainties and time delays in the closed-loop system.

• **Control with state and input delay:**

Time delays are ubiquitous in physical systems and engineering applications. The literature on the control of quadrotors with input delay is very limited. In [59], a robust attitude controller was designed for multiple input multiple output uncertain quadrotors, considering parametric uncertainties, external disturbances, and input time delays. A similar robust controller considering parametric uncertainties, unmodeled uncertainties,

and input, as well as state delays, is designed in [62, 63]. Teleoperation [64] is the next big thing in the robotics industry. But such a task is not without its own set of challenges. The main challenges are packet loss, distortion, and time delay. It is quite desirable to be able to control a robotic device over a network with remote access. There are several examples in the literature of such an operation [65]. In [66, 67, 68], mobile robots have been controlled with communication time delay while in [69], manipulators have been controlled with input time delay. Similarly, in [70], an inverted cart pole pendulum has been controlled, taking into account network-induced delay. All the literature mentioned pertaining to quadrotors does not consider communication time delay. The presence of communication time delay may result in instability in the system. The literature on the control of quadrotors with input delay is very limited. In [71], a robust attitude controller was designed for multiple input multiple output uncertain quadrotors considering parametric uncertainties, external disturbances, and input time delays. A similar robust controller considering parametric uncertainties, unmodeled uncertainties, and input as well as state delays are designed in [62, 63, 72, 73].

• **Control with finite-time convergence:**

A trajectory tracking control law with finite-time convergence on the nonlinear manifold $SE(3)$ is more desirable since most of the existing finite-time control law only stabilizes attitude. The closed-loop systems under finite-time control usually demonstrate a faster convergence rate, higher tracking precision, better disturbance rejection properties, and robustness against uncertainties [74, 51]. Because of above mentioned attractive features and better practical implementation in actuators, the continuous feedback finite-time control method has gained more attention in recent years. Moreover, the continuous feedback stabilization in finite time does not excite unmodeled high-frequency dynamics as compared to discontinuous feedback. A continuous finite-time controller based on homogeneity [75, 76] was developed for robot manipulators in [77]. A continuous finite-time stabilizing feedback law was developed for the double translational, and rotational double integrator in [78]. A finite-time attitude stabilizing result based on a homogeneous method was presented in [79]. Similarly, a finite time attitude tracking control law for single and multiple spacecraft was developed in [80], but the attitude was represented using Modified Rodriguez Parameters (MRPs). To deal with the external disturbances, a finite disturbance observer-based finite-time attitude tracking control of a rigid spacecraft was developed in [81]. In [82], a multi-variable finite-time attitude tracking law, based on a homogeneous method, was presented. The attitude was represented using Euler angles, and a multi-variable super-twisting-like algorithm was proposed with matched disturbances. As an improvement to the above-mentioned method, an adaptive variant

of the controller was developed in [83]. An adaptive multi-variable finite-time stabilizing control algorithm for second-order multi-variable systems is developed based on an improved super-twisting and equivalent control algorithm.

A feedback tracking control scheme was developed for a class of underactuated vehicles on $SE(3)$ in [50] but the position dynamics are only exponentially stable. A finite-time stabilization law with almost global convergence was developed for a rigid body using rotation matrices for representing attitude in [84, 85] but the method was not extended for the position dynamics. An integrated guidance and feedback control scheme for an underactuated aerial vehicle on $SE(3)$ was developed in [86, 52] but there was no mention of robustness to disturbances. Finite time-controllers have also been developed for speed regulation of Permanent Magnet Synchronous Motor in [87] and parallel DC-DC Buck Converters in [88].

1.5 Motivation

The present research work's motivation comes from the author's research interest in robotics, which is evident from his prior work in mobile robots such as PIONEER 3DX and underwater vehicles undertaken in his Master's thesis. The author has developed nonlinear tracking control laws for mobile robots as well as underwater vehicles using differential geometric concepts in his Master's thesis. The tools of differential geometry can be utilized to develop control laws on the manifolds on which the dynamics are evolving and not in the ambient space. This results in the conservation of constraints naturally. One can also avoid singularity associated with using local coordinates. Building upon a limited background in differential geometry and its application in robotics, the author applied these concepts to control aerial vehicles such as quadrotors. The main motivation was to develop globally valid control laws under different conditions for aerial vehicles such as quadrotors.

As mentioned in the literature review section, the present literature on the control of quadrotors mainly utilizes Euler angles or quaternions to represent a quadrotor's attitude. But such a representation introduces singularity in controller design and hence is not valid globally. One cannot have aggressive maneuvers using Euler angles. One singularity-free representation can be achieved by using quaternions. But such a representation introduces ambiguity since an attitude is represented by two antipodal quaternions. This results in an undesirable phenomenon called unwinding.

To avoid singularities introduced due to Euler angles and ambiguities associated with quaternions, one uses rotation matrices to represent a rigid body's attitude. The rotation matrices are a singularity-free representation of the attitude, and the control laws

developed using rotation matrices are globally valid. Due to these advantages, researchers have lately shifted to rotation matrices for attitude representation of a rigid body. In this thesis, we are also representing the rigid bodies' attitude using rotation matrices and developing a globally valid tracking algorithm.

Since, in a mechanical system, external disturbances are inevitable, we need to consider the effect of such disturbances while designing control laws for such a system. This motivated the author to develop a better tracking control law in the presence of disturbances and verify it experimentally. The tracking control law presented in this thesis in the presence of disturbance is an improvement over the current state of work. This has been achieved using a nonlinear disturbance observer and a geometric controller in the loop.

The modeling of a mechanical system is never perfect. This is due to unknown dynamics, imperfect knowledge of its parameters, and its variation with time. This motivated the author to develop an adaptive variant of a control law proposed before. It was also assumed that the center of gravity and origin of the body-fixed frame are different. This results in difficulty in modeling the dynamics of motion.

In physical and engineering systems, time delays are very much a reality. This aspect has not been taken into consideration while designing control laws for a quadrotor. Moreover, teleoperation is a new field of robotics that further results in time delays. The presence of time delay in closed-loop results in instability of the whole system. All the literature mentioned pertaining to quadrotors does not consider communication time delay. This motivated the author to develop a control law in the presence of time delays.

Because of the attractive features of finite-time controllers such as faster convergence, better disturbance rejection, and robustness to disturbances, such a controller is desirable. Moreover, such a controller present in the literature is discontinuous. This motivated the author to develop a robust and continuous geometric controller with finite-time convergence on $SE(3)$. Therefore, the proposed finite-time controller is not only continuous but globally valid also.

1.6 Problem Statement

In this thesis, the author aims to tackle the issue of globally valid control law design for quadrotors in the presence of disturbances and time delays. As previously mentioned, other attitude representations such as Euler angles or quaternions suffer from either singularity or ambiguity of representation. Therefore, the thesis aims to remove these shortcomings and develop control laws free of singularity or ambiguity.

As mentioned, a mechanical system always suffers from disturbances or modeling

uncertainties. Therefore, we aim to develop globally valid control laws in the presence of disturbances and modeling uncertainties. First, this is achieved by designing nonlinear disturbance observers on $SE(3)$. Then, the above is extended to the case of unknown parameters such as mass, the moment of inertia, and offset in the center of gravity. There, the author develops adaptive control design techniques to estimate the unknown parameters and guarantee the boundedness of tracking errors.

There has been very little attention to designing control laws in the presence of time delays. It is well known that time delays are unavoidable when operating a device over a network. The time delays may also introduce instability in the system. Therefore, the methods proposed in this thesis develop control laws for quadrotors in the presence of both input and state time delays. First, the author develops controller-predictor pair architecture to stabilize a quadrotor in the presence of both input and state delays. This is achieved in local coordinates. The second work globally stabilizes the attitude dynamics in the presence of input delay.

Since a controller with finite-time convergence has better disturbance rejection property as compared to exponentially converging control laws, the thesis presents a method to design a finite time stable control for trajectory tracking of a quadrotor. There has been little effort in this direction in the current literature. The robustness of the proposed controller to bounded disturbances is also demonstrated in this thesis.

1.7 Contribution of the thesis

The thesis's main contribution is to design globally valid control laws in the presence of disturbances and time delays by representing the attitude of a quadrotor using rotation matrices. Since the rotation dynamics evolve on Special Orthogonal Group of matrices denoted by $SO(3)$ and the translational dynamics evolve on $\mathbb{R}^3$, the complete dynamics evolve on $SE(3)$. Therefore, global valid control laws are developed directly on $SE(3)$. The contributions of the thesis are mentioned below :

- The dynamics of an underactuated mechanical system, e.g., quadcopters, naturally evolve on a nonlinear manifold. Hence, differential geometric modeling concepts are better suited to arrive at the set of equations describing the dynamic behavior of such systems. Resorting to a differential geometric approach, a generalized dynamical model for a quadcopter is proposed in this paper. The rotation matrices in the forward kinematic map are represented using Euler angles. The modeling has been presented on a single chart. The Riemannian metric, being a crucial ingredient for model development on a chart, is derived from the total kinetic energy. A complete set of dynamic equations of motion neglecting external disturbances

is derived for the quadcopter by representing the Levi-Civita affine connection in local coordinates. Further, based on the derived model, a proportional-derivative (PD) controller is designed for attitude stabilization. Simulation studies validate the proposed model and also demonstrate its robustness to wide variations in initial conditions.

- The thesis proposes a geometric controller with a nonlinear disturbance observer for quadrotors using rotation matrices for attitude dynamics. The thesis utilizes left tracking error while developing the tracking controller. This is because the left tracking error results in a simpler controller structure as compared to the right tracking error proposed in [46, 47, 48, 89]. Further, the proposed observer does not have the assumption that the disturbance is constant or its upper bound is known, which makes the approach much more realistic and general. The only assumption made is that the disturbance and its variations are bounded. Hence the proposed disturbance observer can handle constant disturbance as a special case.

- The thesis proposes an adaptive controller to estimate the center of gravity, mass, and inertia matrix in a coordinate invariant approach when there is an offset between the center of gravity and the origin of the body-fixed frame. The compensation in the system dynamics due to the offset in the center of gravity and geometric center in a coordinate invariant approach is one of this thesis's contributions. The current literature mainly utilizes Euler angles for system dynamics compensation due to the offset in the center of gravity and geometric center, while this thesis uses rotation matrices for the compensation.

- A state predictor is proposed to estimate the future values of the quadrotor's state in the presence of both input and state time delays. The chapter attempts to propose a method to control a quadrotor over a network. According to the authors' best of knowledge, there is no such method in the literature that attempts to control a quadrotor over a network. Then the output of the estimator is used in designing a backstepping controller. A backstepping controller is designed for stabilization and trajectory tracking, assuming no state or input delay. The controller is shown to have asymptotic stability property. To the best of the authors' knowledge, this study is the first to compensate for both states as well as input time delays in a quadrotor system explicitly. All the mentioned literature either does not consider such a scenario or at best handle it as a disturbance.

- The thesis proposes a stabilizing controller for quadrotors with input time delay using rotation matrices for attitude dynamics. There are very few references in

literature compensating input delay in a quadrotor, and this chapter attempts to bridge that gap. Predictor feedback has been developed to compensate for the input time delay in rotation dynamics of the quadrotor. The method does not approximate input delay, which is prevalent in the current literature on input delay compensation.

- The thesis develops a control law that guarantees the convergence of the attitude as well as the translational motion to the equilibrium configuration in finite time, while most of the existing literature develops only finite time attitude tracking control law. Moreover, a finite time control law has been developed for trajectory tracking for an underactuated aerial vehicle on the nonlinear manifold $SE(3)$. The control law is also robust to bounded external disturbances.

1.8 Thesis Organization

The thesis is organized into eight chapters. A brief summary of each chapter is given below :

- **Chapter 2** : This chapter is divided into two sections. The first section presents the mathematical modeling using local parameterization, such as Euler angles. This section also presents the preliminaries of differential geometric concepts used in mathematical modeling. The chapter also presents a brief introduction to Lie Groups and Lie algebras. The second section presents the mathematical modeling on Lie group $SE(3)$.

- **Chapter 3** : Chapter 3 presents a geometric controller's development in the presence of external disturbances when the bound on the disturbances is not known. The external disturbances are estimated using a nonlinear disturbance observer. Both the controller and the disturbance observer are developed on the nonlinear manifold $SE(3)$. This makes the approach globally valid. The proposed control and disturbance observer are also validated on a real-time quadrotor setup.

- **Chapter 4** : An adaptive geometric controller is presented in this chapter in a practical scenario when there is an offset between the center of gravity and the origin of a body-fixed frame of reference. The adaptive control law estimates mass, the moment of inertia, and the offset in the center of gravity in a coordinate invariant approach. The control law, along with the adaptive laws, is shown to be Lyapunov stable.

- **Chapter 5** : A control law in the presence of input as well as state time delay is presented in this chapter. For this scenario, a predictor, as well as a backstepping controller, is presented. The predictor predicts the quadrotor's future states from delayed measurements, while the backstepping controller is designed using the predicted states. The controller predictor pair results in successful steering of a quadrotor when operating over network-induced time delay.

- **Chapter 6** : This chapter presents a geometric control law to stabilize a quadrotor's attitude in the presence of input time delay. The approach does not assume any limitations on input delay. The approach is valid in long input time delay also. The input delay equations are represented using partial differential equations (PDE) such that the overall system is an ODE-PDE cascade. The control law results in exponential stabilization of the attitude dynamics.

- **Chapter 7** : A finite-time stable geometric control law for both attitude as well as translational dynamics of a quadrotor is presented in this chapter. This results in better disturbance rejection and faster convergence to reference trajectory, as demonstrated in numerical simulations and comparison results.

- **Chapter 8** : A summary of the work done and directions for future work are presented in this chapter.

Chapter 2

Mathematical Modeling

The dynamics of an underactuated mechanical system, e.g., quadrotors, naturally evolve on a nonlinear manifold. Hence, differential geometric modeling concepts are better suited to arrive at the set of equations describing the dynamic behavior of such systems. Resorting to a differential geometric approach, a dynamical model for a quadrotor is proposed in this chapter. Since Euler angles are local parameterization of $SO(3)$, the model suffers from singularity because the whole configuration space has not been covered. A globally valid model of the quadrotor on $SE(3)$, derived using variational principles, has been presented in this chapter. This model will be utilized in designing controllers in subsequent chapters.

2.1 Introduction

Attributed to their multifaceted applications, quadrotors have gained immense popularity among aerial vehicles in recent years [90]. Owing to their vertical take-off and landing (VTOL) capabilities in limited spaces and their hovering abilities over a specified target, quadrotors find wide utility in surveillance, search and inspection, and several other social and military applications. Recent advances in miniaturized sensors and high computational efficiency have played a major role in the development of aerial vehicles, especially quadrotors [1, 3, 5, 6]. To introduce, a quadrotor is basically made of four rotors placed perpendicular to each other. One pair of opposite rotors rotates in the same direction while the other pair rotates in the opposite direction. One of the several advantages of a quadrotor over conventional helicopters is its mechanical simplicity, and therefore, these are very easy to build. The other advantage being payload augmentation since four rotors are used, and hence more lift thrust can be generated. Unlike helicopters, a swashplate mechanism is not required to control the movement of the quadrotors, which further simplifies the design. One of the limitations of quadrotors is their high energy

required to control the four rotors.

Modeling a dynamic system is the first and a very important step in designing a controller. Once a system's mathematical model is obtained, various analytical and computational tools can be used for analysis purposes. Control of unmanned aerial vehicles is very challenging due to their highly nonlinear dynamics and parameter variations with flight conditions. Therefore, a good mathematical model of the system is crucial in developing a controller that can give a reasonable performance under various operating conditions. Several linear and nonlinear control techniques have been proposed in the literature for stabilization and tracking control of quadrotors. In [10], PID and LQR control techniques are applied on a simplified linear model for stabilization of a quadrotor. Since the linear model is used, the simulation results are not very satisfactory on account of modeling inaccuracies. To improve performance, initial approaches to nonlinear control of a quadrotor have been through feedback linearization. A dynamic feedback extension of the control input is employed in [12] to develop the controller. Further, the coupling effects between rolling and transverse motion and between pitching and forward motion are neglected in [13] while designing the controller.

The authors in [14] proposed an outer loop approach to stabilize the zero dynamics. Since rotational dynamics are independent of translational dynamics, the former can be controlled independently of the latter. This approach has been applied in [17], where control for the angular subsystem is developed using a Lyapunov function. While compensating gyroscopic and Coriolis effects, a novel feedback controller is proposed in [18]. A Lagrangian-based model is considered, and subsequently, a controller based on nested saturation algorithm [19] is presented in [20]. Thereafter, backstepping and sliding mode control methodologies are reported in [23, 24, 25] for stabilization of quadrotor dynamics. To simplify controller design, the translational dynamics have been represented in the inertial frame while the rotational dynamics have been represented in the body-fixed frame in [47, 89] and subsequently, a geometric approach to controller design has been proposed.

This chapter presents the dynamical model of a quadrotor using differential geometric concepts. Geometric modeling techniques give a better understanding of the dynamic system on manifolds that cannot be obtained using local coordinates. In other words, modeling quadrotor dynamics, adopting a geometric approach results in a global dynamic model. For instance, the configuration space of quadrotor dynamics cannot be globally represented using a single chart since the configuration space is a nonlinear manifold. Hence, multiple charts are needed to represent quadrotor dynamics globally.

The main contribution of the chapter is the modeling of the quadrotor dynamics on $SE(3)$ using variational principles. The derived model is globally valid and hence

singularity free as compared to model derived using Euler angles. This model will be used in subsequent chapters while developing the geometric controllers.

Section 2.2 of the chapter explains some differential geometric concepts used in modeling the dynamics for the sake of clarity in understanding. Section 2.3 presents the basics of Lie Group and Lie algebras used in modeling the quadrotor dynamics on $SE(3)$. Section 2.4 presents the modeling of quadrotor dynamics on $SE(3)$ using variational principles. This model will be used in subsequent chapters for controller design. A summary of the work has been presented in Section 2.5.

2.2 Mathematical Preliminaries

Geometric control [7] [91] is the application of differential geometric tools to nonlinear control theory. Using these tools, one can develop control systems for dynamic systems evolving on the nonlinear manifold, which are only locally Euclidean. The identification of these nonlinear manifolds with Euclidean spaces exhibits singularity. This is the fundamental reason behind the occurrence of singularity when representing attitude with Euler angles since attitude evolves on $SO(3)$, which is a nonlinear manifold. Geometric control techniques give a better understanding of the dynamic system on manifolds that cannot be obtained using local coordinates. For example, there exists no continuous feedback control that asymptotically stabilizes an attitude globally on $SO(3)$. A review of differential geometric tools for a better understanding of the modeling has been presented below ([7], ch.3-4).

2.2.1 Topological Spaces

A topological space is a set $\mathcal{S}$ along with a subset $\mathbb{O}$ of power set of $\mathcal{S}$ called open sets such that following conditions are satisfied :

$$\begin{aligned}
&(i)\ \emptyset \in \mathbb{O} \text{ and } \mathcal{S} \in \mathbb{O},\\
&(ii)\ \text{Arbitrary union of open sets of } \mathbb{O} \text{ is in } \mathbb{O}\\
&i.e. \bigcup_{a\in A} \mathcal{O}_a \in \mathbb{O},\\
&(iii)\ \text{Intersection of any two open sets of } \mathbb{O} \text{ is also in } \mathbb{O}\\
&\text{i.e. if } \mathcal{O}_1, \mathcal{O}_2 \in \mathbb{O} \text{ then } \mathcal{O}_1 \cap \mathcal{O}_2 \text{ is in } \mathbb{O}.
\end{aligned} \tag{2.1}$$

2.2.2 Manifold

A manifold is a topological space that is locally homeomorphic to $\mathbb{R}^n$. Since it is locally homeomorphic to $\mathbb{R}^n$ a continuous bijective map, ι whose inverse is also continuous (called homeomorphism) can be defined from an open neighborhood, $\mathcal{U}$ of the manifold to $\mathbb{R}^n$. The pair $(\mathcal{U},\iota)$ is called a chart. The collection of such charts, such that the whole manifold is covered, is called an atlas. If all the maps in the atlas take value in $\mathbb{R}^n$ then the dimension of the manifold is said to be n. The map ι is said to be of type $\mathcal{C}^r$ if the map $\iota : \mathcal{U} \to \mathbb{R}^n$ is $r-$times differentiable. An atlas, equipped with $\mathcal{C}^r$ maps such that the transition map ι_{12} is $r-$times differentiable, is called a $\mathcal{C}^r-$atlas. A $\mathcal{C}^r-$differentiable structure is an equivalence class of atlases under the equivalence relation that the two $\mathcal{C}^r-$atlases are equivalent if their union is also a $\mathcal{C}^r-$atlas. This is illustrated in Fig.2.1.

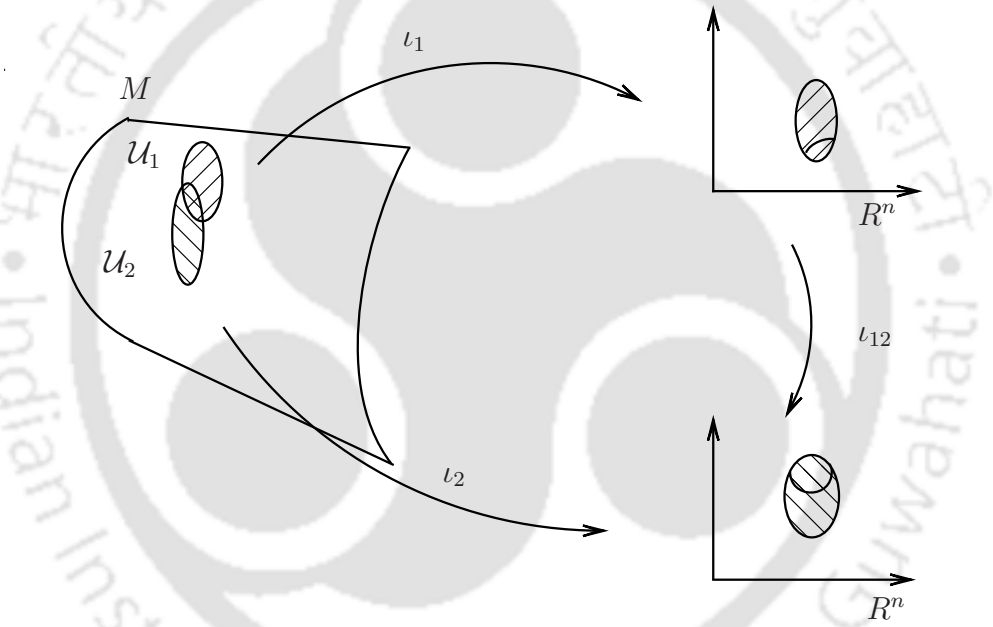

Figure 2.1: Charts and mappings

2.2.3 Immersed Submanifold

A subset $S \subset M$ is a $\mathcal{C}^r-$immersed submanifold if there exists a manifold N and a $\mathcal{C}^r-$injective immersion $f : N \to M$ for which $S = \text{image}(N)$.

2.2.4 Tangent Bundle

A tangent vector at x is an equivalence class of curves under the equivalence relation that the local representative of all curves has the same derivative at their common

intersection point. The collection of all tangent vectors at x is the tangent space at x and is denoted by T_xM. The disjoint union :

$$TM = \overset{\circ}{\bigcup_{x \in M}} T_xM \tag{2.2}$$

of all tangent spaces is called the tangent bundle. The tangent bundle projection is the map $\pi_{TM} : TM \to M$ defined by $\pi_{TM}(v) = x$ when $v \in T_xM$.

2.2.5 Vector fields

A vector field assigns a tangent vector to each point on the manifold in an appropriately smooth way. Similarly, a covector field assigns a cotangent vector to each point on the manifold in an appropriately smooth way.

2.2.6 Tangent Bundle of the configuration manifold

The tangent bundle $TSO(3)$ is isomorphic to $SO(3) \times \mathbb{R}^3$. Let $R \in SO(3)$ and let $A_R \in T_RSO(3)$, then we define isomorphism from $TSO(3)$ to $SO(3) \times \mathbb{R}^3$ as $(R, A_R) \to (R, (R^T A_R)^\vee)$ and $(R, A_R) \to (R, (A_R R^T)^\vee)$ where $(\cdot)^\vee : \mathfrak{so}(3) \to \mathbb{R}^3$ is the inverse of $\widehat{(\cdot)}$. The body angular velocity corresponding to A_R is $R^T A_R$.
The spatial angular velocity corresponding to A_R is $A_R R^T$. The body angular velocity at $R(t)$ is denoted by $\Omega(t)$ while the spatial angular velocity at $R(t)$ is denoted by $\alpha(t)$.

2.2.7 Kinetic Energy of Rigid Body

A rigid body undergoing motion specified by a differential curve $t \to (R(t),r(t))$ has following definition of kinetic energy (KE).

$$KE_{tran} = \frac{1}{2} m ||\dot{r}(t)||^2_{\mathbb{R}^3}; \; KE_{rot} = \frac{1}{2} \mathbb{G}_{\mathbb{R}^3}(\mathbb{I}_c(\Omega(t)), \Omega(t))$$

where KE_{tran} is the translational KE while KE_{rot} is the rotational KE at time t. The total KE is written as :

$$KE = KE_{tran} + KE_{rot} \tag{2.3}$$

2.3 Lie Group and Lie Algebras

2.3.1 Rigid body transformations

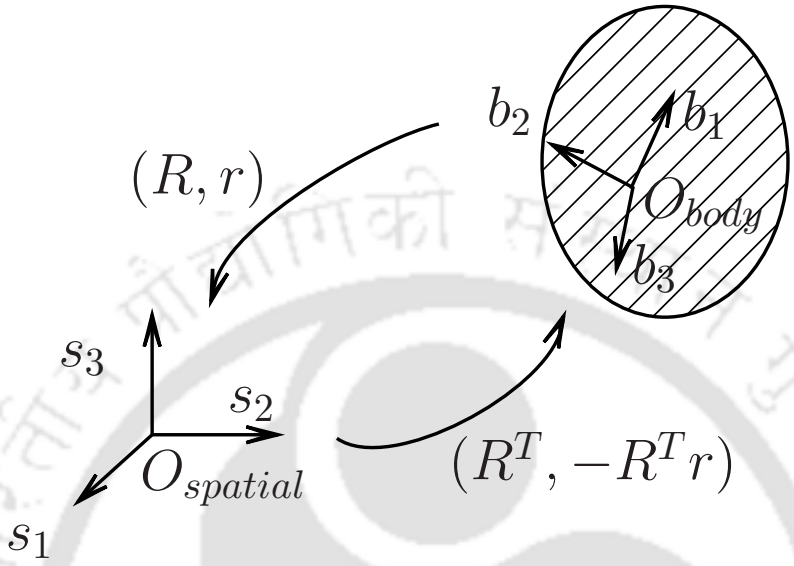

Figure 2.2: Rigid body transformations

Consider a rigid body undergoing motion in 3-dimensional Euclidean space as illustrated in Fig.2.2. The inertial frame is denoted by ($O_{spatial}$,s_1,s_2,s_3) fixed in space and a body frame (O_{body},b_1,b_2,b_3) fixed to the body. The axes (s_1,s_2,s_3) and (b_1,b_2,b_3) are assumed to have same orientation. Let us define following notations :
$r \in \mathbb{R}^3$ connect the origin $O_{spatial}$ to the origin O_{body} i.e. $r = O_{spatial} - O_{body}$.
The matrix $R \in \mathbb{R}^{3\times3}$ has the a^{th}, $a = \{1, 2, 3\}$ column, the components of b_a relative to the basis (s_1,s_2,s_3).
χ_s is coordinate of a point measured in the inertial frame.
χ_b is coordinate of a point measured in the body fixed frame.
Then they are related by:

$$\chi_s = R\chi_b + r$$

If we take $x \in \mathbb{R}^3$ as $x = (x, 1)$, also called homogenous coordinates of x, the transformation and its inverse can be represented as :

$$\bar{\chi}_s = \begin{bmatrix} R & r \\ 0_{1\times3} & 1 \end{bmatrix} \bar{\chi}_b$$

$$\bar{\chi}_b = \begin{bmatrix} R^T & -R^T r \\ 0_{1\times 3} & 1 \end{bmatrix} \bar{\chi}_s$$

The orthogonal group $O(n)$ and the special orthogonal group $SO(n)$ are defined by:

$$O(n) = \{R \in \mathbb{R}^{n\times n} \mid RR^T = I_n\}, \quad SO(n) = \{R \in O(n) \mid \det(R) = 1\},$$

respectively. The Euclidean group $E(n)$ and the special Euclidean group $SE(n)$ are defined by:

$$E(n) = \left\{ g \in \mathbb{R}^{(n+1)\times(n+1)} \;\middle|\; g = \begin{bmatrix} R & r \\ 0_{1\times 3} & 1 \end{bmatrix}, R \in O(n), r \in \mathbb{R}^n \right\},$$

$$SE(n) = \{g \in E(n) \mid \det(g) = 1\}$$

respectively. For $n = 3$, the set $SE(3)$ is the group of rigid displacements in $\mathbb{R}^3$, and the matrix $g \in SE(3)$ is referred to as a rigid displacement matrix. The element of $SO(n) \times \mathbb{R}^n$ is identified with elements of $SE(n)$ by means of the bijection :

$$(R, r) \mapsto \begin{bmatrix} R & r \\ 0_{1\times 3} & 1 \end{bmatrix}$$

For $n \in \mathbb{N}$, we denote the vector space of skew-symmetric matrices in $\mathbb{R}^{n\times n}$ by :

$$\mathfrak{so}(n) = \{S \in \mathbb{R}^{n\times n} \mid S^T = -S\}$$

The linear map $\hat{(\cdot)} : \mathbb{R}^3 \to \mathfrak{so}(3)$ is defined by $\hat{\omega}y = \omega \times y$ for all $\omega, y \in \mathbb{R}^3$. The linear map $\hat{(\cdot)}$ is an isomorphism of vector spaces and is written as $\mathfrak{so}(3) \simeq \mathbb{R}^3$. Similarly we can define :

$$\mathfrak{se}(n) = \left\{ \begin{bmatrix} S & v \\ 0_{1\times n} & 0 \end{bmatrix} \in \mathbb{R}^{(n+1)\times(n+1)} \mid S \in \mathfrak{so}(n), v \in \mathbb{R}^n \right\}.$$

Analogous to $\mathfrak{so}(3)$ case we can define another linear $\hat{(\cdot)} : \mathbb{R}^3 \oplus \mathbb{R}^3 \to \mathfrak{se}(3)$ by :

$$\hat{\xi} = \begin{bmatrix} \hat{\omega} & v \\ 0_{1\times 3} & 0 \end{bmatrix}$$

for $\hat{\xi} = (\omega, v) \in \mathbb{R}^3 \oplus \mathbb{R}^3$. Similarly, we can write $\mathfrak{se}(3) \simeq \mathbb{R}^3 \oplus \mathbb{R}^3$. The elements of $\mathfrak{se}(3)$ are referred to as twists. We can also define inverse isomorphisms for both $\mathfrak{so}(3)$ and $\mathfrak{se}(3)$ case as follows : $(\cdot)^\vee : \mathfrak{so}(3) \to \mathbb{R}^3$ and $(\cdot)^\vee : \mathfrak{se}(3) \to \mathbb{R}^3 \oplus \mathbb{R}^3$. For a rigid body undergoing movement described by a curve $t \mapsto (R(t), r(t)) \in SO(3) \times \mathbb{R}^3$ or equivalently

$t \mapsto g(t) \in SE(3)$, the spatial angular velocity $\omega : \mathbb{R} \to \mathbb{R}^3$ and body angular velocity $\Omega : \mathbb{R} \to \mathbb{R}^3$ are given by :

$$\hat{\omega}(t) = \dot{R}(t)R^T(t), \hat{\Omega}(t) = R^T(t)\dot{R}(t)$$

respectively. For the curve $g : \mathbb{R} \to SE(3)$, the spatial velocity $\xi_s : \mathbb{R} \to \mathbb{R}^3 \oplus \mathbb{R}^3$ and body velocity $\xi_b : \mathbb{R} \to \mathbb{R}^3 \oplus \mathbb{R}^3$ are given by :

$$\hat{\xi}_s(t) = \dot{g}(t)g^{-1}(t), \hat{\xi}_b(t) = g^{-1}(t)\dot{g}(t)$$

respectively. The transformation from the body to inertial reference frame is called the adjoint map $Ad_g : \mathfrak{se}(3) \to \mathfrak{se}(3)$ and is given by :

$$Ad_g\hat{\eta} = g\hat{\eta}g^{-1}$$

For any rigid body trajectory $t \mapsto g(t)$ with spatial velocity $t \mapsto \xi_s(t)$ and body velocity $t \mapsto \xi_b(t)$, following relation holds :

$$\hat{\xi}_s(t) = Ad_{g(t)}\hat{\xi}_b(t).$$

2.3.2 Topological Group

A topological group is a group which is also a topological space for which the group operation and inverse operation are continuous.

2.3.3 Lie Group

A Lie group is a topological group that is also a manifold and in which the group and the inverse operations are smooth. For example, the set of all invertible $n \times n$ matrices with real entries denoted by $\mathsf{GL}(n;\mathbb{R})$ is a Lie group with respect to the operation of matrix multiplication. If the group operation is commutative, then the group is called Abelian. For example, a vector space V with the operation of vector addition is an Abelian group.

2.3.4 Matrix Lie group

A Matrix Lie group is a subgroup of $\mathsf{GL}(n;\mathbb{R})$.

2.3.5 Lie algebra

A Lie algebra V is an $\mathbb{R}-$vector space endowed with a bilinear operation $[\cdot,\cdot] : V \times V \to V$ referred to as bracket operation which satisfies :
(i) anti-commutativity, i.e. $[\xi,\eta] = -[\eta,\xi]$ for all $\xi,\eta \in V$, and
(ii) the Jacobi identity i.e. $[\xi,[\eta,\zeta]] + [\eta,[\zeta,\xi]] + [\zeta,[\xi,\eta]] = 0$ for all $\xi,\eta,\zeta \in V$.
Example : $\mathbb{R}^3$ with operation of vector cross-product is a Lie algebra.

2.3.6 Matrix Lie algebra

A matrix Lie algebra is a subspace of $\mathbb{R}^{n\times n}$ closed under the operation of matrix commutator $[\cdot,\cdot] : \mathbb{R}^{n\times n} \times \mathbb{R}^{n\times n} \to \mathbb{R}^{n\times n}$ given by $[A,B] = AB - BA$.

2.4 Modeling on $SE(3)$ using Variational Principles

The configuration space of quadrotor is $SE(3)$. The material presented in this section is motivated from [92]. The special orthogonal group $SO(3)$ is defined by:

$$SO(3) = \{R \in \mathbb{R}^{3\times 3} \mid R^T R = I_3,\ \det(R) = 1\}, \tag{2.4}$$

Differentiating Eqn.(2.4) we get,

$$\dot{R}^T R + R^T \dot{R} = 0 \tag{2.5}$$

This means $R^T\dot{R}$ is skew symmetric. Let $R^T\dot{R} = \hat{\Omega}$, where the map $\hat{(\cdot)}$ is defined as before. Therefore, we have

$$\dot{R} = R\hat{\Omega} \tag{2.6}$$

This is the kinematic equation of the rotational equation of motion of a quadrotor on $SO(3)$. Here, Ω represents the angular velocity of the quadrotor expressed in the body-fixed frame. The Lagrangian of a mechanical system is defined to be the difference between kinetic and potential energy. Therefore, the Lagrangian of the quadrotor is given by :

$$L = \frac{1}{2}\Omega^T I\Omega + \frac{1}{2}v^T mv - mgz \tag{2.7}$$

where I is the moment of inertia of the quadrotor, v is the linear velocity, m is the mass, $e_3 = [0;0;1]^T$ and z is the z-coordinate of the position vector of the quadrotor. Since rotational kinetic energy is independent of position coordinates and translational kinetic energy is independent of rotational coordinates, one can derive the rotational and translational dynamic equations of motion independent of each other. Let us first

consider rotational kinetic energy. Let

$$L_{rot} = \frac{1}{2}\Omega^T I \Omega \tag{2.8}$$

The equations of motion can be obtained by applying Hamilton's principle i.e.

$$\delta \int_a^b L_{rot}(\Omega) dt = 0 \implies \int_a^b \left\langle \frac{\delta L_{rot}}{\delta \Omega}, \delta\Omega \right\rangle dt = 0 \tag{2.9}$$

The variations $\delta\Omega$ are induced by the variations on δR. By taking the variation of $\hat{\Omega} = R^{-1}\dot{R}$, one gets :

$$\delta\hat{\Omega} = -R^{-1}\delta R R^{-1}\dot{R} + R^{-1}\delta\dot{R} = -(R^{-1}\delta R)\hat{\Omega} + R^{-1}\delta\dot{R} \tag{2.10}$$

The variations δR are taken among paths $R(t) \in SO(3)$ with fixed endpoints, so that $\delta R(a) = \delta R(b) = 0$. Defining $\hat{\Sigma} \in \mathfrak{so}(3)$ by

$$\hat{\Sigma} = R^{-1}\delta R \tag{2.11}$$

$\hat{\Sigma}$ vanishes at the endpoints since δR does. Differentiating Eqn.(2.11) gives :

$$\frac{d\hat{\Sigma}}{dt} = -R^{-1}\dot{R}R^{-1}\delta R + R^{-1}\delta\dot{R} \implies R^{-1}\delta\dot{R} = \frac{d\hat{\Sigma}}{dt} + R^{-1}\dot{R}R^{-1}\delta R \tag{2.12}$$

Substituting in Eqn.(2.10) gives :

$$\delta\hat{\Omega} = -\hat{\Sigma}\hat{\Omega} + \frac{d\hat{\Sigma}}{dt} + \hat{\Omega}\hat{\Sigma} = \frac{d\hat{\Sigma}}{dt} + [\hat{\Omega}, \hat{\Sigma}] \tag{2.13}$$

where $[\cdot,\cdot]$ is the matrix commutator. Since $[\hat{\Omega}, \hat{\Sigma}] = \widehat{\Omega \times \Sigma}$, one can write :

$$\delta\Omega = \dot{\Sigma} + \Omega \times \Sigma \tag{2.14}$$

Substituting in Eqn.(2.9), we get

$$\begin{aligned}
&\int_a^b \left\langle \frac{\delta L_{rot}}{\delta\Omega}, \dot{\Sigma} + \Omega\times\Sigma \right\rangle dt = 0 \implies \int_a^b \left\langle \frac{\delta L_{rot}}{\delta\Omega}, \frac{d\Sigma}{dt} \right\rangle + \int_a^b \left\langle \frac{\delta L_{rot}}{\delta\Omega}, \Omega\times\Sigma \right\rangle dt = 0 \\
&\implies \int_a^b \left\langle -\frac{d}{dt}\left(\frac{\delta L_{rot}}{\delta\Omega}\right), \Sigma \right\rangle + \int_a^b \left\langle -\Omega\times\frac{\delta L_{rot}}{\delta\Omega}, \Sigma \right\rangle dt = 0 \\
&\implies \int_a^b \left\langle -\frac{d}{dt}\left(\frac{\delta L_{rot}}{\delta\Omega}\right) + \frac{\delta L_{rot}}{\delta\Omega}\times\Omega, \Sigma \right\rangle dt = 0
\end{aligned} \tag{2.15}$$

Since Eqn.(2.15) vanishes for any path $\Sigma(t) \in \mathfrak{so}(3)$, the motion is given by the equation :

$$\frac{d}{dt}\left(\frac{\delta L_{rot}}{\delta \Omega}\right) = \frac{\delta L_{rot}}{\delta \Omega} \times \Omega \tag{2.16}$$

which simplifies to

$$I\dot{\Omega} = I\Omega \times \Omega \tag{2.17}$$

Similarly the translational equation of motion can be derived and is found to be :

$$m\dot{v} = -mge_3 \tag{2.18}$$

Therefore, the complete equations of motion of a quadrotor on $SE(3)$ in presence of forces assumes the form :

$$\begin{aligned} \dot{R} &= R\hat{\Omega} \\ I\dot{\Omega} &= I\Omega \times \Omega + \tau \end{aligned} \tag{2.19}$$

$$\begin{aligned} \dot{x} &= v \\ m\dot{v} &= -mge_3 + Rf_b \end{aligned} \tag{2.20}$$

where τ and f_b are the external torque and force acting in the body-fixed frame. $x \in \mathbb{R}^3$ is the position vector of the quadrotor.

2.5 Conclusion

Since Euler angles are local parameterization of $SO(3)$, the model suffers from singularity because the whole configuration space has not been covered. Moreover the quaternions suffer from ambiguity of representation since two anti-podal quaternions represent same rotation matrix. Therefore, a globally valid model of the quadrotor on $SE(3)$, derived using variational principles, has been presented in this chapter. This model will be utilized in designing controllers in subsequent chapters.

Chapter 3

Nonlinear Disturbance Observer Based Geometric Control of a Quadrotor

A mechanical system inherently suffers from disturbances. Therefore, this chapter presents a nonlinear disturbance observer-based controller (NDOBC) for quadrotors utilizing the rotation matrices for attitude dynamics. The proposed observer does not make the assumption that the disturbance is constant or its upper bound is known. The only assumptions are that the disturbance and its derivatives are bounded and hence can handle constant disturbance as a special case. The proposed disturbance observer can handle a large class of disturbances. The NDOBC is shown to be locally input to state stable with respect to the derivatives of the disturbances present in attitude dynamics and translational dynamics. The proposed controller, as well as the nonlinear disturbance observer, has been formulated on the nonlinear manifold $SE(3)$, where the rotational dynamics evolve on $SO(3)$ while the translational dynamics evolve on $\mathbb{R}^3$.

3.1 Introduction

To remove the singularities associated with Euler angles and ambiguities with quaternions, rotation matrices have been used to develop controllers in [46, 47, 48, 89]. The effect of external disturbances was considered in [47, 48] where it is assumed that the bound on the disturbances is known a priori. A time-varying disturbance with bounded amplitude and bounded derivative was considered in [93] but the control law was developed using quaternions.

The contributions of this chapter are mentioned below. Firstly, the chapter presents a geometric controller with a nonlinear disturbance observer for quadrotors using rota-

tion matrices for attitude dynamics. The second novelty of this chapter is the utilization of left tracking errors while developing the tracking controller. This is because the left tracking error results in a simpler controller structure as compared to the right tracking error proposed in [46, 47, 48, 89]. The third contribution of this chapter is that the proposed observer does not have the assumption that the disturbance is constant or its upper bound is known, which makes the approach much more realistic and general. The proposed geometric controller, along with the nonlinear disturbance observer, is shown to render closed-loop error dynamics locally input to state stable with respect to the derivatives of disturbances present in attitude as well as translational dynamics.
Section 3.2 of the chapter explains the dynamic model used in developing the controller. Various configuration errors and nonlinear disturbance observer design have been presented in section 3.3. Section 3.4 explains the development of the geometric controller while compensating for the external disturbances along with the proofs. Simulation results and experimental results on a hardware setup have been presented in section 3.5 and section 3.6, respectively.

3.2 Dynamic Model

The dynamic equations of motion of a quadrotor can be recalled from section 2.4. In the presence of external disturbances, the equations of motion become :

$$\dot{x} = v$$
$$\dot{R} = R\hat{\Omega}$$
$$m\dot{v} = -mge_3 + Rf_b + d_x \tag{3.1}$$
$$I\dot{\Omega} = -\Omega \times I\Omega + \tau_b + d_\Omega \tag{3.2}$$

where, d_x : disturbance vector in translational dynamics,
d_Ω : disturbance vector in rotational dynamics.
$\hat{(\cdot)}$: map from $\mathbb{R}^3$ to $\mathfrak{so}(3)$, space of skew symmetric matrices i.e. if $\Omega = [b_1 \quad b_2 \quad b_3]^T$, then

$$\hat{\Omega} = \begin{bmatrix} 0 & -b_3 & b_2 \\ b_3 & 0 & -b_1 \\ -b_2 & b_1 & 0 \end{bmatrix}$$

3.3 Geometric Controller

3.3.1 Configuration Error

The configuration error for the position and velocity are defined in the inertial frame as :

$$e_x = x - x_d, \quad e_v = v - v_d$$

where, $v_d = \dot{x}_d$ is the desired inertial velocity. For the attitude dynamics, left error representation is employed as:

$$R_e = RR_d^T \in SO(3)$$

where R_d represents the desired attitude. This choice allows us to obtain a simple control law design as opposed to the right error representation given below:

$$R_r = R_d^T R \in SO(3)$$

The error function on $SO(3)$ is chosen to be :

$$\Psi = \frac{1}{2}\text{tr}(K(I - RR_d^T))$$

for a symmetric positive definite matrix $K \in \mathbb{R}^{3\times3}$. Here $\text{tr}(\cdot)$ denotes trace of the matrix. For the sake of simplicity, the gain matrix is taken to be diagonal i.e., $K = \text{diag}(k_1, k_2, k_3)$, where k_1, k_2, k_3 are strictly positive constants. The properties of the left error function used in this chapter can be recalled from [54] but is mentioned below for the sake of completeness.

(1) Ψ is locally positive definite about $R_e = I_{3\times3}$.

(2) The time derivative of Ψ is

$$\frac{d}{dt}\Psi = (\text{skew}(KR_e)^\vee)^T R_d e_\Omega = e_R^T R_d e_\Omega. \tag{3.3}$$

where $(\cdot)^\vee$ denotes map from $\mathfrak{so}(3)$ to $\mathbb{R}^3$ and e_R is attitude error vector.

(3) For $\Psi < \psi < p_1$, it is locally quadratic

$$h_1||e_R||^2 \leq \Psi \leq h_2||e_R||^2$$

$$h_1 = \frac{p_1}{p_2 + p_3^2}, \quad h_2 = \frac{p_3}{p_1(p_1 - \psi)} \tag{3.4}$$

where the constants, p_i are given by

$$\begin{aligned} p_1 &= \min\{k_1 + k_2, k_2 + k_3, k_3 + k_1\} \\ p_2 &= \max\{(k_1 - k_2)^2, (k_2 - k_3)^2, (k_3 - k_1)^2\} \\ p_3 &= \max\{k_1 + k_2, k_2 + k_3, k_3 + k_1\} \end{aligned}$$

(4) The time derivative of the attitude error vector e_R is given by

$$\begin{aligned} \dot{e}_R &= E(K, R_e) e_\Omega \\ \text{where} \quad E(K, R_e) &= \frac{1}{2}(\text{tr}(K R_e) I_{3\times 3} - R_e^T K) R_d \end{aligned}$$

The norm of $\dot{e}_R$ satisfies the following inequality and will be used in the stability analysis [54]

$$||\dot{e}_R|| \leq \frac{1}{\sqrt{2}} \text{tr}(K) ||e_\Omega||$$

To find the error in angular velocity, we need the concept of transport map [7]. The transport map allows us to compare velocities in different tangent spaces. Since $\dot{R} \in T_R SO(3)$ and $\dot{R}_d \in T_{R_d} SO(3)$, we cannot subtract them naively to obtain the error in angular velocity, which is the case in $T\mathbb{R}^3$. The error in angular velocity is calculated as:

$$\dot{R} - \tau_l(\dot{R}_d) = R(\hat{\Omega} - \hat{\Omega}_d) = R\hat{e}_\Omega$$

where τ_l represents transport map. For left error representation $\tau_l = R_e$. Hence left velocity error is given by :

$$e_\Omega = \Omega - \Omega_d$$

3.3.2 Nonlinear Disturbance Observer

One of the advantages of disturbance observer-based control (DOBC) over robust control methods is good disturbance rejection property without sacrificing the nominal performance. In case of no external disturbances, its estimates are zero, and hence the DOBC law reduces to baseline control law. In this scenario, excessive control energy is not wasted in rejecting the disturbances. Other advantages of disturbance observers are better transient performance and better dynamic response. Owing to these advantages, we have

chosen to utilize disturbance observers to estimate external disturbances. The nonlinear disturbance observer proposed here is motivated from [94] and is used to estimate the external disturbances. The structure of the observer is given by:

$$\dot{z}_\Omega = -l(\Omega)[I^{-1}(\lambda(\Omega) + z_\Omega) - I^{-1}(\Omega \times J\Omega) + I^{-1}\tau_b]$$
$$\bar{d}_\Omega = z_\Omega + \lambda(\Omega) \tag{3.5}$$
$$\dot{z}_x = -l(v)[\frac{1}{m}(\lambda(v) + z_x) - ge_3 + \frac{Rf_b}{m}]$$
$$\bar{d}_x = z_x + \lambda(v) \tag{3.6}$$

where, $\bar{d}_\Omega$ and $\bar{d}_x$ represent disturbance estimates in attitude and translational dynamics. z_i, $i \in \{x, \Omega\}$ represents the internal state of the observer. $\lambda(i)$ is a nonlinear function and $l(i)$ is designed as:

$$l(i) = \frac{\partial \lambda(i)}{\partial i}$$

where $i \in \{v, \Omega\}$. In this work, we have chosen the above parameters as:

$$\lambda(\Omega) = K_m\Omega \text{ therefore } l(\Omega) = K_m I_{3\times 3}$$

Similarly,

$$\lambda(v) = K_s v \text{ and therefore } l(v) = K_s I_{3\times 3}$$

where K_m and K_s are positive definite gain matrices and $I_{3\times 3}$ is identity matrix.
The dynamics of the disturbance estimation error $\Delta_x = d_x - \bar{d}_x$ and $\Delta_\Omega = d_\Omega - \bar{d}_\Omega$ is given by :

$$\dot{\Delta}_x = -\frac{l(v)}{m}\Delta_x + \dot{d}_x$$
$$\dot{\Delta}_\Omega = -l(\Omega)I^{-1}\Delta_\Omega + \dot{d}_\Omega$$

Lemma 3.3.1. *[95] If the disturbances are bounded, the estimation error of the disturbance observer is locally input to state stable(ISS) if the observer gain $l(v)$ and $l(\Omega)$ are chosen such that*

$$\dot{\Delta}_x + \frac{l(v)}{m}\Delta_x = 0 \text{ and } \dot{\Delta}_\Omega + l(\Omega)I^{-1}\Delta_\Omega = 0$$

are asymptotically stable.

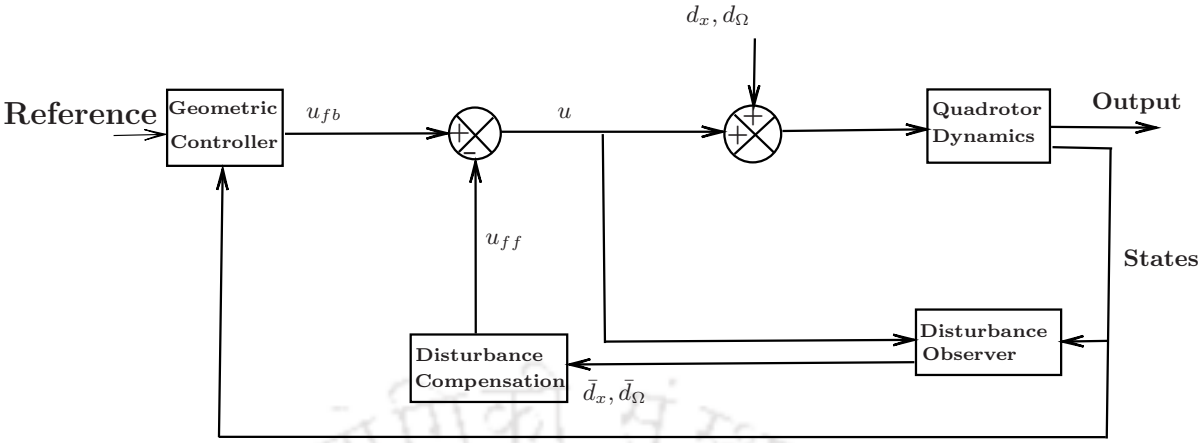

Figure 3.1: Controller with the disturbance observer

3.4 Controller Design

For a fully actuated rigid body, the control force and torque required to track any desired trajectory $(x_d(t), v_d(t), R_d(t), \Omega_d(t))$ while compensating for external disturbances, are given by [54]:

$$f_c^d = -K_x e_x - K_v e_v + m(\dot{v}_d + g e_3) - \bar{d}_x \tag{3.7}$$

$$\tau_c = -R_d^T e_R - K_\Omega e_\Omega + I\dot{\Omega}_d + \Omega \times I\Omega - \bar{d}_\Omega \tag{3.8}$$

where $K_x, K_v, K_\Omega \in \mathbb{R}^{3\times3}$ are positive definite gain matrices. The control torque (3.8) proposed in [7] has simpler expression as compared to the one based on right attitude error representation [46]. In our approach we propose to apply following control law and torque to the quadrotor :

$$f_b = ||f_c^d|| e_3 \quad \text{and} \quad \tau_b = \tau_c \tag{3.9}$$

The choice of control f_b always results in positive thrust to the quadrotor, whereas in [46] the total thrust becomes negative when the angle between the desired thrust and vertical body axis becomes greater than 90°. For a standard VTOL vehicle, it is required that $f_b^T e_3 > 0$. A conceptual diagram of the geometric controller with the nonlinear disturbance observer in the loop is shown in Fig.3.1. In the figure u_{ff} denotes feedforward compensation input while u_{fb} denotes feedback control input. u is given as sum of u_{ff} and u_{fb} i.e. $u = u_{ff} + u_{fb}$. $\bar{d}_\Omega$ and $\bar{d}_x$ depict disturbance estimates in attitude and translational dynamics respectively. d_Ω and d_x depict additive external disturbances present in attitude and translational dynamics respectively.

3.4.1 Finding Reference Attitude

For a desired heading direction $b_{1d}(t)$, we can calculate the desired attitude $R_d(t)$ [46] as :

$$R_d(t) = [b_{2d}(t) \times b_{3d}(t) \quad b_{2d}(t) \quad b_{3d}(t)]$$

where,

$$b_{3d}(t) = \frac{f_c^d}{||f_c^d||}, \quad b_{2d}(t) = \frac{b_{3d}(t) \times b_{1d}(t)}{||b_{3d}(t) \times b_{1d}(t)||}$$

f_c^d is defined in Eqn.(3.7). Thus, the attitude reference depends among others on the translational movement errors. It is assumed that $||f_c^d|| \neq 0$. It is also assumed that $b_{3d}(t)$ is not parallel to $b_{1d}(t)$.

3.4.2 Input to State Stability

The nonlinear system

$$\dot{x} = f(t, x, u) \tag{3.10}$$

is said to be input to state (ISS) [96, 97] stable if there exist a class $\mathcal{KL}$ function β and a class $\mathcal{K}$ function γ such that for any initial state $x(t_0)$ and any bounded input $u(t)$, the solution exists for all $t \geq t_0$ and satisfies

$$||x(t)|| \leq \beta(||x(t_0)||, t - t_0) + \gamma(sup_{t_0 \leq \tau \leq t}||u(\tau)||)$$

The above notion of input to state stability (ISS) is defined for the global case where the initial state and the input can be arbitrarily large. If the above inequality is satisfied in the region $||x|| < r$ and $||u|| < r_u$ for $||x(t_0)|| < k_1$ and $sup_{t \geq t_0}||u(t)|| < k_2$ where k_1 and k_2 are positive constants, then the system is said to be locally input to state stable (LISS) [98].

Theorem 3.4.1. *[96] Let $V : [0, \infty) \times R^n \to R$ be a continuously differentiable function such that*

$$\alpha_1(||x||) \leq V(t, x) \leq \alpha_2(||x||)$$
$$\frac{\partial V}{\partial t} + \frac{\partial V}{\partial x} f(t, x, u) \leq -W_3(x), \quad \forall \; ||x|| \geq \rho(||u||) > 0$$

$\forall(t,x,u) \in [0,\infty) \times R^n \times R^m$, *where* α_1, α_2 *are class* $\mathcal{K}_\infty$ *functions,* ρ *is a class* $\mathcal{K}$ *function, and* $W_3(x)$ *is a continuous positive definite function on* R^n. *Then the system 3.10 is input to state stable with* $\gamma = \alpha_1^{-1} \circ \alpha_2 \circ \rho$.

For local input to state stability (LISS) α_1 and α_2 can be class $\mathcal{K}$ functions and are not necessarily class $\mathcal{K}_\infty$ functions.

Following propositions are the contributions of this chapter.

Proposition 3.1. *The attitude dynamics* (3.2) *driven by control law* (3.8) *with the disturbance estimates given by* (3.5) *renders the closed loop attitude error dynamics locally input to state stable (ISS) with respect to derivative of the disturbance,* d_Ω *if the following conditions are satisfied :*
(i) $\Psi < \psi < p_1$,
(ii) $||\dot{d_\Omega}||$ *is bounded,*
(iii) The matrices A, L_1 *and* L_2 *defined in the proof below are positive definite for positive constant* c_1

Proof. Consider the following Lyapunov candidate for the rotational motion

$$V_R = \frac{1}{2} e_\Omega^T I e_\Omega + \Psi + c_1 e_\Omega^T e_R + \frac{1}{2} \Delta_\Omega^T \Delta_\Omega$$

where c_1 is a positive constant. Letting $z_R = [||e_R|| \;\; ||e_\Omega|| \;\; ||\Delta_\Omega||]^T$, we can write

$$\lambda_m(L_1)||z_R||^2 \leq V_R \leq \lambda_M(L_2)||z_R||^2 \tag{3.11}$$

where

$$L_1 = \begin{bmatrix} h_1 & -c_1 & 0 \\ -c_1 & \frac{1}{2}\lambda_m(I) & 0 \\ 0 & 0 & \frac{1}{2} \end{bmatrix} \quad L_2 = \begin{bmatrix} h_2 & c_1 & 0 \\ c_1 & \frac{1}{2}\lambda_M(I) & 0 \\ 0 & 0 & \frac{1}{2} \end{bmatrix}$$

$\lambda_m(\cdot)$ represents minimum eigenvalue of its argument and
$\lambda_M(\cdot)$ represents maximum eigenvalue of its argument
We can observe that

$$I\dot{e}_\Omega = I(\dot{\Omega} - \dot{\Omega}_d) = -\Omega \times I\Omega + \tau_b + d_\Omega - I\dot{\Omega}_d = -R_d^T e_R - K_\Omega e_\Omega + \Delta_\Omega$$

Then,

$$\begin{aligned}\dot{V}_R &= e_\Omega^T I\dot{e}_\Omega + \frac{1}{2}\text{tr}(-K\dot{R}R_d^T - KR\dot{R}_d^T) + c_1\dot{e}_\Omega^T e_R + c_1 e_\Omega^T\dot{e}_R + \Delta_\Omega^T\dot{\Delta}_\Omega \\ &= e_\Omega^T(-R_d^T e_R - K_\Omega e_\Omega + \Delta_\Omega) - \frac{1}{2}\text{tr}(KR\hat{e}_\Omega R_d^T) + c_1 e_R^T I^{-1}(-R_d^T e_R - K_\Omega e_\Omega + \Delta_\Omega) \\ &+ c_1 e_\Omega^T E e_\Omega + \Delta_\Omega^T(-l(\Omega)I^{-1}\Delta_\Omega + \dot{d}_\Omega)\end{aligned}$$

From the equality $A\hat{x}A^T = \widehat{Ax}$, we can write :

$$\begin{aligned}\dot{V}_R &= e_\Omega^T(-R_d^T e_R - K_\Omega e_\Omega + \Delta_\Omega) - \frac{1}{2}\text{tr}(KRR_d^T\widehat{R_d e_\Omega}) + c_1 e_R^T I^{-1}(-R_d^T e_R - K_\Omega e_\Omega + \Delta_\Omega) \\ &+ c_1 e_\Omega^T E e_\Omega + \Delta_\Omega^T(-l(\Omega)I^{-1}\Delta_\Omega + \dot{d}_\Omega)\end{aligned}$$

From the equality $-\frac{1}{2}\text{tr}(\hat{x}\hat{y}) = x\cdot y$ and further simplification, we can write :

$$\begin{aligned}\dot{V}_R &= -e_\Omega^T K_\Omega e_\Omega - c_1 e_R^T I^{-1}R_d^T e_R - c_1 e_R^T I^{-1}K_\Omega e_\Omega + c_1 e_R^T I^{-1}\Delta_\Omega + c_1 Ee\Omega^T e_\Omega \\ &- \Delta_\Omega^T l(\Omega)I^{-1}\Delta_\Omega + e_\Omega^T\Delta_\Omega + \Delta_\Omega^T\dot{d}_\Omega \\ &\leq -\lambda_m(K_\Omega)||e_\Omega||^2 + ||e_\Omega||||\Delta_\Omega|| - \frac{c_1}{\lambda_M(I)}||e_R||^2 + \frac{c_1}{\lambda_m(I)}\lambda_M(K_\Omega)||e_R||||e_\Omega|| \\ &+ \frac{c_1}{\lambda_m(I)}||e_R||||\Delta_\Omega|| + \frac{c_1}{\sqrt{2}}\text{tr}(K)||e_\Omega||^2 - \lambda_m(K_m I^{-1})||\Delta_\Omega||^2 + ||\Delta_\Omega||||\dot{d}_\Omega|| \\ &\leq -\lambda_m(K_\Omega)||e_\Omega||^2 + ||e_\Omega||||\Delta_\Omega|| - \frac{c_1}{\lambda_M(I)}||e_R||^2 + \frac{c_1}{\lambda_m(I)}\lambda_M(K_\Omega)||e_R||||e_\Omega|| \\ &+ \frac{c_1}{\lambda_m(I)}||e_R||||\Delta_\Omega|| + \frac{c_1}{\sqrt{2}}\text{tr}(K)||e_\Omega||^2 - \lambda_m(K_m I^{-1})||\Delta_\Omega||^2 + \frac{||\Delta_\Omega||^2}{2} + \frac{||\dot{d}_\Omega||^2}{2}\end{aligned}$$

If $z_R = [||e_R||\ \ ||e_\Omega||\ \ ||\Delta_\Omega||]^T$, then we can write

$$\dot{V}_R \leq -z_R^T A z_R + \frac{||\dot{d}_\Omega||^2}{2} \leq -\lambda_m(A)||z_R||^2 + \frac{||\dot{d}_\Omega||^2}{2} \tag{3.12}$$

where matrix A is given by:

$$A = \begin{bmatrix} \frac{c_1}{\lambda_M(I)} & -\frac{c_1}{2\lambda_m(I)}\lambda_M(K_\Omega) & -\frac{c_1}{2\lambda_m(I)} \\ -\frac{c_1}{2\lambda_m(I)}\lambda_M(K_\Omega) & \lambda_m(K_\Omega) - \frac{c_1}{\sqrt{2}}\text{tr}(K) & -\frac{1}{2} \\ -\frac{c_1}{2\lambda_m(I)} & -\frac{1}{2} & \lambda_m(K_m I^{-1}) - \frac{1}{2} \end{bmatrix}$$

Eqn.(3.12) can be written as :

$$\dot{V}_R \leq -\lambda_m(A)(1-\theta)||z_R||^2 - \lambda_m(A)\theta||z_R||^2 + \frac{||\dot{d}_\Omega||^2}{2}$$

for $0 < \theta < 1$.

$$\dot{V}_R \leq -\lambda_m(A)(1-\theta)||z_R||^2 \ \ \forall \ \ ||z_R|| \geq \frac{1}{\sqrt{2\theta\lambda_m(A)}}||\dot{d}_\Omega|| \tag{3.13}$$

From Eqns.(3.11) and (3.13), we have

$$\alpha_1(r) = \lambda_m(L_1)r^2, \ \alpha_2(r) = \lambda_M(L_2)r^2 \ and \ \rho(r) = \frac{1}{\sqrt{2\theta\lambda_m(A)}}r$$

Therefore the attitude error dynamics is locally ISS w.r.t. $\dot{d}_\Omega$ with

$$\gamma(r) = \sqrt{\frac{\lambda_M(L_2)}{2\theta\lambda_m(A)\lambda_m(L_1)}}\ r$$

□

Proposition 3.2. *The complete dynamics* (3.1), (3.2) *driven by control law* (3.7), (3.8) *with the disturbance estimates given by* (3.5), (3.6) *renders the complete closed loop error dynamics locally input to state stable with respect to derivative of disturbances in rotational and translational dynamics if the conditions in Proposition 1 as well as the following conditions are satisfied.*
(i) $||\dot{d}_x||$ *is bounded,*
(ii) $||\dot{d}||$ *is bounded,*
(iii) The matrices B, P_1 *and* P_2 *defined in the proof below are positive definite for positive constant* c_2
$d = [d_\Omega, d_x]$ *represents total disturbance vector.*

Proof. Consider the following Lyapunov candidate for the translational motion

$$V_x = \frac{1}{2}me_v^Te_v + \frac{1}{2}e_x^TK_xe_x + c_2e_x^Te_v + \frac{1}{2}\Delta_x^T\Delta_x$$

Defining $z_x = [||e_x|| \ \ ||e_v|| \ \ |||\Delta_x|||]^T$, we have

$$\lambda_m(P_1)||z_x||^2 \leq V_x \leq \lambda_M(P_2)||z_x||^2$$

where

$$P_1 = \begin{bmatrix} \frac{1}{2}\lambda_m(K_x) & -c_2 & 0 \\ -c_2 & \frac{1}{2}m & 0 \\ 0 & 0 & \frac{1}{2} \end{bmatrix} \quad P_2 = \begin{bmatrix} \frac{1}{2}\lambda_M(K_x) & p_2 & 0 \\ p_2 & \frac{1}{2}m & 0 \\ 0 & 0 & \frac{1}{2} \end{bmatrix}$$

We can observe that

$$m\dot{e}_v = m(\dot{v} - \dot{v}_d) = -mge_3 + Rf_b + d_x - m\dot{v}_d = -mge_3 + Rf_b + f_c^d - f_c^d + d_x - m\dot{v}_d$$
$$= -K_x e_x - K_v e_v + \Delta_x + Rf_b - f_c^d = -K_x e_x - K_v e_v + \Delta_x + \Delta f$$

where $\Delta f = Rf_b - f_c^d$. Then,

$$\dot{V}_x = me_v^T\dot{e}_v + e_x^T K_x e_v + c_2\dot{e}_x^T e_v + c_2 e_x^T\dot{e}_v + \Delta_x^T\dot{\Delta}_x$$
$$= e_v^T(-K_x e_x - K_v e_v + \Delta_x + \Delta f) + e_x^T K_x e_v + c_2 e_v^T e_v$$
$$+ \frac{c_2}{m}e_x^T(-K_x e_x - K_v e_v + \Delta_x + \Delta f) + \Delta_x^T(-\frac{l(v)}{m}\Delta_x + \dot{d}_x)$$

Further simplification results in

$$\dot{V}_x = -e_v^T K_v e_v + e_v^T\Delta_x + e_v^T\Delta f + c_2 e_v^T e_v - \frac{c_2}{m}e_x^T K_x e_x - \frac{c_2}{m}e_x^T K_v e_v + \frac{c_2}{m}e_x^T\Delta_x$$
$$+ \frac{c_2}{m}e_x^T\Delta f - \Delta_x^T K_s m^{-1}\Delta_x + \Delta_x^T\dot{d}_x$$
$$\leq -(\lambda_m(K_v) - c_2)||e_v||^2 - \frac{c_2}{m}\lambda_m(K_x)||e_x||^2 - \lambda_m(\frac{K_s}{m})||\Delta_x||^2 + ||e_v||||\Delta_x||$$
$$+ ||e_v||||\Delta_f|| + \frac{c_2}{m}\lambda_M(K_v)||e_x||||e_v|| + \frac{c_2}{m}||e_x||||\Delta_x|| + \frac{c_2}{m}||e_x||||\Delta_f|| + \frac{||\Delta_x||^2}{2}$$
$$+ \frac{||\dot{d}_x||^2}{2} \tag{3.14}$$

where, $\Delta f = Rf_b - f_c^d$, the norm of which can be written as :

$$||\Delta f|| = ||Rf_b - f_c^d|| = \big|\big|R||f_c^d||e_3 - ||f_c^d||R_d e_3\big|\big|$$
$$\leq \big|\big|Re_3 - R_d e_3\big|\big|||f_c^d||$$
$$= \sqrt{(Re_3 - R_d e_3)^T(Re_3 - R_d e_3)}||f_c^d||$$
$$= \sqrt{2 - 2e_3^T R_d^T Re_3}||f_c^d||$$

$e_3^T R_d^T Re_3$ represents cosine of angle between b_3 and b_{3d} where b_3 represents current thrust direction. Since $1 - \Psi$ represents the cosine of the eigen-axis rotation angle between R_d and R [46], we have:

$$1 > e_3^T R_d^T Re_3 > 1 - \Psi > 0 \Rightarrow 0 < 1 - e_3^T R_d^T Re_3 < \Psi$$

Since

$$h_1||e_R||^2 \leq \Psi \leq h_2||e_R||^2, \quad \text{we have}$$

$$||\Delta f|| < \sqrt{2h_2}||e_R||f_M \tag{3.15}$$

where f_M represents maximum thrust delivered by the propellers i.e. $||f_c^d|| \leq f_M$. Therefore,

$$\begin{aligned}\dot{V}_x \leq & -(\lambda_m(K_v) - c_2)||e_v||^2 - \frac{c_2}{m}\lambda_m(K_x)||e_x||^2 - \lambda_m(\frac{K_s}{m})||\Delta_x||^2 + ||e_v||||\Delta_x|| \\ & + \sqrt{2h_2}||e_v||||e_R||f_M + \frac{c_2}{m}\lambda_M(K_v)||e_x||||e_v|| + \frac{c_2}{m}||e_x||||\Delta_x|| \\ & + \sqrt{2h_2}\frac{c_2}{m}||e_x||||e_R||f_M + \frac{||\Delta_x||^2}{2} + \frac{||\dot{d}_x||^2}{2}\end{aligned} \tag{3.16}$$

The complete error dynamics can be proved to be locally input to state stable by taking $V = V_x + V_R$ as the Lyapunov function candidate for the complete dynamics. Therefore, letting $z = [||e_R||\ \ ||e_\Omega||\ \ ||\Delta_\Omega||\ \ ||e_x||\ \ ||e_v||\ \ ||\Delta_x||]^T$, we can write

$$\lambda_m(T_1)||z||^2 \leq V \leq \lambda_M(T_2)||z||^2 \tag{3.17}$$

where

$$T_1 = \begin{bmatrix} L_1 & 0 \\ 0 & P_1 \end{bmatrix} \quad T_2 = \begin{bmatrix} L_2 & 0 \\ 0 & P_2 \end{bmatrix}$$

Therefore, T_1 will be positive definite if both L_1 and P_1 are positive definite. Similarly, T_2 will be positive definite if both L_2 and P_2 are positive definite.
We can write

$$\begin{aligned}\dot{V} = & \dot{V}_x + \dot{V}_R \\ & \leq -(\lambda_m(K_v) - c_2)||e_v||^2 - \frac{c_2}{m}\lambda_m(K_x)||e_x||^2 - \lambda_m(\frac{K_s}{m})||\Delta_x||^2 + ||e_v||||\Delta_x|| \\ & + \sqrt{2h_2}||e_v||||e_R||f_M + \frac{c_2}{m}\lambda_M(K_v)||e_x||||e_v|| + \frac{c_2}{m}||e_x||||\Delta_x|| \\ & + \sqrt{2h_2}\frac{c_2}{m}||e_x||||e_R||f_M + \frac{||\Delta_x||^2}{2} + \frac{||\dot{d}_x||^2}{2} - \lambda_m(K_\Omega)||e_\Omega||^2 + ||e_\Omega||||\Delta_\Omega|| \\ & - \frac{c_1}{\lambda_M(I)}||e_R||^2 + \frac{c_1}{\lambda_m(I)}\lambda_M(K_\Omega)||e_R||||e_\Omega|| + \frac{c_1}{\lambda_m(I)}||e_R||||\Delta_\Omega|| + \frac{c_1}{\sqrt{2}}\mathrm{tr}(K)||e_\Omega||^2 \\ & - \lambda_m(K_m I^{-1})||\Delta_\Omega||^2 + \frac{||\Delta_\Omega||^2}{2} + \frac{||\dot{d}_\Omega||^2}{2}\end{aligned} \tag{3.18}$$

If $z = [||e_R||\ \ ||e_\Omega||\ \ ||\Delta_\Omega||\ \ ||e_x||\ \ ||e_v||\ \ ||\Delta_x||]^T$, then we can write (3.18) as:

$$\dot{V} \leq -z^T B z + \frac{||\dot{d}_x||^2}{2} + \frac{||\dot{d}_\Omega||^2}{2} \leq -\lambda_m(B)||z||^2 + \frac{||\dot{d}||^2}{2} \tag{3.19}$$

where

$$B = \begin{bmatrix} A & B_{12} \\ B_{12}^T & B_{22} \end{bmatrix}$$

$$B_{12} = \begin{bmatrix} -\sqrt{\frac{h_2}{2}}\frac{c_2}{m} f_M & -\sqrt{\frac{h_2}{2}} f_M & 0 \\ 0 & 0 & 0 \\ 0 & 0 & 0 \end{bmatrix}$$

$$B_{22} = \begin{bmatrix} \frac{c_2}{m}\lambda_m(K_x) & -\frac{c_2}{2m}\lambda_M(K_v) & -\frac{c_2}{2m} \\ -\frac{c_2}{2m}\lambda_M(K_v) & \lambda_m(K_v) - c_2 & -\frac{1}{2} \\ -\frac{c_2}{2m} & -\frac{1}{2} & \lambda_m(\frac{K_s}{m}) \end{bmatrix}$$

Here $d = [d_\Omega, d_x]^T$ is the total disturbance vector and hence $||\dot{d}||^2 = ||\dot{d}_x||^2 + ||\dot{d}_\Omega||^2$. Eqn. (3.19) can be written as:

$$\begin{aligned} \dot{V} &\leq -\lambda_m(B)(1-\theta_1)||z||^2 - \lambda_m(B)\theta_1||z||^2 + \frac{||\dot{d}||^2}{2} \\ &\leq -\lambda_m(B)(1-\theta_1)||z||^2 \quad \forall \quad ||z|| \geq \frac{1}{\sqrt{2\theta_1\lambda_m(B)}}||\dot{d}|| \end{aligned} \tag{3.20}$$

for $0 < \theta_1 < 1$. From Eqns.(3.17) and (3.20), the complete error dynamics will be locally input to state stable (ISS) with respect to the derivate of disturbances, $\dot{d}$ with the following parameters

$$\alpha_1(r) = \lambda_m(T_1)r^2, \ \alpha_2(r) = \lambda_M(T_2)r^2, \ \rho(r) = \frac{1}{\sqrt{2\theta_1\lambda_m(B)}}r$$

and

$$\gamma(r) = \sqrt{\frac{\lambda_M(T_2)}{2\theta_1\lambda_m(B)\lambda_m(T_1)}}\ r$$

□

3.5 Simulation Results

A numerical simulation [MATLAB/SIMULINK] of the geometric controller developed in the previous section is performed with the designed nonlinear disturbance observer in the loop. Various parameters used in the simulations are given in Table 3.1. Positive definite diagonal gain matrices have been chosen to quickly stabilize the attitude dynamics. Yaw dynamics will be stabilized first due to higher inertia value which will result in higher control effort in feedback control law. This results

Table 3.1: Parameters used in simulation

Parameter	Values	Units	Parameter	Values	Units
g	9.81	m/s^2	I_{xx}	0.082	kg m^2
m	4.34	kg	I_{yy}	0.0845	kg m^2
K_x	$4I_3$	-	I_{zz}	0.1377	kg m^2
K_v	$10I_3$	-	K_Ω	$5I_3$	-
K_m	$5I_3$	-	K_s	$5I_3$	-
K	$10I_3$	-			

in better stability of the vehicle. Then pitch dynamics will be stabilized because of greater control effort as compared to roll dynamics. The reference trajectory is given by $x_d(t) = [2\cos\left[\frac{\pi t}{10}\right]; 2\sin\left[\frac{\pi t}{10}\right]; \frac{t}{2}]$ and $b_{1d}(t) = \frac{\dot{x}_d(t)}{||\dot{x}_d(t)||}$. The initial conditions for simulation are assumed to be $[x(0); y(0); z(0))] = [0; 0; 0]$ and $R(0) = I_3$.

3.5.1 Scenario I : Finite Slope and bounded Disturbance

The external disturbances generated in the simulation environment are given by $d_x(t) = d_\Omega(t) = [0.13\tan^{-1}\left(\frac{t}{2}\right); 0.2\tan^{-1}\left(\frac{t}{2}\right); 0.26\tan^{-1}\left(\frac{t}{2}\right)]$. The position tracking performance and the disturbance estimates in position and attitude dynamics are shown in Figs 3.2-3.3. It is observed from Fig. 3.2 that better position tracking is obtained with the nonlinear disturbance observer than without the disturbance observer. The RMS error in position tracking without the disturbance observer is found to be $[0.4069; 0.2450; 0.1039]m$ while RMS error in position tracking with the disturbance observer is found to be $[0.3363; 0.0771; 0.0253]m$, which is a substantial improvement. The transient performance and the dynamic response of the NDOBC are also better compared to the one without the disturbance observer. A good estimate of the disturbances present in position and attitude dynamics is also obtained by the disturbance observer, as illustrated in Figs. 3.3. All the disturbance estimates were initialized with zero initial conditions. The disturbance estimates quickly converge to the actual ones within few seconds with some bounded errors. The configuration error function, Ψ as seen from Fig.3.4*b*, decreases very fast and settles around zero with some small bounded positive error. The control force f_b is also smooth, bounded, and settles to a final value of 42.3 N within 5 seconds.

3.5.2 Scenario II : Constant Disturbance

The external disturbances generated in the simulation environment are assumed to be constants and are given by $d_x(t) = d_\Omega(t) = [0.13; 0.2; 0.26]$. This type of scenario might occur when there is a change in dynamic parameters like mass, the moment of inertia, or the center of gravity. It is observed from Fig. 3.5 that better position tracking is

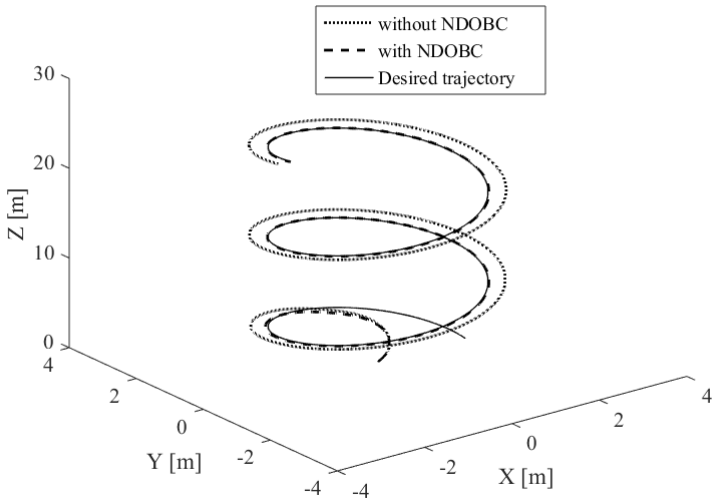

Figure 3.2: Trajectory tracking

Table 3.2: Comparison Table

RMS Error	with NDOBC	without NDOBC
Scenario I	$[0.3363; 0.0771; 0.0253]m$	$[0.4069; 0.2450; 0.1039]m$
Scenario II	$[0.3358; 0.0749; 0.0245]m$	$[0.3634; 0.1809; 0.0716]m$

obtained with the nonlinear disturbance observer than without the disturbance observer. The RMS error in position tracking without the disturbance observer is found to be $[0.3634; 0.1809; 0.0716]m$ while RMS error in position tracking with the disturbance observer is found to be $[0.3358; 0.0749; 0.0245]m$. The estimates of the disturbances present in position and attitude dynamics converge to the actual disturbances within few seconds, as illustrated in Fig. 3.6. One can also observe that the convergence rate is also fast, and the disturbance estimates converge to the actual disturbances in less than 5 secs.
Table 3.2 shows the RMS error in position tracking with and without the disturbance observer in the loop for both scenarios.

Table 3.3: Parameters used in experiment

Parameter	Values	Units	Parameter	Values	Units
K	I_3	-	I_{xx}	0.006	kg m^2
K_Ω	$\{0.15, 0.15, 0.2\}$	-	I_{yy}	0.008	kg m^2
K_x	$\{0.95, 0.95, 1.0\}$	-	I_{zz}	0.02	kg m^2
K_v	$\{0.09, 0.09, 0.2\}$	-	m	1	kg
K_m	$\{0.2, 0.2, 0.05\}$	-	K_s	$0.02I_3$	-

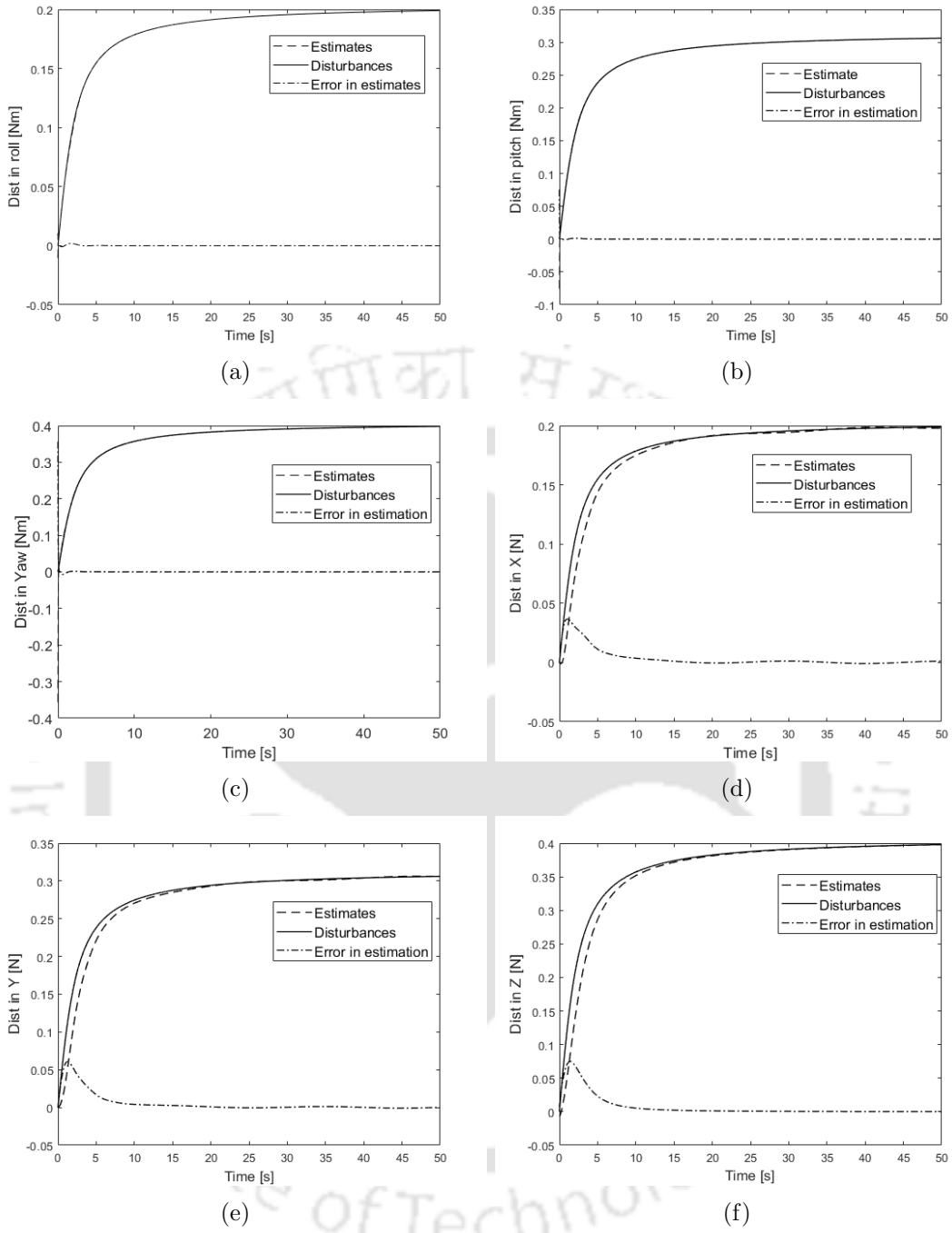

Figure 3.3: Disturbance estimates in (a) Roll [Nm]; (b) Pitch [Nm]; (c) Yaw [Nm]; (d) X [N]; (e) Y [N]; (f) Z [N].

3.6 Experimental Results

The above designed geometric controller with the nonlinear disturbance observer was implemented on an open-source Pixhawk[99] board with the parameters listed in Table 3.3. The quadrotor was made from a DJI F450 frame with a frame length of 45cm from one diagonal end to another. The quadrotor was given a circular trajectory to follow

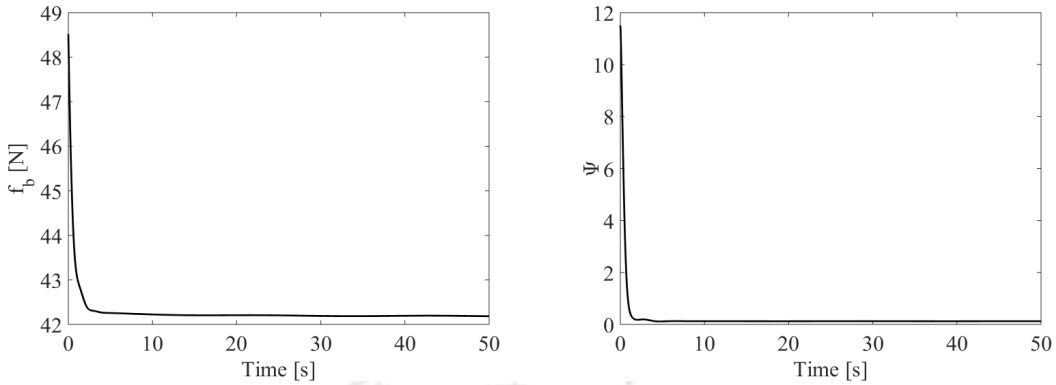

(a) (b)

Figure 3.4: (a) f_b [N]; (b) Ψ.

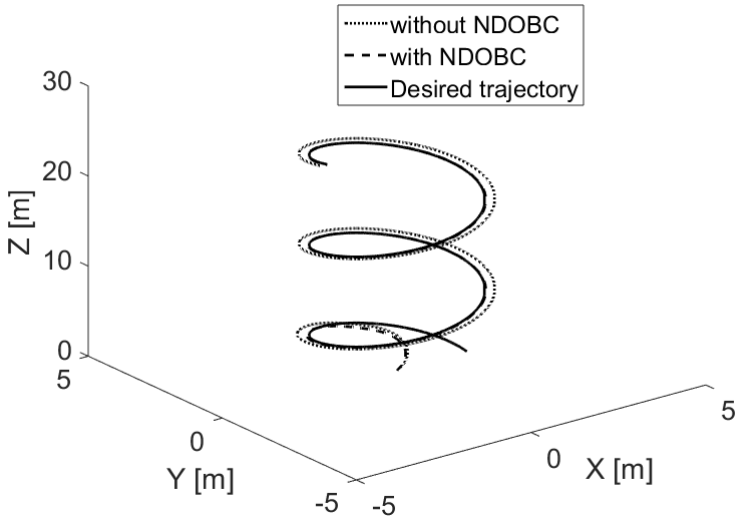

Figure 3.5: Trajectory tracking

with a radius of $2m$ at an altitude of $5m$ as described below :

$$x_d(t) = 0 \quad y_d(t) = 0 \quad z_d(t) = 0.5t \text{ for } 0 \leq t \leq 10s;$$
$$x_d(t) = 2\cos\left[2\pi\frac{(t-10)}{20}\right] \quad y_d(t) = 2\sin\left[2\pi\frac{(t-10)}{20}\right]$$
$$z_d(t) = 5m \text{ for } 10s \leq t \leq 90s;$$
$$x_d(t) = 0 \quad y_d(t) = 0 \quad z_d(t) = 5m \text{ for } 90s \leq t \leq 100s;$$
$$x_d(t) = 0 \; y_d(t) = 0 \; z_d(t) = -0.5(t-110) \text{ for } 100s \leq t \leq 110s$$

The experiment was done on a slightly windy day. The initial condition was taken to be $x(0) = 0; y(0) = 0; z(0) = 0$ and $R(0) = I_3$. The various experimental results are shown

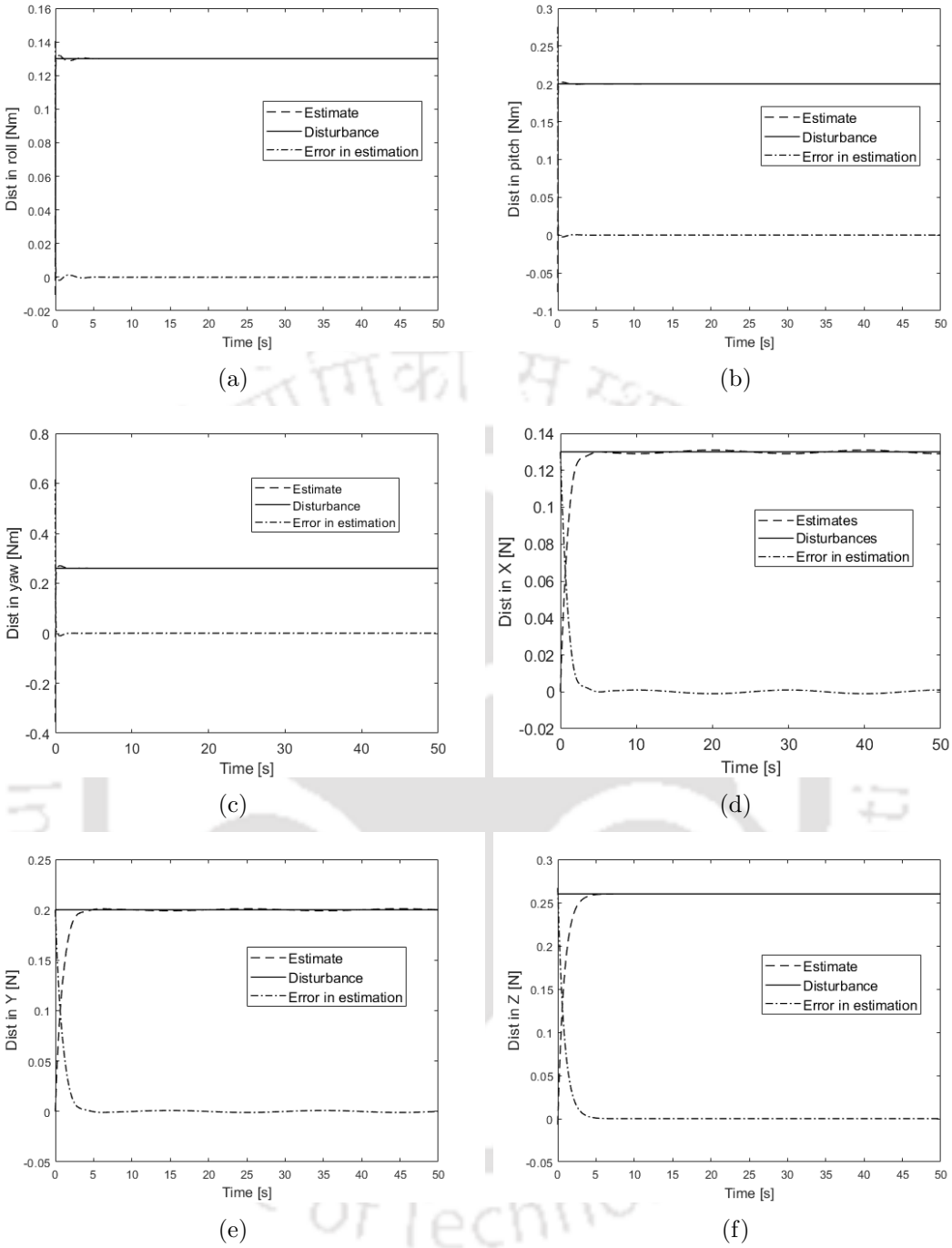

Figure 3.6: Disturbance estimates in (a) Roll [Nm]; (b) Pitch [Nm]; (c) Yaw [Nm]; (d) X [N]; (e) Y [N]; (f) Z [N].

in Figs. 3.7-3.10. Decent tracking performance is observed from Figs. 3.7-3.8 while the tracking errors can be attributed to lack of better localization methods. Here GPS was used for localization of the quadrotor due to the unavailability of motion capture systems. The various control torques and the throttle input are shown in Fig. 3.9. It is observed that the control inputs are bounded and finite. The control torques vary

around zero, while the throttle input varies around 0.425. Nominal values of dynamic parameters were used in designing the disturbance observers. The disturbance estimates shown in Fig. 3.10 are due to the deviation of parameters from their nominal values as well as disturbances due to wind. It can be observed from the experimental results that the disturbance estimates in yaw, as well as z-direction, become almost constant after some time if the measurement noises are neglected. Small disturbances are also logged in other directions, which can be considered almost constant if the measurement noises are neglected. The periodic nature of disturbance estimates in the X and Y direction might represent unmodelled dynamics.

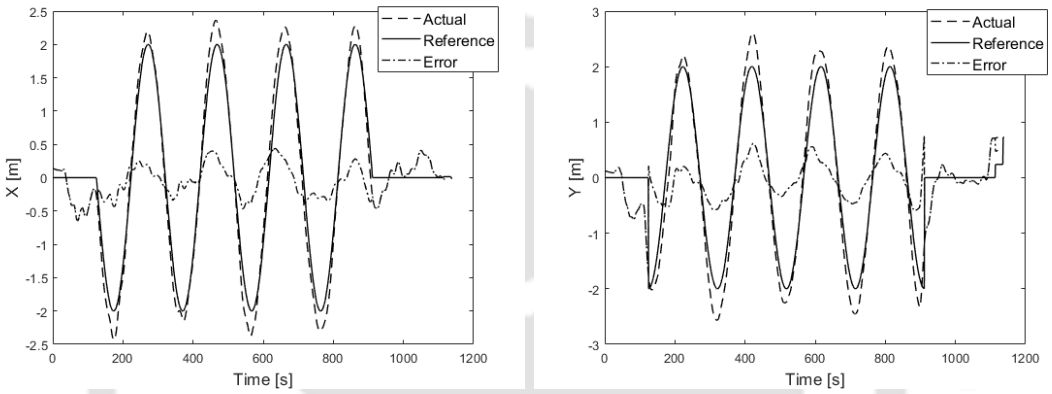

(a) (b)

Figure 3.7: Position Tracking in (a) X [m]; (b) Y [m].

3.7 Conclusion

A nonlinear disturbance observer-based controller was designed for a quadrotor. The proposed disturbance observer-based controller's main advantage is that the bound

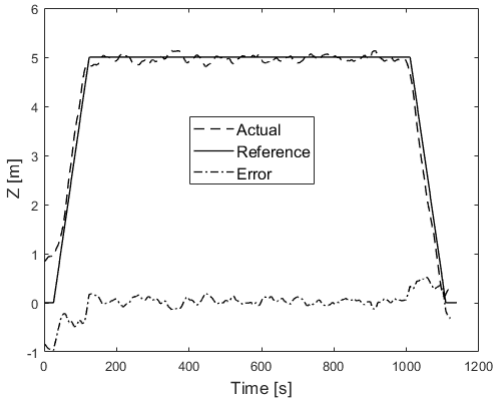

Figure 3.8: Position Tracking in Z [m]

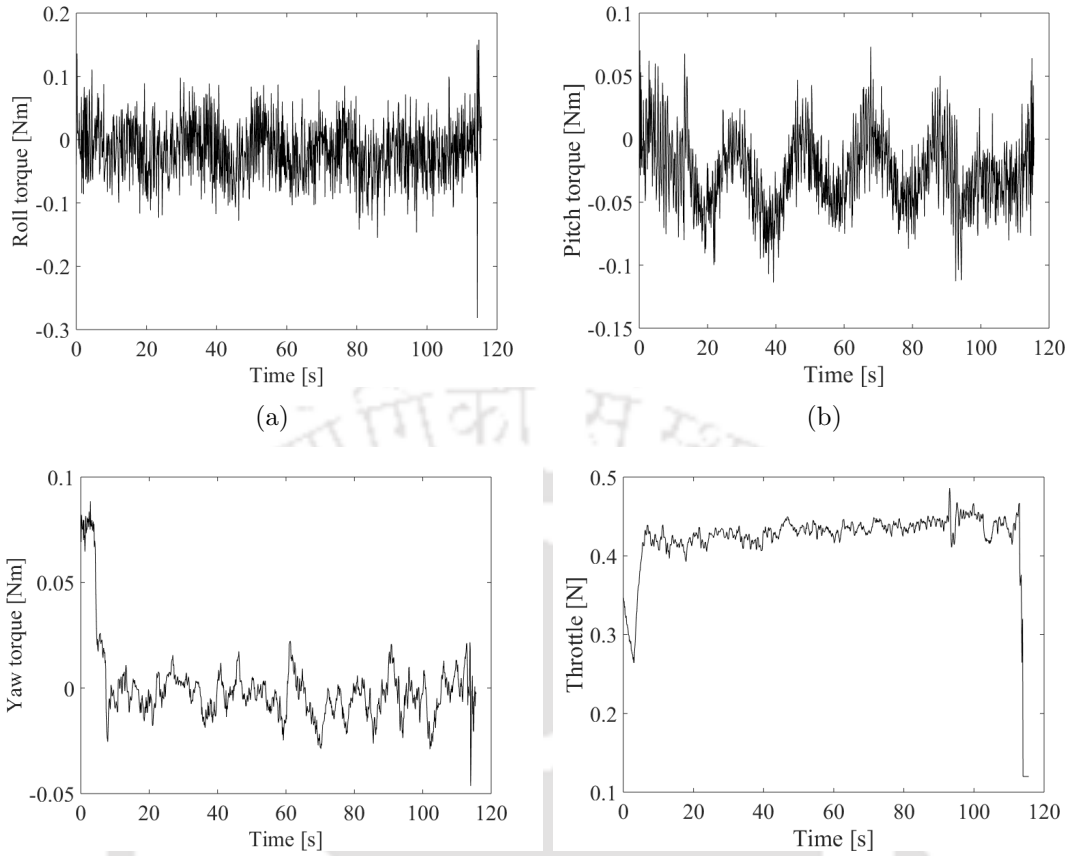

Figure 3.9: (a) Roll torque [Nm]; (b) Pitch torque [Nm];(c) Yaw torque [Nm];(d) Throttle [N].

on the disturbance is not assumed to be known. The controller is also shown to have a simpler structure. The theoretical proof shows that the proposed controller is locally input to state stable with respect to the derivative of the disturbances if the disturbance, as well as its derivatives, are bounded, and hence the tracking errors are also bounded. The simulation results and the experimental results show the proposed controller's effectiveness in the presence of disturbances and modeling inaccuracies.

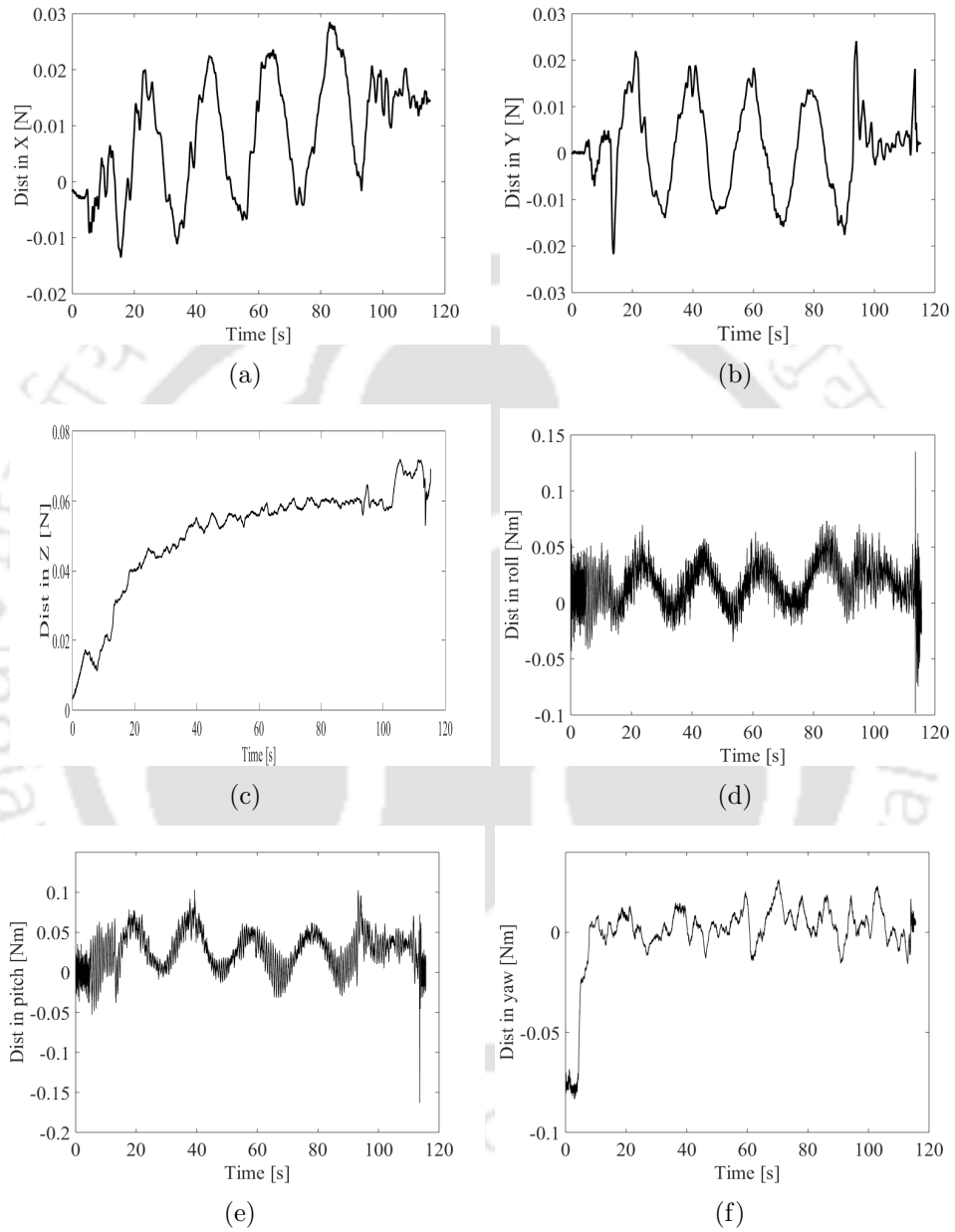

Figure 3.10: Disturbance estimates in (a) X [N]; (b) Y [N];(c) Z [N]; (d) Roll [Nm];(e) Pitch [Nm]; (f) Yaw [Nm].

Chapter 4

Geometric Adaptive Control of a Quadrotor with Location of Center of Gravity Different from Geometric Center

In the previous chapter, a nonlinear disturbance observer-based geometric control of a quadrotor was presented. It was assumed that the origin of the body-fixed frame and the center of gravity was coincident. This shortcoming of the previous chapter will be removed in this chapter. Geometric adaptive control of quadrotors has been presented in this chapter when the center of gravity of the quadrotor is different from its geometric center. The controller's unique feature is the use of the left tracking error function to simplify controller design. The inertia matrix, mass as well as center of gravity are assumed to be unknown, and coordinate invariant adaptive laws have been derived for the estimate of these mentioned parameters. The coordinate invariant approach is another unique feature of the proposed method as opposed to the literature. Rigorous mathematical proofs have been prescribed to show the complete closed-loop dynamics' stability under the proposed adaptive laws. The controller has been derived under the assumption that the rotational dynamics are faster than the translational dynamics.

4.1 Introduction

The offset between the center of gravity and geometric center was explicitly compensated in [100, 101, 102] wherein the 6-DOF rigid body dynamic model was considered while designing the adaptive controller. This offset may be compensated through integral actions, but if the nonlinear dynamic model is not properly considered, additional dis-

turbances may result. In [100], it was shown through simulations that an input-output feedback linearization-based controller was insufficient in the presence of dynamic changes in the center of gravity, and so the authors developed an adaptive control algorithm. In [101, 102], authors considered a transformation between frames of reference placed at the center of mass and geometric center and developed separate adaptive algorithms for altitude, attitude, and horizontal position control.

The contributions of this chapter are mentioned below. Firstly, the chapter presents a nonlinear geometric controller with a nonlinear adaptive controller for quadrotors using rotation matrices for attitude dynamics. The second novelty of this chapter is the utilization of left tracking errors while developing the tracking controller. The third contribution of this chapter is that adaptive controllers are used to estimate the center of gravity, mass, and inertia matrix in a coordinate invariant approach. The compensation in the system dynamics due to the offset in the center of gravity and geometric center in a coordinate invariant approach is one of this chapter's main contributions. The current literature [100, 101, 102] mainly utilizes Euler angles for system dynamics compensation due to the offset in the center of gravity and geometric center, while this chapter utilizes rotation matrices for the compensation.

Section 4.2 of the chapter explains the dynamic model used in developing the controller. Section 4.3 explains the development of the geometric controller while compensating for the offset in the center of gravity along with the proofs. Numerical simulation results have been presented in Section 4.4.

4.2 Dynamic Model

The mathematical model of a rigid body with its center of gravity shifted from the geometric center as shown in Fig.4.1 is derived from [103] and is presented below:

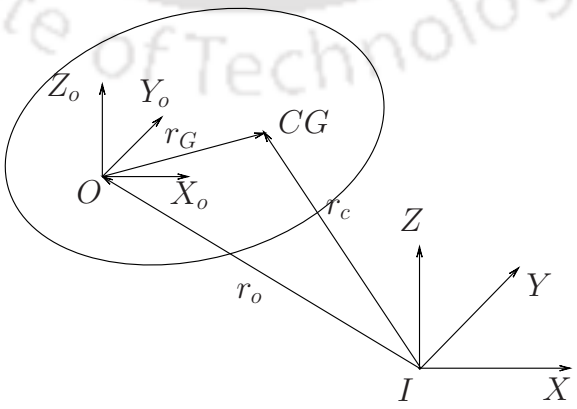

Figure 4.1: Rigid Body Model with offset between CG and body-fixed frame

Rotational motion:

$$\dot{R} = R\Omega^{\dagger}$$
$$I_o\bar{\Omega} + \Omega \times I_o\Omega + mr_G \times \bar{v}_o + mr_G \times (\Omega \times v_o) = \tau - mg(r_G \times R^T e_3) \tag{4.1}$$

Translational motion:

$$\dot{x}_o = v_o$$
$$\dot{v}_o = -ge_3 + \frac{Rf_b}{m} \tag{4.2}$$

In the above representation, the translational dynamics evolve in the inertial frame while the rotational dynamics evolve in the body-fixed frame. This representation of motion helps us in developing a simplified control law. The following nomenclature has been used in defining the mathematical model (Eqn.(4.1)-Eqn.(4.2)):

$\{O_B,X_B,Y_B,Z_B\}$ or $\{O,X_o,Y_o,Z_o\}$: Body reference frame with origin O_B or O respectively.
$\{O_I,X_I,Y_I,Z_I\}$ or $\{I,X,Y,Z\}$: Inertial reference frame with origin O_I or I respectively.
T_i : thrust from rotor i.
$R \in SO(3)$: Rotation matrix from body reference frame to inertial reference frame.
Ω : angular velocity of rigid body w.r.t inertial frame.
$(\cdot)^{\dagger}$: map from $\mathbb{R}^3$ to $\mathfrak{so}(3)$, space of skew symmetric matrices i.e. if $\Omega = [b_1 \;\; b_2 \;\; b_3]^T$, then

$$\Omega^{\dagger} = \begin{bmatrix} 0 & -b_3 & b_2 \\ b_3 & 0 & -b_1 \\ -b_2 & b_1 & 0 \end{bmatrix}$$

I_o : Moment of Inertia w.r.t. body frame origin O or O_B.
m : mass of the rigid body.
r_G : location of center of gravity w.r.t. O or O_B.
v_o : velocity of origin O or O_B of the rigid body w.r.t. I or O_I respectively.
τ : external torque input in the body frame.
g : acceleration due to gravity $= 9.81m/s^2$.
e_3 : $[0,0,1]^T$.
x_o or r_o : position of O_B or O w.r.t. O_I or I.
r_c : position of CG w.r.t. O_I or I.
f_b : thrust input in the body frame$=[0,0,\sum_{i=0}^{4} T_i]^T$

$\bar{c}$: represents time derivative in body frame.

$\dot{c}$: represents time derivative in inertial frame.

The time derivative in inertial frame and body frame is related by following relationship : $\dot{c} = \bar{c} + \Omega \times c$ and we know $\bar{\Omega} = \dot{\Omega}$. Therefore, rotational equation of motion can also be written as :

$$\begin{aligned} \dot{R} &= R\Omega^{\dagger} \\ I_o\dot{\Omega} + \Omega \times I_o\Omega + m(r_G \times \dot{v}_o) &= \tau - mg(r_G \times R^T e_3) \end{aligned} \tag{4.3}$$

Assumption 1.
- *$\dot{v}_o$ is bounded i.e. $||\dot{v}_0|| \leq a$ due to the actuator saturation.*
- *r_G is bounded i.e. $||r_G|| \leq b$ which is quite realistic.*

4.3 Controller Design

The reader may refer to Section 3.3.1 for definition of various configuration error functions used in subsequent controller design. Following propositions are the contributions of this chapter.

Proposition 4.1. *The attitude dynamics* (4.1) *driven by control law* (4.4) *with the adaptive laws given by* (4.5) *and* (4.6) *renders the closed loop attitude error dynamics* $\{e_R, e_\Omega\}$ *stable :*

$$\tau = -R_d^T e_R - K_\Omega e_\Omega + \hat{I}_o\dot{\Omega}_d + \Omega \times \hat{I}_o\Omega + \hat{m}g(\hat{r}_G \times R^T e_3) + \hat{m}(\hat{r}_G \times \dot{v}_o) \tag{4.4}$$

$$\dot{\hat{I}}_o = \frac{k_1}{2}(\dot{\Omega}_d e_\Omega^T - e_\Omega \dot{\Omega}_d^T + \Omega\Omega^T e_\Omega^{\dagger} - e_\Omega^{\dagger}\Omega\Omega^T) \tag{4.5}$$

$$\dot{\hat{r}}_G = \hat{m}k_2(-\dot{v}_o \times e_\Omega - g(R^T e_3 \times e_\Omega)) \tag{4.6}$$

where $\hat{I}_o$ is the estimate of I_o. $\hat{r}_G$ is the estimate of r_G. $\hat{m}$ is the estimate of m. The matrices $I_o, \hat{I}_o, \tilde{I}_o$ are symmetric. $K_\Omega \in \mathbb{R}^{3\times3}$ is a positive definite gain matrix.

Proof. Let the Lyapunov function for the attitude dynamics be :

$$\begin{aligned} V_R &= \frac{1}{2}e_\Omega^T I_o e_\Omega + \Psi + \frac{1}{2k_1}||\tilde{I}_o||_F^2 + \frac{1}{2k_2}\tilde{r}_G \cdot \tilde{r}_G \\ &= \frac{1}{2}e_\Omega^T I_o e_\Omega + \frac{1}{2}\mathrm{tr}(K(I - RR_d^T)) + \frac{1}{2k_1}\mathrm{tr}(\tilde{I}_o\tilde{I}_o) + \frac{1}{2k_2}\tilde{r}_G \cdot \tilde{r}_G \end{aligned} \tag{4.7}$$

where $||\tilde{I}_o||_F$ represents Frobenius norm, $e_\Omega = \Omega - \Omega_d$, k_1 and k_2 are positive constants.

$\tilde{I}_o = I_o - \hat{I}_o$. $\tilde{r}_G = r_G - \hat{r}_G$ and $\tilde{m} = m - \hat{m}$. Then

$$\begin{aligned}
&I_o\dot{e}_\Omega = I_o\dot{\Omega} - I_o\dot{\Omega}_d \\
&= -\Omega \times I_o\Omega - m(r_G \times \dot{v}_o) + \tau - mg(r_G \times R^T e_3) - I_o\dot{\Omega}_d \\
&= -\Omega \times I_o\Omega - (\hat{m} + \tilde{m})(r_G \times \dot{v}_o) - R_d^T e_R - K_\Omega e_\Omega + \hat{I}_o\dot{\Omega}_d \\
&+ \Omega \times \hat{I}_o\Omega + \hat{m}g(\hat{r}_G \times R^T e_3) + \hat{m}(\hat{r}_G \times \dot{v}_o) - (\hat{m} + \tilde{m})g(r_G \times R^T e_3) - I_o\dot{\Omega}_d \\
&= -\Omega \times \tilde{I}_o\Omega - \hat{m}(\tilde{r}_G \times \dot{v}_o) - R_d^T e_R - K_\Omega e_\Omega - \tilde{I}_o\dot{\Omega}_d - \hat{m}g(\tilde{r}_G \times R^T e_3) \\
&- \tilde{m}(r_G \times \dot{v}_o) - \tilde{m}g(r_G \times R^T e_3)
\end{aligned} \tag{4.8}$$

The time derivative of Lyapunov function Eqn.(4.7) is given by :

$$\begin{aligned}
&\dot{V}_R = e_\Omega^T I_o\dot{e}_\Omega - \frac{1}{2}(K\dot{R}R_d^T + KR\dot{R}_d^T) + \frac{1}{k_1}\mathrm{tr}(\tilde{I}_o\dot{\tilde{I}}_o) + \frac{1}{k_2}\tilde{r}_G \cdot \dot{\tilde{r}}_G \\
&= -e_\Omega \cdot (\Omega \times \tilde{I}_o\Omega) - e_\Omega \cdot \hat{m}(\tilde{r}_G \times \dot{v}_o) - e_\Omega^T R_d^T e_R - e_\Omega \cdot K_\Omega e_\Omega \\
&- e_\Omega \cdot \tilde{I}_o\dot{\Omega}_d - \hat{m}ge_\Omega \cdot (\tilde{r}_G \times R^T e_3) - \frac{1}{2}\mathrm{tr}(KRe_\Omega^\dagger R_d^T) \\
&- \frac{1}{k_1}\mathrm{tr}(\tilde{I}_o\dot{\tilde{I}}_o) - \frac{1}{k_2}\tilde{r}_G \cdot \dot{\hat{r}}_G - e_\Omega \cdot \tilde{m}(r_G \times \dot{v}_o) - e_\Omega \cdot \tilde{m}g(r_G \times R^T e_3)
\end{aligned} \tag{4.9}$$

From the scalar triple product identity $A \cdot (B \times C) = B \cdot (C \times A) = C \cdot (A \times B)$ and the identity $Ax^\dagger A^T = (Ax)^\dagger$, we can write :

$$\begin{aligned}
&\dot{V}_R = -\tilde{I}_o\Omega \cdot (e_\Omega \times \Omega) - \hat{m}\tilde{r}_G \cdot (\dot{v}_o \times e_\Omega) - e_\Omega^T R_d^T e_R - e_\Omega^T K_\Omega e_\Omega \\
&- e_\Omega^T \tilde{I}_o\dot{\Omega}_d - \hat{m}g\tilde{r}_G \cdot (R^T e_3 \times e_\Omega) - \frac{1}{2}\mathrm{tr}(KRR_d^T(R_d e_\Omega)^\dagger) \\
&- \frac{1}{k_1}\mathrm{tr}(\tilde{I}_o\dot{\tilde{I}}_o) - \frac{1}{k_2}\tilde{r}_G \cdot \dot{\hat{r}}_G - \tilde{m}e_\Omega \cdot (r_G \times \dot{v}_o) - \tilde{m}e_\Omega \cdot g(r_G \times R^T e_3)
\end{aligned} \tag{4.10}$$

From the equality $-\frac{1}{2}\mathrm{tr}(x^\dagger y^\dagger) = x \cdot y$ and $x \cdot y = \mathrm{tr}(xy^T) = \mathrm{tr}(yx^T)$, we can write :

$$\begin{aligned}
&\dot{V}_R = -\mathrm{tr}(\tilde{I}_o\Omega(e_\Omega \times \Omega)^T) - \hat{m}\tilde{r}_G \cdot (\dot{v}_o \times e_\Omega) - e_\Omega^T K_\Omega e_\Omega - \mathrm{tr}(\tilde{I}_o\dot{\Omega}_d e_\Omega^T) - \\
&\hat{m}g\tilde{r}_G \cdot (R^T e_3 \times e_\Omega) - \frac{1}{k_1}\mathrm{tr}(\tilde{I}_o\dot{\tilde{I}}_o) - \frac{1}{k_2}\tilde{r}_G \cdot \dot{\hat{r}}_G - \tilde{m}e_\Omega \cdot (r_G \times \dot{v}_o) - \tilde{m}e_\Omega \cdot g(r_G \times R^T e_3) \\
&= -e_\Omega^T K_\Omega e_\Omega - \mathrm{tr}(-\tilde{I}_o\Omega\Omega^T e_\Omega^\dagger + \tilde{I}_o\dot{\Omega}_d e_\Omega^T + \frac{1}{k_1}\tilde{I}_o\dot{\tilde{I}}_o) - \hat{m}\tilde{r}_G \cdot (\dot{v}_o \times e_\Omega + g(R^T e_3 \times e_\Omega) - \frac{\dot{\hat{r}}_G}{k_2}) \\
&- \tilde{m}e_\Omega \cdot (r_G \times \dot{v}_o) - \tilde{m}e_\Omega \cdot g(r_G \times R^T e_3)
\end{aligned}$$

$$= -e_\Omega^T K_\Omega e_\Omega - \text{tr}(\tilde{I}_o(-\Omega\Omega^T e_\Omega^\dagger + \dot{\Omega}_d e_\Omega^T + \frac{1}{k_1}\dot{\hat{I}}_o)) - \hat{m}\tilde{r}_G \cdot (\dot{v}_o \times e_\Omega + g(R^T e_3 \times e_\Omega) + \frac{\dot{\hat{r}}_G}{k_2})$$
$$- \tilde{m} e_\Omega \cdot (r_G \times \dot{v}_o) - \tilde{m} e_\Omega \cdot g(r_G \times R^T e_3)$$

If we choose

$$\dot{\hat{I}}_o = \frac{k_1}{2}(\dot{\Omega}_d e_\Omega^T - e_\Omega \dot{\Omega}_d^T + \Omega\Omega^T e_\Omega^\dagger - e_\Omega^\dagger \Omega\Omega^T)$$
$$\dot{\hat{r}}_G = \hat{m} k_2(-\dot{v}_o \times e_\Omega - g(R^T e_3 \times e_\Omega))$$

then

$$\begin{aligned}
\dot{V}_R &= -e_\Omega^T K_\Omega e_\Omega - \tilde{m} e_\Omega \cdot (r_G \times \dot{v}_o) - \tilde{m} e_\Omega \cdot g(r_G \times R^T e_3) \\
&\leq -\lambda_m(K_\Omega)||e_\Omega||^2 + |\tilde{m}|||e_\Omega||||r_G||(||\dot{v}_o|| + g) \\
&\leq -\lambda_m(K_\Omega)||e_\Omega||^2(1-\theta) - \lambda_m(K_\Omega)||e_\Omega||^2\theta + |\tilde{m}|||e_\Omega||||r_G||(||\dot{v}_o|| + g) \\
&\leq -\lambda_m(K_\Omega)||e_\Omega||^2(1-\theta) \quad \forall \quad ||e_\Omega|| \geq \frac{|\tilde{m}|||r_G||(||\dot{v}_o|| + g)}{\lambda_m(K_\Omega)\theta}
\end{aligned} \tag{4.11}$$

for $0 < \theta < 1$. In the following proposition, it will be proved that $|\tilde{m}|$ is bounded. This means Lyapunov function, V_R is bounded and therefore the attitude errors are bounded with the following bound on $||e_\Omega||$:

$$||e_\Omega|| \leq \frac{|\tilde{m}|||r_G||(||\dot{v}_o|| + g)}{\lambda_m(K_\Omega)} \leq \frac{|\tilde{m}|b(a+g)}{\lambda_m(K_\Omega)}$$

where $\lambda_m(\cdot)$ denotes minimum eigenvalue of its argument. □

Proposition 4.2. *The translational dynamics* (4.2) *driven by control law* (4.12) *with the adaptive law for mass given by* (4.13) *renders the closed loop translational error dynamics* $\{e_x, e_v\}$ *stable :*

$$f_c^d = -K_x e_x - K_v e_v + \hat{m}(\dot{v}_d + g e_3) \tag{4.12}$$
$$\dot{\hat{m}} = -k_3(g e_v^T e_3 + e_v^T \dot{v}_d) \tag{4.13}$$

where $K_x, K_v \in \mathbb{R}^{3\times3}$ *are positive definite gain matrices,* $e_x = x - x_d$ *and* $e_v = v_o - v_d$. $\hat{m}$ *is the estimate of* m *and* $\tilde{m} = m - \hat{m}$.

Proof. Let the Lyapunov function for the translation dynamics be :

$$V_T = \frac{1}{2} e_v^T m e_v + \frac{1}{2} e_x^T K_x e_x + \frac{1}{2k_3}\tilde{m}^2 \tag{4.14}$$

where k_3 is a positive constant. In our approach we propose to apply following control

law and torque to the quadrotor :

$$f_b = ||f_c^d||e_3 \tag{4.15}$$

The choice of control f_b always results in positive thrust to the quadrotor, whereas in [46] the total thrust becomes negative when the angle between the desired thrust and vertical body axis becomes greater than 90°. For a standard VTOL vehicle, it is required that $f_b^T e_3 > 0$. Then the time derivative of V_T is

$$\dot{V}_T = e_v^T m\dot{e}_v + e_x^T K_x e_v + \frac{1}{k_3}\tilde{m}\dot{\tilde{m}} \tag{4.16}$$

We can find $m\dot{e}_v$ as

$$\begin{aligned} m\dot{e}_v &= m\dot{v}_o - m\dot{v}_d \\ &= -mge_3 + Rf_b - m\dot{v}_d \\ &= -mge_3 + Rf_b + f_c^d - f_c^d - m\dot{v}_d \\ &= -mge_3 + Rf_b - K_x e_x - K_v e_v + \hat{m}(\dot{v}_d + ge_3) - f_c^d - m\dot{v}_d \\ &= -\tilde{m}ge_3 + Rf_b - K_x e_x - K_v e_v - \tilde{m}\dot{v}_d - f_c^d \end{aligned} \tag{4.17}$$

From Eqn.(4.17), eqn.(4.16) becomes :

$$\begin{aligned} \dot{V}_T &= e_v^T(-\tilde{m}ge_3 + Rf_b - K_x e_x - K_v e_v - \tilde{m}\dot{v}_d - f_c^d) + e_x^T K_x e_v - \frac{1}{k_3}\tilde{m}\dot{\hat{m}} \\ &= -e_v^T K_v e_v - \tilde{m}(e_v^T ge_3 + e_v^T \dot{v}_d + \frac{1}{k_3}\dot{\hat{m}}) + e_v^T(Rf_b - f_c^d) \end{aligned} \tag{4.18}$$

If we choose :

$$\dot{\hat{m}} = -k_3(ge_v^T e_3 + e_v^T \dot{v}_d) \text{ then} \tag{4.19}$$

$$\dot{V}_T = -e_v^T K_v e_v + e_v^T(Rf_b - f_c^d) = -e_v^T K_v e_v + e_v^T \Delta f$$

where, $\Delta f = Rf_b - f_c^d$. From (3.15), the norm of Δ_f can be written as :

$$||\Delta f|| < \sqrt{2h_2}||e_R||f_M$$

Therefore, eqn.(4.18) becomes :

$$\begin{aligned}
\dot{V}_T &\leq -\lambda_m(K_v)||e_v||^2 + ||e_v||||\Delta f|| \\
&< -\lambda_m(K_v)||e_v||^2 + \sqrt{2h_2}||e_v||||e_R||f_M \\
&< -\lambda_m(K_v)||e_v||^2(1-\theta_1) - \lambda_m(K_v)||e_v||^2\theta_1 + \sqrt{2h_2}||e_v||||e_R||f_M \\
&\leq -\lambda_m(K_v)||e_v||^2(1-\theta_1) \;\; \forall \;\; ||e_v|| \geq \frac{\sqrt{2h_2}||e_v||||e_R||f_M}{\lambda_m(K_v)\theta_1}
\end{aligned} \tag{4.20}$$

for $0 < \theta_1 < 1$. From Eqns. (3.3) and (3.4), $||e_R||$ is bounded, therefore translational error dynamics is bounded and hence $|\tilde{m}|$ is also bounded. □

Proposition 4.3. *The closed loop error dynamics* $\{e_x, e_v, e_R, e_\Omega\}$ *is rendered stable if the complete system dynamics* (4.1), (4.2) *is driven by the control laws* (4.4), (4.12) *along with the adaptive laws given by* (4.5), (4.6) *and* (4.13).

Proof. This can be proved by taking the Lypaunov function as :

$$V = V_T + V_R \tag{4.21}$$

Taking the time derivative of Eqn.(4.21) and using Eqns.(4.11) and (4.20), we can prove the boundedness of the complete closed loop error dynamics $\{e_x, e_v, e_R.e_\Omega\}$. □

Desired angular velocity

To avoid complex analytic derivative of R_d while calculating Ω_d and $\dot{\Omega}_d$, we used a first-order command filter [26] to estimate these values as given below :

$$\begin{aligned}
&\dot{R}_d = [\dot{b}_{d1c}\ \dot{b}_{d2c}\ \dot{b}_{d3c}] \text{ where} \\
&\dot{b}_{dic} = -\bar{T}(b_{dic} - b_{dit}) \text{ for } i = 1,2,3 \text{ and} \\
&R_d = [b_{d1t}\ b_{d2t}\ b_{d3t}] \\
&\Omega_d = [R_d^T \dot{R}_d]^\vee \text{ where } (\cdot)^\vee : \mathfrak{so}(3) \to \mathbb{R}^3
\end{aligned}$$

Similarly,

$$\dot{\Omega}_{dc} = -\bar{T}(\Omega_{dc} - \Omega_d) \text{ and } \dot{\Omega}_d = \dot{\Omega}_{dc}$$

$\bar{T} = \text{diag}(t_1, t_2, t_3) > 0$ is the filter time constant which should be high to ensure fast tracking.

Projection operation

The initial values of estimates of the center of gravity are set to be in a given compact set. To limit the update of the center of gravity to a given compact set, projection operation [104] is used as given below :

Assumption 2. *There exist* r_{Gmax}, r_{Gmin} *and a small positive constant* σ *so that* $r_{Gmin} + \sigma < r_G < r_{Gmax} - \sigma$.

$$\text{If } r_{est} = -(\dot{v}_o \times e_\Omega) - g(R^T e_3 \times e_\Omega)$$

The update law of $\hat{r}_G$ is modified as:

$$\dot{\hat{r}}_G(i) = mk_2 r_{est}(i) \text{ if } r_{Gmin}(i) + \sigma < \hat{r}_G(i) < r_{Gmax}(i) - \sigma$$
$$\dot{\hat{r}}_G(i) = mk_2(r_{est}(i) + \frac{1}{2}(1 + r_{est}(i)^2)) \text{ if } \hat{r}_G(i) \leq r_{Gmin}(i) + \sigma$$
$$\dot{\hat{r}}_G(i) = mk_2(r_{est}(i) - \frac{1}{2}(1 + r_{est}(i)^2)) \text{ if } \hat{r}_G(i) \geq r_{Gmax}(i) - \sigma$$

for $i = 1, 2, 3$. $r_G(i)$ and $r_{est}(i)$ represent i^{th} component of r_G and r_{est} respectively .

The initial value of r_G is chosen such that $r_{Gmin} < \hat{r}_G(0) < r_{Gmax}$. If $\hat{r}_G \leq r_{Gmin} + \sigma$,then we have $\dot{\hat{r}}_G \geq 0$ and this will not let $\hat{r}_G$ getting smaller than r_{Gmin}. Similarly, if $\hat{r}_G \geq r_{Gmax} - \sigma$, then we have $\dot{\hat{r}}_G \leq 0$ and this will not let $\hat{r}_G$ getting greater than r_{Gmax}. The projection operation has not been used for other parameters.

4.4 Numerical simulations

To illustrate the theoretical results, numerical simulations were carried out for the system whose parameters are shown in Table.4.1. The reference trajectory is given by

$$x_d(t) = [2\cos\left[\frac{\pi t}{10}\right]; 2\sin\left[\frac{\pi t}{10}\right]; \frac{t}{2}] \text{ and } b_{1d}(t) = \frac{\dot{x}_d(t)}{||\dot{x}_d(t)||}$$

The initial conditions for simulation are assumed to be

$$[x(0), y(0), z(0)] = [0, 0, 0], [\dot{x}(0), \dot{y}(0), \dot{z}(0)] = [0, 0, 0] \text{ and}$$
$$R(0) = I_3.$$

Table 4.1: Parameters used in simulation

Parameter	Values	Units	Parameter	Values	Units
g	9.81	m/s^2	I_{xx}	0.006	kg m^2
m	1.0	kg	I_{yy}	0.008	kg m^2
K_x	$3I_3$	-	I_{zz}	0.015	kg m^2
K_v	$2I_3$	-	K_Ω	$5I_3$	-
k_1	0.2	-	k_2	0.2	-
K	$2I_3$	-	k_3	0.2	-
$\bar{T}$	$50I_3$	-	σ	0.005	-

The value of moment of inertia is given in Table 4.1 while its initial estimate is given by $\hat{I}_o = \text{diag}[0.005, 0.007, 0.012]$.

4.4.1 Scenario I

The value of center of gravity with its initial estimate and its minimum and maximum values are mentioned below :

$$r_G = [0.02, 0.02, 0.01]^T m, \quad \hat{r}_G = [0.01, 0.01, 0.005]^T m,$$
$$r_{Gmin} = -[0.01, 0.01, 0.005]^T m, r_{Gmax} = [0.03, 0.03, 0.015]^T m$$

The various simulation results are shown in Figs. 4.2-4.3. It is seen from Figs.4.2 that better trajectory tracking response is observed when the offset in the center of gravity is explicitly compensated. The increase in the offset of the center of gravity results in worse tracking performance, shown through simulations. The RMS error in position tracking without the compensation is found to be $[0.3287; 0.2652; 0.0275]$ m while RMS error in position tracking with the compensation is found to be $[0.2627; 0.1157; 0.0328]$ m, which is a good improvement in horizontal position tracking. The dynamic response in altitude with compensation is better than without the compensation. The transient performance of altitude response with compensation has better settling time and less overshoot as compared to the response without compensation.

The estimates in the center of gravity with projection is shown in Fig.4.3 (a)-(c), which tends to be around the actual values used in the simulation. The estimates oscillate around the actual value and the reason seems to be sinusoidal reference. Since the sinusoidal references are used in $X-$ and $Y-$ axes, the $X-$ and $Y-$ estimates oscillate. No sinusoidal references are used in $Z-$ axes and hence estimates converge to a final value. The initial estimate of mass was taken to be 0.9 kg. The estimates in mass tend to converge to a value of 0.99 kg, which is very close to the actual value. The throttle input

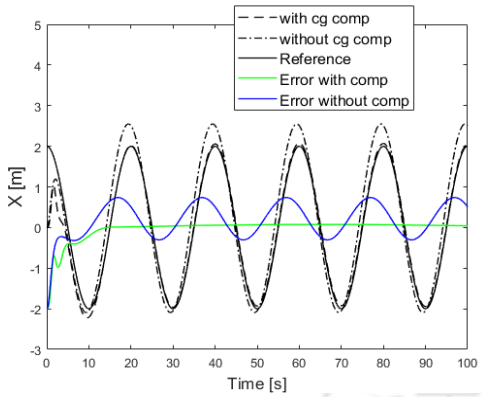

(a)

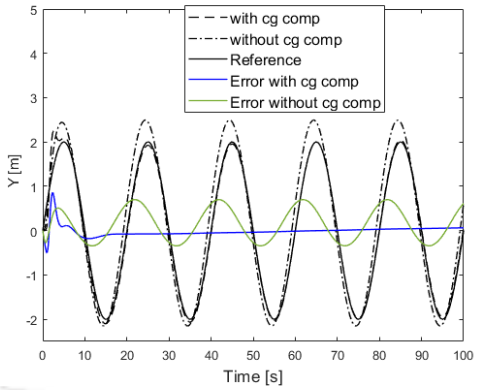

(b)

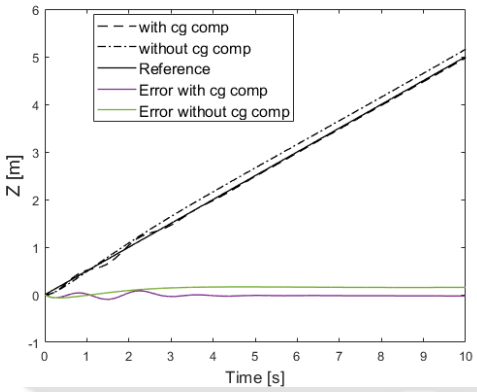

(c)

Figure 4.2: Tracking in (a) X [m] (b) Y [m] (c) Z [m] for $r_G = [0.02, 0.02, 0.01]^T m$

and torque input are stable, finite, and converge to finite values, as can be seen from Figs.4.3(e)-(f). Initially high throttle is required as expected but soon it settles to a finite value as steady state is reached. The attitude error vector, angular velocity error vector, and linear velocity error vector also tend to a small value around zero in finite time as seen from Fig.4.4(a)-(c). The moment of inertia and product of inertias as seen from Fig.4.4(d)-4.5 also converge to some finite values. Since only boundedness of moment of inertia and product of inertia is guaranteed in theoretical analysis, therefore, these values do not tend to their actual values used in the simulation. We see a slight jump in the estimation values during initial times which is expected during transient phase of the response.

4.4.2 Scenario II

The tracking performance with $r_G = [0.04, 0.04, 0.02]^T m$ is shown in Figs.4.6. The RMS error in position tracking without the compensation is found to be [0.5497, $0.5049, 0.0930]^T m$ while RMS error in position tracking with the compensation is found

to be $[0.2625, 0.1159,\ 0.0329]^T m$ which is a substantial improvement. The transient response of the proposed controller in altitude dynamics is much better as compared to the controller without the compensation. Once again, it is observed that the transient performance of altitude response with compensation has better settling time and less overshoot as compared to the response without compensation. It is also observed that the tracking error has increased with the increase in offset between the center of gravity and the geometric center. The center of gravity estimates is shown in Fig.4.6(d). The estimate in the center of gravity tends to be around the actual value, as can be seen from Fig.4.6(d)-(f). We see a slight jump in the estimation values during initial times which is expected during transient phase of the response. If the offset is increased beyond a certain threshold, the system without compensation even becomes unstable. This shows that the compensation in system dynamics due to offset is necessary. The other error vectors in Scenario II reported similar behavior as that in Scenario I and hence their plots are not presented for the sake of repetitions.

4.5 Conclusion

A nonlinear geometric adaptive controller is proposed for quadrotors when its location of the center of gravity is different from the geometric center. The theoretical proof shows that the proposed control law along with coordinate invariant adaptive laws is stable. Simulation results show better tracking performance when the offset is explicitly compensated as compared to when it is not. It can be observed through simulations that beyond a certain threshold in the offset, if the system dynamics is not compensated explicitly with the proposed method, then the system becomes unstable. Hence the proposed method gives a tracking adaptive controller, which is stable and verified through numerical simulations. The proposed method renders the closed-loop dynamics stable irrespective of the magnitude of the offset. The hardware implementation is one of the future works of these theoretical findings.

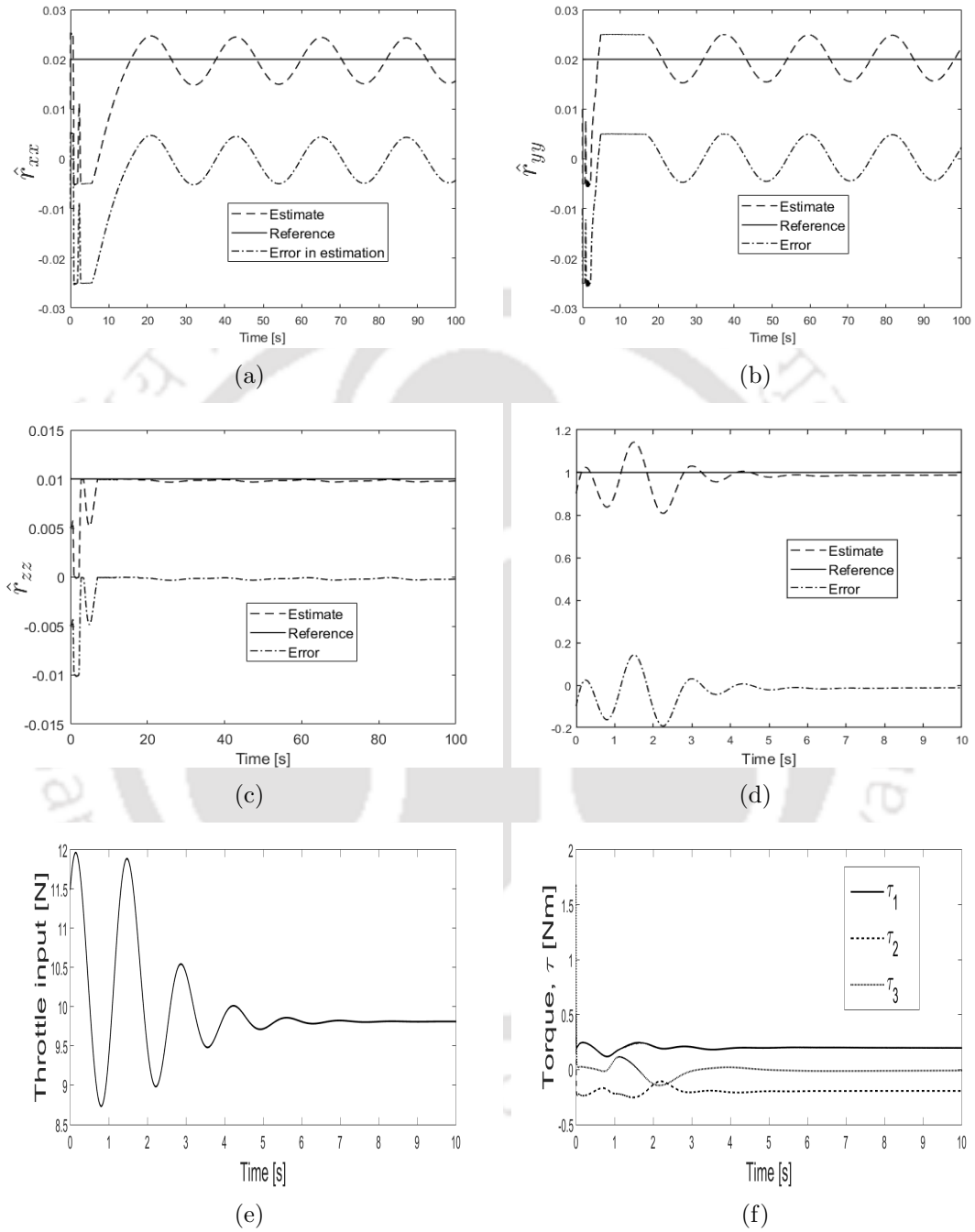

Figure 4.3: (a)-(c) Center of gravity estimates for $r_G = [0.02, 0.02, 0.01]^T m$ (d)Mass estimate (e)Throttle input (f) Torque input

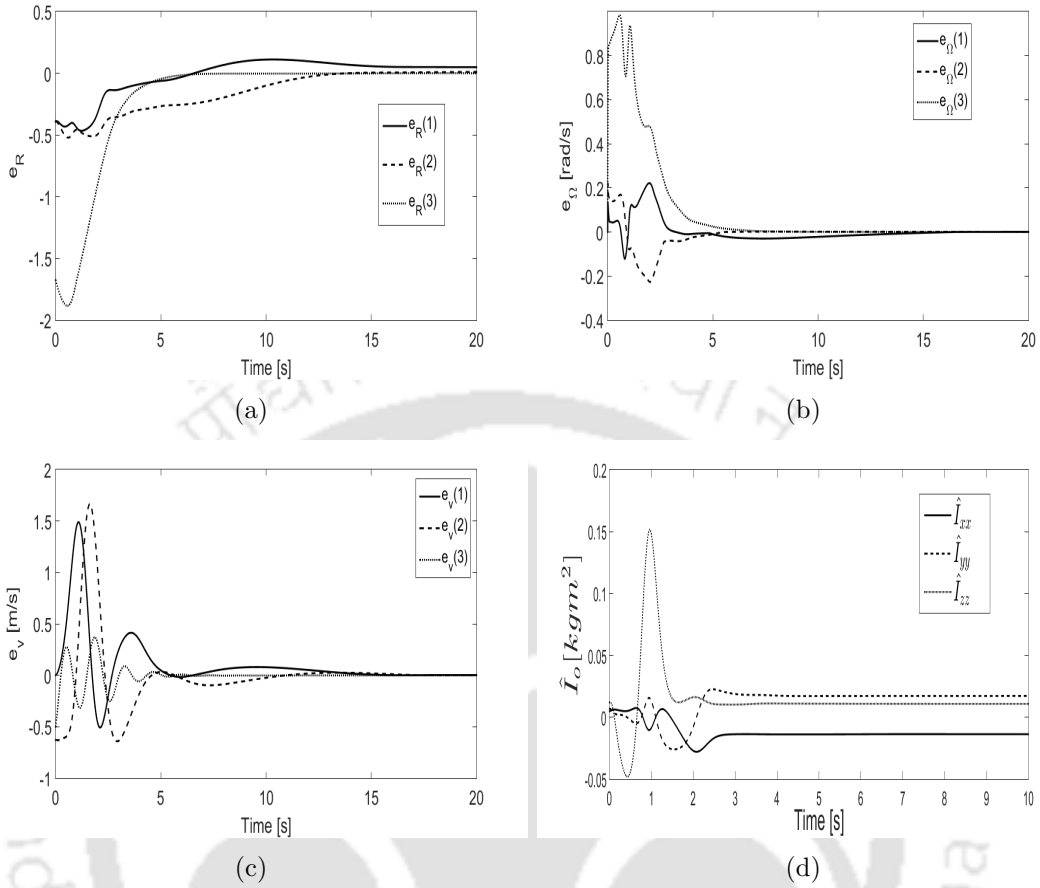

Figure 4.4: (a) Attitude error (b) Angular velocity error (c) Linear velocity error (d) Moment of Inertia estimate

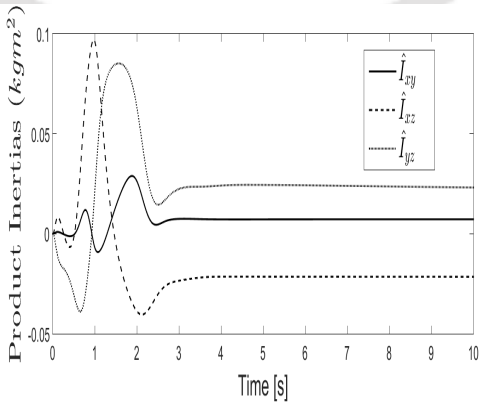

Figure 4.5: Product of Inertia estimate

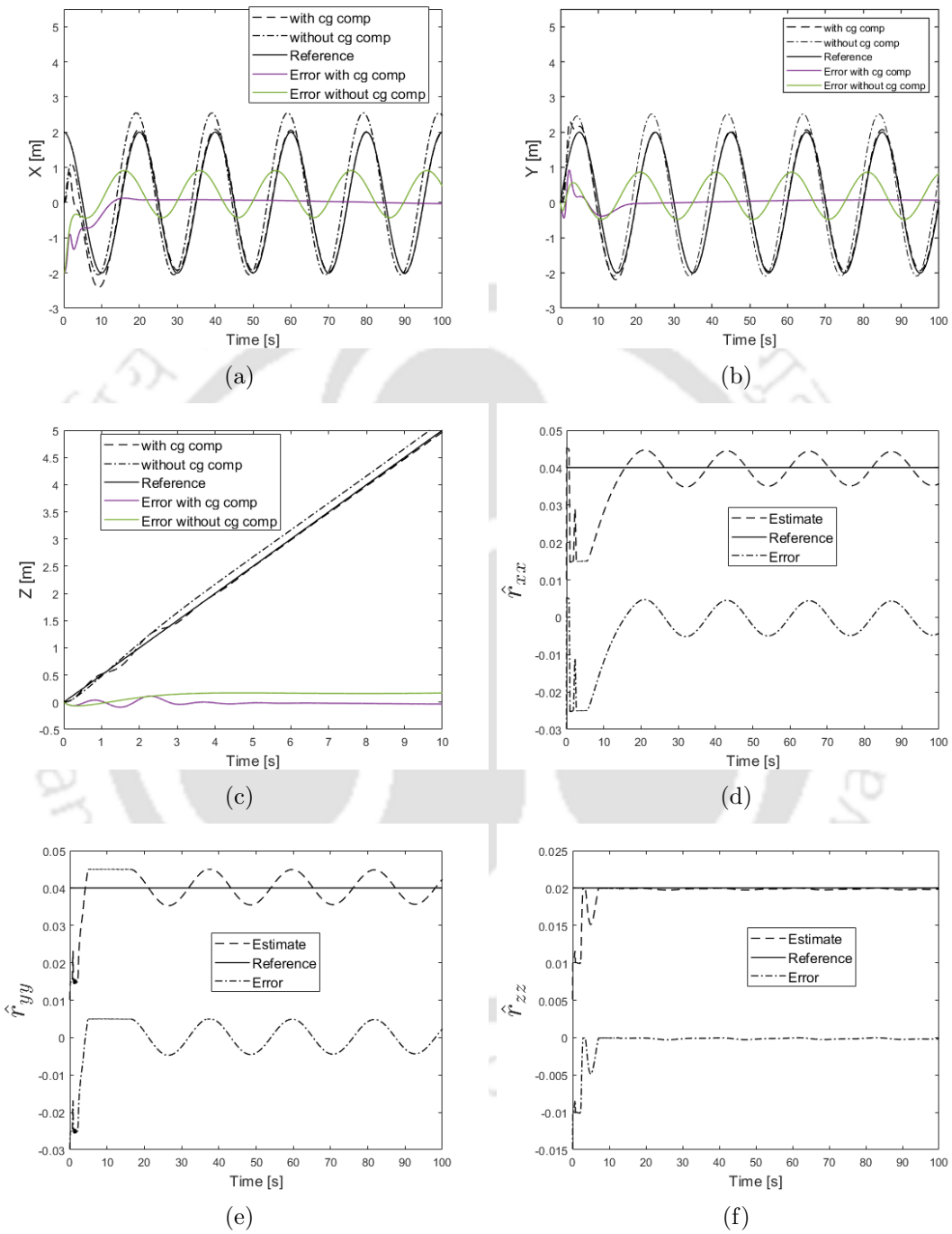

Figure 4.6: Tracking in (a) X [m] (b) Y [m] (c) Z [m] (d)-(f) Center of gravity estimates for $r_G = [0.04, 0.04, 0.02]^T m$

Chapter 5

Control of a Quadrotor with Network Induced Time Delay

In the first two chapters, time delays were not taken into account, but it is well known that a physical system suffers from time delays. Therefore, a backstepping controller augmented with a state predictor is presented in this chapter to control a quadrotor over a network subjected to both state and input time delay. The state predictor predicts the future values of the states by taking the measured delayed states as input. A backstepping control law is further designed based on these predicted states. It is shown with the aid of the Lyapunov Razumikhin theorem that the error dynamics of the predictor are asymptotically stable. The cascade of state predictor and backstepping controller makes the tracking error dynamics of the quadrotor asymptotically stable. Simulation results are presented to validate the proposed approach.

5.1 Introduction

Teleoperation [64] is a challenging task given the challenges faced in its implementation, such as packet loss, distortion, and time delay. But the advantages of such an operation give the research community the motivation to overcome such challenges with the present set of mathematical tools. There are several successful attempts in the literature of such an operation [65, 66, 67, 68, 69, 70]. All the literature mentioned pertaining to quadrotors does not consider communication time delay. The presence of communication time delay may result in instability in the system. Unfortunately, such an approach has not been extended for the remote operation of quadrotors. In [71], a robust attitude controller was designed for multiple input multiple output uncertain quadrotors considering parametric uncertainties, external disturbances, and input time delays. A similar robust controller considering parametric uncertainties, unmodeled uncertainties, and in-

put as well as state delays are designed in [62, 63, 72, 73]. Motivated by the current state of the literature, a controller considering both inputs as well as state delay experienced while operating the device over a network is designed.

The contributions of this chapter are threefold. Firstly, we design a state predictor to estimate the future values of the quadrotor's state in the presence of both input and state time delay. We assume bilateral operation such that the forward, as well as the backward time delay, is constant and known. The chapter attempts to propose a method to control a quadrotor over a network. According to the authors' best of knowledge, there is no such method in the literature that attempts to control a quadrotor over a network. Since the network will inherently induce time delays in the state as well as the control input, an estimator has been proposed to predict the future states from the measured states, which are delayed. Then the output of the estimator is used in designing a backstepping controller. Secondly, we design a backstepping [97, 105] controller for stabilization and trajectory tracking, assuming no state or input delay. We have chosen the backstepping technique since it is recursive and suitable for our needs. Such an algorithm can also be easily extended to handle unknown parameters by using the adaptive backstepping technique. The controller is shown to have asymptotic stability property. Then state predictor is cascaded with the controller, where the output of the predictor is used in place of the state requirement in the controller. To the best of the authors' knowledge, this study is the first to compensate for both states as well as input time delay in a quadrotor system explicitly. All the mentioned literature either does not consider such a scenario or at best handle it as a disturbance. Thirdly, the backstepping control law has been designed to control an underactuated system, i.e., quadrotor. For a quadrotor, its dynamics are highly coupled, and moreover, it is underactuated. This is another challenge of the controller design, which we have addressed by designing the controller of the attitude subsystem independently of the translational subsystem. Numerical simulation results have been given at the end to validate the proposed method.

The chapter is organized as follows. Section 5.2 of the chapter defines the quadrotor's dynamic model while developing the controller and the predictor. Section 5.3 defines the Lyapunov Razumikhin theorem used in the stability proof of the predictor. Section 5.4 gives the structure of the proposed state predictor along with its stability proof. Section 5.5 presents the backstepping controller design. Section 5.6 gives some numerical simulation results to validate the proposed approach. The section also contains comparison results with the existing literature and further discussion of the results obtained.

5.2 Dynamic Model

The reader is referred to section 1.2 to refresh the dynamic model of a quadrotor in local coordinates (Eqn. 1.3). The above equations of motion are in the presence of zero states and zero input delay. We will neglect gyroscopic effects in the subsequent analysis. In the presence of bilateral time delay, i.e., delay in both forward and backward transmission, the equations of motion become :

$$\begin{aligned}
\ddot{\phi}(t-\tau_b) &= \dot{\theta}(t-\tau_b)\dot{\psi}(t-\tau_b)\frac{I_y - I_z}{I_x} + \frac{l}{I_x}U_2(t-\tau) \\
\ddot{\theta}(t-\tau_b) &= \dot{\phi}(t-\tau_b)\dot{\psi}(t-\tau_b)\frac{I_z - I_x}{I_y} + \frac{l}{I_y}U_3(t-\tau) \\
\ddot{\psi}(t-\tau_b) &= \dot{\theta}(t-\tau_b)\dot{\phi}(t-\tau_b)\frac{I_x - I_y}{I_z} + \frac{1}{I_z}U_4(t-\tau) \\
\ddot{x}(t-\tau_b) &= (cos\phi(t-\tau_b)sin\theta(t-\tau_b)cos\psi(t-\tau_b) + sin\phi(t-\tau_b)sin\psi(t-\tau_b))\frac{1}{m} \\
& U_1(t-\tau) \\
\ddot{y}(t-\tau_b) &= (cos\phi(t-\tau_b)sin\theta(t-\tau_b)sin\psi(t-\tau_b) - sin\phi(t-\tau_b)cos\psi(t-\tau_b))\frac{1}{m} \\
& U_1(t-\tau) \\
\ddot{z}(t-\tau_b) &= -g + (cos\phi(t-\tau_b)cos\theta(t-\tau_b))\frac{1}{m}U_1(t-\tau)
\end{aligned} \tag{5.1}$$

where τ_b is the backward transmission delay while τ_f is the forward transmission delay and $\tau = \tau_f + \tau_b$. Let us denote the measured states by the following symbols : $\phi_{\tau_b} = \phi(t-\tau_b), \dot{\phi}_{\tau_b} = \dot{\phi}(t-\tau_b), \theta_{\tau_b} = \theta(t-\tau_b), \dot{\theta}_{\tau_b} = \dot{\theta}(t-\tau_b), \psi_{\tau_b} = \psi(t-\tau_b), \dot{\psi}_{\tau_b} = \dot{\psi}(t-\tau_b), x_{\tau_b} = x(t-\tau_b), \dot{x}_{\tau_b} = \dot{x}(t-\tau_b), y_{\tau_b} = y(t-\tau_b), \dot{y}_{\tau_b} = \dot{y}(t-\tau_b), z_{\tau_b} = z(t-\tau_b), \dot{z}_{\tau_b} = \dot{z}(t-\tau_b)$. The control objective is to design a state predictor to predict future states from the delayed states and design a backstepping controller based on these predicted states to take care of network delay. Let ζ be the states of the quadrotor i.e. $\zeta = [\phi, \theta, \psi, z, x, y]$, $\hat{\zeta}$ be the output of the predictor and ζ_{τ_b} be the delayed measurement. Then the predictor and the control inputs U_1, U_2, U_3, U_4 have to be designed in such a way that :

$$\begin{aligned}
&\lim_{t\to\infty}[\hat{\zeta}(t-\tau) - \zeta_{\tau_b}] = 0; \quad \lim_{t\to\infty}[\hat{\dot{\zeta}}(t-\tau) - \dot{\zeta}_{\tau_b}] = 0 \\
&\lim_{t\to\infty}[x - x_d, y - y_d, z - z_d] = [0,0,0]; \\
&\lim_{t\to\infty}[\dot{x} - \dot{x}_d, \dot{y} - \dot{y}_d, \dot{z} - \dot{z}_d] = [0,0,0]; \\
&\lim_{t\to\infty}[\phi - \phi_d, \theta - \theta_d, \psi - \psi_d] = [0,0,0]; \quad \lim_{t\to\infty}[\dot{\phi}, \dot{\theta}, \dot{\psi}] = [0,0,0]
\end{aligned} \tag{5.2}$$

5.3 Lyapunov Razumikhin Theorem

For systems without time delay, one resorts to Lyapunov functions to test the stability of the system. Unfortunately, such an approach is not suitable for systems with time delays. One approach is to use Lyapunov Krassovski functionals to test the stability, but such an approach suffers from complexity arising out of differentiating functionals. An alternative is to use the Lyapunov Razumikhin theorem, where one deals with functions rather than functionals, which simplifies the analysis and design. The same approach has been used in this text to prove the asymptotic stability of the predictor. The statement of Lyapunov Razumikhin theorem is given below :

Definition 1. *[106, 107] Let us consider the following retarded functional differential equation :*

$$\dot{x} = f(t, x_t) \tag{5.3}$$

where $x(t) \in \mathbb{R}^n$ *and* $f : \mathbb{R} \times \mathcal{C} \to \mathbb{R}^n$. $\mathcal{C}$ *represents set of continuous functions that map* $[-h, 0]$ *to* $\mathbb{R}^n$ *and* $x_t = x(t+\theta)$ *for* $-h \leq \theta \leq 0$. *Let* $u, v, w : \bar{\mathbb{R}}_+ \to \bar{\mathbb{R}}_+$ *be functions such that* $u(\tau), v(\tau) > 0$ *for* $\tau > 0$, $u(0) = v(0) = 0$, *then*

• *If one can infer the existence of a continuous and differentiable function* $V : \mathbb{R} \times \mathbb{R}^n \to \mathbb{R}$ *such that*

$$\begin{aligned} &u(||x||) \leq V(t,x) \leq v(||x||), \quad t \in \mathbb{R}, \quad x \in \mathbb{R}^n, \quad \textit{and} \\ &\dot{V}(t, x(t)) \leq -w(||x(t)||) \quad \textit{if} \\ &V(t+\theta, x(t+\theta)) \leq pV(t, x(t)) \end{aligned} \tag{5.4}$$

$\theta \in [-h, 0]$,$w(\tau) > 0$ *and* $p(\tau) > \tau$ *for* $\tau > 0$ *then the equilibrium solution of* (5.3) *is uniformly asymptotically stable.*

5.4 State Predictor

The present section aims to design a state predictor to compensate for the bilateral time delay induced due to the network's presence on the input and the states' measurement. This predictor's output will be used to design the backstepping controller by replacing the actual states with the states predicted by the predictor. A schematic diagram of the controller predictor pair is shown in Fig. 5.1. Let the state space representation

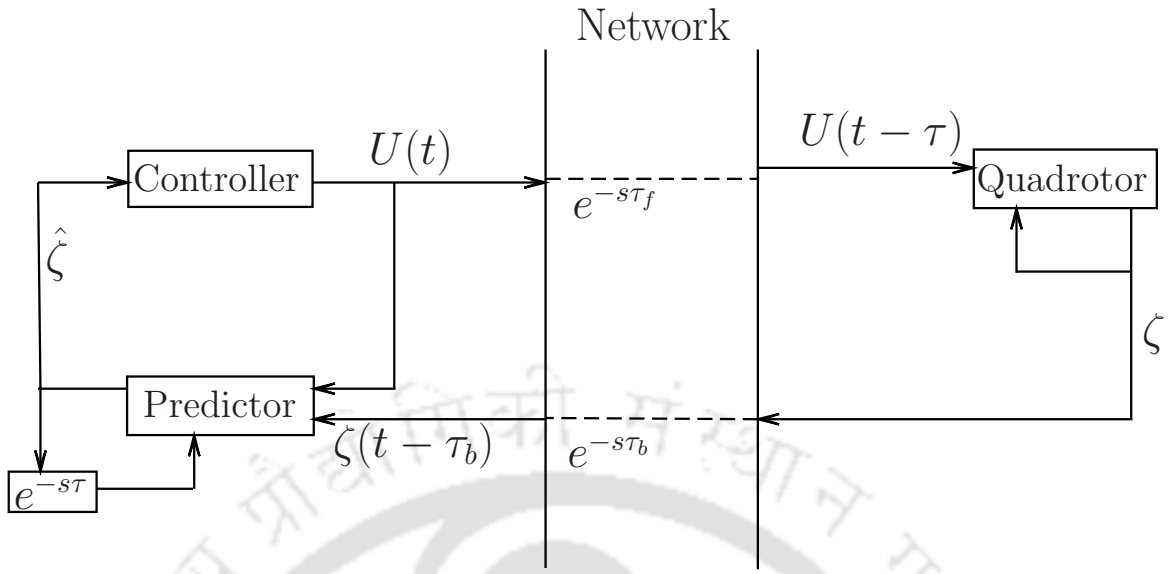

Figure 5.1: Controller-Predictor pair

of the equation (5.1) be given below :

$$
\begin{aligned}
\dot{\phi}_{\tau_b} &= q_{\phi_{\tau_b}} \\
\dot{q}_{\phi_{\tau_b}} &= \frac{I_y - I_z}{I_x}\dot{\theta}_{\tau_b}\dot{\psi}_{\tau_b} + \frac{1}{I_x}U_2(t-\tau) \\
\dot{\theta}_{\tau_b} &= q_{\theta_{\tau_b}} \\
\dot{q}_{\theta_{\tau_b}} &= \frac{I_z - I_x}{I_y}\dot{\phi}_{\tau_b}\dot{\psi}_{\tau_b} + \frac{1}{I_y}U_3(t-\tau) \\
\dot{\psi}_{\tau_b} &= q_{\psi_{\tau_b}} \\
\dot{q}_{\psi_{\tau_b}} &= \frac{I_x - I_y}{I_z}\dot{\theta}_{\tau_b}\dot{\phi}_{\tau_b} + \frac{1}{I_z}U_4(t-\tau) \\
\dot{x}_{\tau_b} &= q_{x_{\tau_b}} \\
\dot{q}_{x_{\tau_b}} &= (cos\phi_{\tau_b} sin\theta_{\tau_b} cos\psi_{\tau_b} + sin\phi_{\tau_b} sin\psi_{\tau_b})\frac{1}{m}U_1(t-\tau) \\
\dot{y}_{\tau_b} &= q_{y_{\tau_b}} \\
\dot{q}_{y_{\tau_b}} &= (cos\phi_{\tau_b} sin\theta_{\tau_b} sin\psi_{\tau_b} - sin\phi_{\tau_b} cos\psi_{\tau_b})\frac{1}{m}U_1(t-\tau) \\
\dot{z}_{\tau_b} &= q_{z_{\tau_b}} \\
\dot{q}_{z_{\tau_b}} &= -g + (cos\phi_{\tau_b} cos\theta_{\tau_b})\frac{1}{m}U_1(t-\tau)
\end{aligned}
\tag{5.5}
$$

We propose the following predictor scheme to estimate the future values of the quadrotor's states :

$$
\begin{aligned}
\dot{\hat{\phi}} &= \bar{q}_\phi - k_1(\hat{\phi}(t-\tau) - \phi_{\tau_b}(t)) \\
\dot{\bar{q}}_\phi &= \frac{I_y - I_z}{I_x}\bar{q}_\theta\bar{q}_\psi + \frac{U_2(t)}{I_x} - k_2(\bar{q}_\phi(t-\tau) - q_{\phi_{\tau_b}}(t)) \\
\dot{\hat{\theta}} &= \bar{q}_\theta - k_3(\hat{\theta}(t-\tau) - \theta_{\tau_b}(t)) \\
\dot{\bar{q}}_\theta &= \frac{I_z - I_x}{I_y}\bar{q}_\phi\bar{q}_\psi + \frac{U_3(t)}{I_y} - k_4(\bar{q}_\theta(t-\tau) - q_{\theta_{\tau_b}}(t)) \\
\dot{\hat{\psi}} &= \bar{q}_\psi - k_5(\hat{\psi}(t-\tau) - \psi_{\tau_b}(t)) \\
\dot{\bar{q}}_\psi &= \frac{I_x - I_y}{I_z}\bar{q}_\phi\bar{q}_\theta + \frac{U_4(t)}{I_z} - k_6(\bar{q}_\psi(t-\tau) - q_{\psi_{\tau_b}}(t)) \\
\dot{\hat{x}} &= \bar{q}_x - k_7(\hat{x}(t-\tau) - x_{\tau_b}(t)) \\
\dot{\bar{q}}_x &= (cos\hat{\phi}\ sin\hat{\theta}\ cos\hat{\psi} + sin\hat{\phi}\ sin\hat{\psi})\frac{U_1(t)}{m} - k_8(\bar{q}_x(t-\tau) - q_{x_{\tau_b}}(t)) \\
\dot{\hat{y}} &= \bar{q}_y - k_9(\hat{y}(t-\tau) - y_{\tau_b}(t)) \\
\dot{\bar{q}}_y &= (cos\hat{\phi}\ sin\hat{\theta}\ sin\hat{\psi} - sin\hat{\phi}\ cos\hat{\psi})\frac{U_1(t)}{m} - k_{10}(\bar{q}_y(t-\tau) - q_{y_{\tau_b}}(t)) \\
\dot{\hat{z}} &= \bar{q}_z - k_{11}(\hat{z}(t-\tau) - z_{\tau_b}(t)) \\
\dot{\bar{q}}_z &= -g + (cos\hat{\phi}\ cos\hat{\theta})\frac{U_1(t)}{m} - k_{12}(\bar{q}_z(t-\tau) - q_{z_{\tau_b}}(t))
\end{aligned} \tag{5.6}
$$

where k_i for $i = 1 \cdots 12$ are positive constants.

5.4.1 Error Dynamics for Rotational Subsystem

Let the prediction errors in rotational subsystem be given by :

$$
\begin{aligned}
e_\phi(t) &= \hat{\phi}(t-\tau) - \phi_{\tau_b}(t) \\
e_{q_\phi}(t) &= \bar{q}_\phi(t-\tau) - q_{\phi_{\tau_b}}(t) \\
e_\theta(t) &= \hat{\theta}(t-\tau) - \theta_{\tau_b}(t) \\
e_{q_\theta}(t) &= \bar{q}_\theta(t-\tau) - q_{\theta_{\tau_b}}(t) \\
e_\psi(t) &= \hat{\psi}(t-\tau) - \psi_{\tau_b}(t) \\
e_{q_\psi}(t) &= \bar{q}_\psi(t-\tau) - q_{\psi_{\tau_b}}(t)
\end{aligned} \tag{5.7}
$$

Then the error dynamics is given by :

$$
\dot{e}_\phi(t) = \dot{\hat{\phi}}(t-\tau) - \dot{\phi}_{\tau_b}(t) = e_{q_\phi}(t) - k_1 e_\phi(t-\tau) \tag{5.8}
$$

and

$$\dot{e}_{q_\phi}(t) = \frac{(I_y - I_z)}{I_x}(\bar{q}_\theta(t-\tau)\bar{q}_\psi(t-\tau) - q_{\theta_{\tau_b}} q_{\psi_{\tau_b}}) - k_2 e_{q_\phi}(t-\tau) \tag{5.9}$$

Let $a = \frac{(I_y - I_z)}{I_x}$, then from (5.7), we get

$$\dot{e}_{q_\phi}(t) = a(e_{q_\theta} e_{q_\psi} + e_{q_\theta} q_{\psi_{\tau_b}} + e_{q_\psi} q_{\theta_{\tau_b}}) - k_2 e_{q_\phi}(t-\tau) \tag{5.10}$$

Similarly,

$$\begin{aligned}
\dot{e}_\theta(t) &= e_{q_\theta}(t) - k_3 e_\theta(t-\tau) \\
\dot{e}_{q_\theta}(t) &= b(e_{q_\phi} e_{q_\psi} + e_{q_\phi} q_{\psi_{\tau_b}} + e_{q_\psi} q_{\phi_{\tau_b}}) - k_4 e_{q_\theta}(t-\tau) \\
\dot{e}_\psi(t) &= e_{q_\psi}(t) - k_5 e_\psi(t-\tau) \\
\dot{e}_{q_\psi}(t) &= c(e_{q_\phi} e_{q_\theta} + e_{q_\phi} q_{\theta_{\tau_b}} + e_{q_\theta} q_{\phi_{\tau_b}}) - k_6 e_{q_\psi}(t-\tau)
\end{aligned} \tag{5.11}$$

where $b = \frac{I_z - I_x}{I_y}$ and $c = \frac{I_x - I_y}{I_z}$.
Let $e_R = [e_\phi \;\; e_{q_\phi} \;\; e_\theta \;\; e_{q_\theta} \;\; e_\psi \;\; e_{q_\psi}]^T$. It can be observed that $e_R = 0$ is an equilibrium point of the error dynamics. Therefore it will act as a state predictor if and only if $e_R = 0$ is an asymptotically stable equilibrium point. The linearized error dynamics is given by :

$$\begin{aligned}
\dot{e}_\phi(t) &= e_{q_\phi}(t) - k_1 e_\phi(t-\tau) \\
\dot{e}_{q_\phi}(t) &= a(e_{q_\theta} q_{\psi_{\tau_b}} + e_{q_\psi} q_{\theta_{\tau_b}}) - k_2 e_{q_\phi}(t-\tau) \\
\dot{e}_\theta(t) &= e_{q_\theta}(t) - k_3 e_\theta(t-\tau) \\
\dot{e}_{q_\theta}(t) &= b(e_{q_\phi} q_{\psi_{\tau_b}} + e_{q_\psi} q_{\phi_{\tau_b}}) - k_4 e_{q_\theta}(t-\tau) \\
\dot{e}_\psi(t) &= e_{q_\psi}(t) - k_5 e_\psi(t-\tau) \\
\dot{e}_{q_\psi}(t) &= c(e_{q_\phi} q_{\theta_{\tau_b}} + e_{q_\theta} q_{\phi_{\tau_b}}) - k_6 e_{q_\psi}(t-\tau)
\end{aligned} \tag{5.12}$$

The equilibrium point $e_R = 0$ is asymptotically stable for the original error dynamics if and only if it is an asymptotically stable equilibrium point for the linearized error dynamics (5.12). We will derive the sufficient condition for the equilibrium point $e_R = 0$ to be an asymptotically stable equilibrium point for the linearized error dynamics (5.12). The linearized error dynamics can be written in compact form as :

$$\dot{e}_R = -K_R e_R(t-\tau) + D \tag{5.13}$$

where $K_R = diag(k_1, k_2, k_3, k_4, k_5, k_6)$ and D is given by :

$$D = \begin{bmatrix} e_{q_\phi}(t) \\ a(e_{q_\theta} q_{\psi_{\tau_b}} + e_{q_\psi} q_{\theta_{\tau_b}}) \\ e_{q_\theta}(t) \\ b(e_{q_\phi} q_{\psi_{\tau_b}} + e_{q_\psi} q_{\phi_{\tau_b}}) \\ e_{q_\psi}(t) \\ c(e_{q_\phi} q_{\theta_{\tau_b}} + e_{q_\theta} q_{\phi_{\tau_b}}) \end{bmatrix}$$

One should note the following assumption before proceeding:

Assumption 3. *The magnitudes of angular velocities q_ϕ, q_θ and q_ψ are bounded.*

From Assumption 3, the norm of D can be written as :

$$\begin{aligned} ||D|| \leq & |e_{q_\phi}| + a_1|e_{q_\theta}| + a_2|e_{q_\psi}| + |e_{q_\theta}| + b_1|e_{q_\phi}| + b_2|e_{q_\psi}| \\ & + |e_{q_\psi}| + c_1|e_{q_\phi}| + c_2|e_{q_\theta}| \leq \gamma_1||e_R|| \end{aligned} \tag{5.14}$$

where $a_1 = max(a|q_{\psi_{\tau_b}}|)$, $a_2 = max(a|q_{\theta_{\tau_b}}|)$, $b_1 = max(b|q_{\psi_{\tau_b}}|)$, $b_2 = max(b|q_{\phi_{\tau_b}}|)$, $c_1 = max(c|q_{\theta_{\tau_b}}|)$, $c_2 = max(c|q_{\phi_{\tau_b}}|)$, $\gamma_1 = max((1 + b_1 + c_1), (1 + a_1 + c_2), (1 + a_2 + b_2))$.

5.4.2 Stability Proof for Rotational Subsystem

Proposition 5.1. *The state predictor* (5.6) *for the rotational subsystem with the error dynamics given by* (5.12) *for the state equation* (5.5) *is asymptotically stable if the following condition is satisfied :*

$$\lambda_m(K_R) - \lambda_m(K_R^2)\sqrt{q}\tau - \lambda_m(K_R)\gamma_1\tau - \gamma_1 > 0 \tag{5.15}$$

where $\lambda_m(\cdot)$ is the minimum eigenvalue of its argument.

Proof. Let us begin by observing that

$$e_R(t - \tau) = e_R(t) - \int_{t-\tau}^{t} \dot{e_R}(s)ds \tag{5.16}$$

Therefore,

$$\dot{e}_R = -K_R e_R - K_R^2 \int_{t-\tau}^{t} e_R(s - \tau)ds + K_R \int_{t-\tau}^{t} D(s)ds + D \tag{5.17}$$

Let us consider the following Lyapunov function candidate :

$$V_R = \frac{1}{2} e_R^T e_R \tag{5.18}$$

The time derivative of (5.18), along the solutions of (5.17) and using the relation $V_R(e_R(t+\zeta)) \leq qV_R(e_R(t))$ for all $-2\tau \leq \zeta \leq 0$ and $q > 1$, becomes :

$$\begin{aligned}
&\dot{V}_R = e_R^T \dot{e}_R \\
&= e_R^T(-K_R e_R - K_R^2 \int_{t-\tau}^{t} e_R(s-\tau)ds + K_R \int_{t-\tau}^{t} D(s)ds + D) \\
&\leq -\lambda_m(K_R)||e_R||^2 - e_R^T K_R^2 \int_{t-\tau}^{t} e_R(s-\tau)ds + e_R^T K_R \int_{t-\tau}^{t} ||D(s)||ds + 2||e_R||||D|| \\
&\leq -\lambda_m(K_R)||e_R||^2 + \lambda_m(K^2)\sqrt{q}\tau||e_R||^2 + \lambda_m(K)\gamma_1\tau||e_R||^2 + \gamma_1||e_R||^2 \\
&= -(\lambda_m(K_R) - \lambda_m(K_R^2)\sqrt{q}\tau - \lambda_m(K_R)\gamma_1\tau - \gamma_1)||e_R||^2
\end{aligned} \tag{5.19}$$

From Lyapunov Razumikhin theorem, one can conclude that the prediction error is asymptotically stable if $(\lambda_m(K_R) - \lambda_m(K_R^2)\sqrt{q}\tau - \lambda_m(K_R)\gamma_1\tau - \gamma_1) > 0$. This proves Proposition 5.1. □

5.4.3 Complete Error Dynamics

Let the prediction error for the translational subsystem be given by :

$$\begin{aligned}
e_x(t) &= \hat{x}(t-\tau) - x_{\tau_b}(t) \\
e_{q_x}(t) &= \bar{q}_x(t-\tau) - q_{x_{\tau_b}}(t) \\
e_y(t) &= \hat{y}(t-\tau) - y_{\tau_b}(t) \\
e_{q_y}(t) &= \bar{q}_y(t-\tau) - q_{y_{\tau_b}}(t) \\
e_z(t) &= \hat{z}(t-\tau) - z_{\tau_b}(t) \\
e_{q_z}(t) &= \bar{q}_z(t-\tau) - q_{z_{\tau_b}}(t)
\end{aligned} \tag{5.20}$$

Then the error dynamics is given by :

$$\dot{e}_x(t) = \dot{\hat{x}}(t-\tau) - \dot{x}_{\tau_b}(t) = e_{q_x}(t) - k_7 e_x(t-\tau)$$

and

$$\begin{aligned}
\dot{e}_{q_x} &= \dot{\hat{q}}_x(t-\tau) - \dot{q}_{x_{\tau_b}}(t) \\
&= \big(cos\hat{\phi}(t-\tau)sin\hat{\theta}(t-\tau)cos\hat{\psi}(t-\tau) + sin\hat{\phi}(t-\tau)sin\hat{\psi}(t-\tau) \\
&- cos\phi_{\tau_b}sin\theta_{\tau_b}cos\psi_{\tau_b} - sin\phi_{\tau_b}sin\psi_{\tau_b}\big)\frac{U_1(t-\tau)}{m} - k_8 e_{q_x}(t-\tau) \\
&= \Bigg(cos(e_\phi + \phi_{\tau_b})sin(e_\theta + \theta_{\tau_b})cos(e_\psi + \psi_{\tau_b}) + sin(e_\phi + \phi_{\tau_b}) \\
&sin(e_\psi + \psi_{\tau_b}) - cos\phi_{\tau_b}sin\theta_{\tau_b}cos\psi_{\tau_b} - sin\phi_{\tau_b}sin\psi_{\tau_b}\Bigg)\frac{U_1(t-\tau)}{m} - k_8 e_{q_x}(t-\tau)
\end{aligned}$$

The linearization of the above equation is

$$\begin{aligned}
\dot{e}_{q_x} &= \Bigg((-sin\phi_{\tau_b}sin\theta_{\tau_b}cos\psi_{\tau_b} + cos\phi_{\tau_b}sin\psi_{\tau_b})e_\phi + (cos\phi_{\tau_b}cos\theta_{\tau_b}cos\psi_{\tau_b})e_\theta \\
&+ (-cos\phi_{\tau_b}sin\theta_{\tau_b}sin\psi_{\tau_b} + sin\phi_{\tau_b}cos\psi_{\tau_b})e_\psi\Bigg)\frac{U_1(t-\tau)}{m} - k_8 e_{q_x}(t-\tau) \\
&= EU_1(t-\tau) - k_8 e_{q_x}(t-\tau) \qquad (5.21)
\end{aligned}$$

where

$$\begin{aligned}
E =& \frac{(-sin\phi_{\tau_b}sin\theta_{\tau_b}cos\psi_{\tau_b} + cos\phi_{\tau_b}sin\psi_{\tau_b})e_\phi + (cos\phi_{\tau_b}cos\theta_{\tau_b}cos\psi_{\tau_b})e_\theta}{m} \\
&+ \frac{(-cos\phi_{\tau_b}sin\theta_{\tau_b}sin\psi_{\tau_b} + sin\phi_{\tau_b}cos\psi_{\tau_b})e_\psi}{m} \qquad (5.22)
\end{aligned}$$

The magnitude of E is bounded by

$$|E| \leq \frac{2}{m}|e_\phi| + \frac{1}{m}|e_\theta| + \frac{2}{m}|e_\psi| \leq \frac{2}{m}(|e_\phi| + |e_\theta| + |e_\psi|) \qquad (5.23)$$

Similarly,

$$\dot{e}_y(t) = e_{q_y}(t) - k_9 e_y(t-\tau) \qquad (5.24)$$

$$\dot{e}_{q_y} = FU_1(t-\tau) - k_{10} e_{q_y}(t-\tau) \qquad (5.25)$$

$$\dot{e}_z(t) = e_{q_z}(t) - k_{11} e_z(t-\tau) \qquad (5.26)$$

$$\dot{e}_{q_y} = GU_1(t-\tau) - k_{12} e_{q_y}(t-\tau) \qquad (5.27)$$

where

$$F = \frac{(-sin\phi_{\tau_b} sin\theta_{\tau_b} sin\psi_{\tau_b} - cos\phi_{\tau_b} cos\psi_{\tau_b})e_\phi + (cos\phi_{\tau_b} cos\theta_{\tau_b} sin\psi_{\tau_b})e_\theta}{m} + \frac{(cos\phi_{\tau_b} sin\theta_{\tau_b} cos\psi_{\tau_b} + sin\phi_{\tau_b} sin\psi_{\tau_b})e_\psi}{m} \tag{5.28}$$

and

$$G = \frac{\left(- sin\phi_{\tau_b} cos\theta_{\tau_b} e_\phi - cos\phi_{\tau_b} sin\theta_{\tau_b} e_\theta \right)}{m} \tag{5.29}$$

The magnitudes of F and G are bounded by

$$|F| \leq \frac{2}{m}|e_\phi| + \frac{1}{m}|e_\theta| + \frac{2}{m}|e_\psi| \leq \frac{2}{m}(|e_\phi| + |e_\theta| + |e_\psi|) \tag{5.30}$$

$$|G| \leq \frac{1}{m}(|e_\phi| + |e_\theta|) \tag{5.31}$$

Therefore the linearized dynamics for the translational subsystem is given by :

$$\begin{aligned}
\dot{e}_x(t) &= e_{q_x}(t) - k_7 e_x(t-\tau) \\
\dot{e}_{q_x} &= EU_1(t-\tau) - k_8 e_{q_x}(t-\tau) \\
\dot{e}_y(t) &= e_{q_y}(t) - k_9 e_y(t-\tau) \\
\dot{e}_{q_y} &= FU_1(t-\tau) - k_{10} e_{q_y}(t-\tau) \\
\dot{e}_z(t) &= e_{q_z}(t) - k_{11} e_z(t-\tau) \\
\dot{e}_{q_y} &= GU_1(t-\tau) - k_{12} e_{q_y}(t-\tau)
\end{aligned} \tag{5.32}$$

Let $e_X = [e_x \quad e_{q_x} \quad e_y \quad e_{q_y} \quad e_z \quad e_{q_z}]^T$ and $e = [e_X \quad e_R]^T$. It can be observed that $e = 0$ is an equilibrium point of the linearized error dynamics. Therefore, it will act as a state predictor if and only if $e = 0$ is an asymptotically stable equilibrium point. The equilibrium point $e = 0$ is asymptotically stable for the original error dynamics if and only if it is an asymptotically stable equilibrium point for the linearized error dynamics (5.12) and (5.32). We will derive the sufficient condition for the equilibrium point $e = 0$ to be an asymptotically stable equilibrium point for the linearized error dynamics (5.12) and (5.32). The linearized error dynamics of the complete system can be written in compact form as :

$$\dot{e} = -Ke(t-\tau) + H \tag{5.33}$$

where $K = diag\{k_i\}$ for $i = 1 \cdots 12$, and

$$H = \begin{bmatrix} e_{q_x}(t) \\ EU_1(t-\tau) \\ e_{q_y}(t) \\ FU_1(t-\tau) \\ e_{q_z}(t) \\ GU_1(t-\tau) \\ D \end{bmatrix}$$

Assumption 4. *The magnitude of control input U_1 is bounded i.e. $|U_1| \leq \bar{U}$.*

From Assumption 4, the norm of H is bounded as shown below :

$$||H|| \leq |e_{q_x}| + |E|\bar{U} + |e_{q_y}| + |F|\bar{U} + |e_{q_z}| + |G|\bar{U} + ||D|| \tag{5.34}$$

Substituting the values of $|E|, |F|$ and $|G|$, one gets,

$$\begin{aligned} ||H|| &\leq |e_{q_x}| + |e_{q_y}| + |e_{q_z}| + 5\bar{U}|e_\phi| + 3\bar{U}|e_\theta| + 4\bar{U}|e_\psi| + \gamma_1||e_R|| \\ &\leq \gamma_2||e|| + \gamma_1||e|| \leq \gamma||e|| \end{aligned} \tag{5.35}$$

where $\gamma_2 = max\{1, 5\bar{U}\}$ and $\gamma = \{\gamma_1 + \gamma_2\}$.

5.4.4 Stability Proof for Complete System

Proposition 5.2. *The state predictor* (5.6) *for the complete system with the error dynamics given by* (5.12) *and* (5.32) *for the state equation* (5.5) *is asymptotically stable if the following condition is satisfied :*

$$\lambda_m(K) - \lambda_m(K^2)\sqrt{q}\tau - \lambda_m(K)\gamma\tau - \gamma > 0 \tag{5.36}$$

where $\lambda_m(\cdot)$ is the minimum eigenvalue of its argument.

Proof. Let us begin by observing that

$$e(t-\tau) = e(t) - \int_{t-\tau}^{t} \dot{e}(s)ds \tag{5.37}$$

Therefore,

$$\dot{e} = -Ke - K^2 \int_{t-\tau}^{t} e(s-\tau)ds + K \int_{t-\tau}^{t} H(s)ds + H \tag{5.38}$$

Let us consider the following Lyapunov function candidate :

$$V = \frac{1}{2}e^T e \tag{5.39}$$

The time derivative of (5.39) along the solutions of (5.38) and using the relation $V(e(t+\zeta)) \leq qV(e(t))$ for all $-2\tau \leq \zeta \leq 0$ and $q > 1$ becomes :

$$\begin{aligned}
\dot{V} &= e^T\dot{e} \\
&= e^T(-Ke - K^2\int_{t-\tau}^{t} e(s-\tau)ds + K\int_{t-\tau}^{t} H(s)ds + H) \\
&\leq -\lambda_m(K)||e||^2 - e^T K^2\int_{t-\tau}^{t} e(s-\tau)ds + e^T K\int_{t-\tau}^{t} ||H(s)||ds + ||e||||H|| \\
&\leq -\lambda_m(K)||e||^2 + \lambda_m(K^2)\sqrt{q}\tau||e||^2 + \lambda_m(K)\gamma\tau||e||^2 + \gamma||e||^2 \\
&= -(\lambda_m(K) - \lambda_m(K^2)\sqrt{q}\tau - \lambda_m(K)\gamma\tau - \gamma)||e_R||^2
\end{aligned} \tag{5.40}$$

From Lyapunov Razumikhin theorem, one can conclude that the prediction error is asymptotically stable if $(\lambda_m(K) - \lambda_m(K^2)\sqrt{q}\tau - \lambda_m(K)\gamma\tau - \gamma) > 0$. This proves Proposition 5.2. □

5.5 Controller Design

In this section, a control law based on the backstepping technique is designed to enable the quadrotor to track a reference trajectory. The control design technique for the whole system is divided into the control design technique of three subsystems. First, we will design the control law for the z-subsystem, and the heading direction, i.e., $\psi-$ subsystem, since both $z-$ and $\psi-$ subsystems are independent of other subsystems. Finally, we will design the control law for the horizontal subsystem, i.e., $x-\phi$ and $y-\theta$ subsystem, since these are dependent on each other. Let us start by giving the state space representation of (1.3) neglecting gyroscopic effects. Let $x_1 = \phi, x_2 = \dot{\phi}, x_3 = \theta, x_4 = \dot{\theta}, x_5 = \psi, x_6 = \dot{\psi}, x_7 = x, x_8 = \dot{x}, x_9 = y, x_{10} = \dot{y}, x_{11} = z, x_{12} = \dot{z}, a = \frac{I_y - I_z}{I_x}, b =$

$\frac{I_z-I_x}{I_y}, c = \frac{I_x-I_y}{I_z}$, then the state space representation is given by :

$$\begin{aligned}
\dot{x}_1 &= x_2 \quad & \dot{x}_2 &= ax_4x_6 + \frac{l}{I_x}U_2 \\
\dot{x}_3 &= x_4 \quad & \dot{x}_4 &= bx_2x_6 + \frac{l}{I_x}U_3 \\
\dot{x}_5 &= x_6 \quad & \dot{x}_6 &= cx_2x_4 + \frac{1}{I_z}U_4 \\
\dot{x}_7 &= x_8 \quad & \dot{x}_8 &= (cosx_1\ sinx_3\ cosx_5 + sinx_1\ sinx_5)\frac{1}{m}U_1 \\
\dot{x}_9 &= x_{10} \quad & \dot{x}_{10} &= (cosx_1\ sinx_3\ sinx_5 - sinx_1\ cosx_5)\frac{1}{m}U_1 \\
\dot{x}_{11} &= x_{12} \quad & \dot{x}_{12} &= -g + (cosx_1\ cosx_5)\frac{1}{m}U_1
\end{aligned} \tag{5.41}$$

Let us proceed towards the control design in a step wise manner. In the following sections all the $c_i's$ for $i = 1 \cdots 12$ are positive constants. The control law has been designed, assuming that there is no delay in the state and input. In actual implementation, the states in the control input are replaced by the output of the state predictor proposed in the previous section.

5.5.1 $Z-$subsystem

The $Z-$ subsystem is given by :

$$\dot{x}_{11} = x_{12} \quad \dot{x}_{12} = -g + (cosx_1 cosx_5)\frac{1}{m}U_1 \tag{5.42}$$

Let the error variables be given by :

$$z_1 = x_{11} - z_d \qquad z_2 = x_{12} - \alpha_1 - \dot{z}_d \tag{5.43}$$

where z_d is the reference position and α_1 is the virtual control variable. Then,

$$\dot{z}_1 = \dot{x}_{11} - \dot{z}_d = x_{12} - \dot{z}_d = z_2 + \alpha_1 \tag{5.44}$$

Let the Lyapunov function for the first subsystem be given by :

$$V_1 = \frac{1}{2}z_1^2 \tag{5.45}$$

The time derivative of above Lyapunov function along the subsystem trajectory is given by :

$$\dot{V}_1 = z_1\dot{z}_1 = z_1(z_2 + \alpha_1) \tag{5.46}$$

Let us choose $\alpha_1 = -c_1 z_1$. Such a choice will become apparent in the next step. Then,

$$\dot{V}_1 = z_1 z_2 - c_1 z_1^2 \tag{5.47}$$

The time derivative of α_1 is given by :

$$\dot{\alpha}_1 = -c_1\dot{z}_1 = -c_1 x_{12} + c_1\dot{z}_d \tag{5.48}$$

To design the control input, consider the following Lyapunov function candidate for the whole subsystem :

$$V_2 = V_1 + \frac{1}{2}z_2^2 \tag{5.49}$$

Then, the time derivative of the above Lyapunov function candidate along the system trajectories become :

$$\begin{aligned}\dot{V}_2 &= z_1 z_2 - c_1 z_1^2 + z_2(\dot{x}_{12} - \dot{\alpha}_1 - \ddot{z}_d) \\ &= z_1 z_2 - c_1 z_1^2 + z_2(-g + cosx_1 cosx_3\frac{U_1}{m} + c_1 x_{12} - c_1\dot{z}_d - \ddot{z}_d)\end{aligned} \tag{5.50}$$

If we choose

$$U_1 = \frac{m}{cosx_1 cosx_3}(g - z_1 - c_2 z_2 - c_1 x_{12} + c_1\dot{z}_d + \ddot{z}_d) \tag{5.51}$$

Then $\dot{V}_2$ becomes :

$$\dot{V}_2 = -c_1 z_1^2 - c_2 z_2^2 < 0 \tag{5.52}$$

Therefore, the $z-$ subsystem becomes asymptotically stable and $z \to z_d$ as $t \to \infty$.

5.5.2 Heading($\psi-$) Subsystem

The $\psi-$ subsystem is given by :

$$\dot{x}_5 = x_6 \qquad \dot{x}_6 = cx_2 x_4 + \frac{1}{I_z}U_4 \tag{5.53}$$

Let us take the error variables to be :

$$z_3 = x_5 - \psi_d \qquad z_4 = x_6 - \alpha_2 - \dot{\psi}_d \tag{5.54}$$

where ψ_d is the reference heading direction and α_2 is the virtual control variable. Then,

$$\dot{z}_3 = \dot{x}_5 - \dot{\psi}_d = x_6 - \dot{\psi}_d = z_4 + \alpha_2 \tag{5.55}$$

Consider the following Lyapunov function for the first subsystem :

$$V_3 = \frac{1}{2} z_3^2 \tag{5.56}$$

The time derivative of above Lyapunov function is given by :

$$\dot{V}_3 = z_3 \dot{z}_3 = z_3(z_4 + \alpha_2) \tag{5.57}$$

Let us choose $\alpha_2 = -c_3 z_3$. Then,

$$\dot{V}_3 = z_3 z_4 - c_3 z_3^2 \tag{5.58}$$

The time derivative of α_2 is given by :

$$\dot{\alpha}_2 = -c_3 \dot{z}_3 = -c_3 x_6 + c_3 \dot{\psi}_d \tag{5.59}$$

Consider the following Lyapunov function candidate for the whole subsystem :

$$V_4 = V_3 + \frac{1}{2} z_4^2 \tag{5.60}$$

Then,

$$\begin{aligned} \dot{V}_4 &= z_3 z_4 - c_3 z_3^2 + z_4(\dot{x}_6 - \dot{\alpha}_2 - \ddot{\psi}_d) \\ &= z_3 z_4 - c_3 z_3^2 + z_4(c x_2 x_4 + c_3 x_6 - c_3 \dot{\psi}_d + \frac{1}{I_z} U_4 - \ddot{\psi}_d) \end{aligned} \tag{5.61}$$

Let us choose

$$U_4 = I_z(-c x_2 x_4 - c_3 x_6 + c_3 \dot{\psi}_d + \ddot{\psi}_d - z_3 - c_4 z_4) \tag{5.62}$$

then $\dot{V}_4$ becomes :

$$\dot{V}_4 = -c_3 z_3^2 - c_4 z_4^2 < 0 \tag{5.63}$$

Therefore, $\psi \to \psi_d$ as $t \to \infty$.

5.5.3 Horizontal Subsystem

Since the control input U_1 appears in the dynamics of both $x-$ and $y-$ subsystem, the quadrotor dynamics are underactuated. Instead of designing the control input U_1, we will design the virtual control inputs u_x and u_y defined below.

$$\begin{aligned} u_x &= cosx_1 sinx_3 cosx_5 + sinx_1 sinx_5 \\ u_y &= cosx_1 sinx_3 sinx_5 - sinx_1 cosx_5 \end{aligned} \tag{5.64}$$

Therefore, the state representation for the horizontal subsystem becomes :

$$\begin{aligned} \dot{x}_7 &= x_8 \quad \dot{x}_8 = u_x \frac{1}{m} U_1 \\ \dot{x}_9 &= x_{10} \quad \dot{x}_{10} = u_y \frac{1}{m} U_1 \end{aligned} \tag{5.65}$$

Let $u = [u_x \;\; u_y]^T$,

$$M = \begin{bmatrix} cosx_5 & sinx_5 \\ sinx_5 & -cosx_5 \end{bmatrix}$$

and

$$v = \begin{bmatrix} cosx_1 sinx_3 \\ sinx_1 \end{bmatrix}$$

Then,

$$u = Mv \implies v = M^{-1}u \tag{5.66}$$

Therefore, the desired roll and pitch angles are given by :

$$\phi_d = sin^{-1}[v(2)] \;\text{ and }\; \theta_d = sin^{-1}\left[\frac{v(1)}{cos\phi_d}\right] \tag{5.67}$$

These desired values will be used while designing the control law for $\phi-$ and $\theta-$ subsystem.

5.5.4 $Y-$subsystem

The state representation for the $Y-$ subsystem is :

$$\dot{x}_9 = x_{10} \quad \dot{x}_{10} = u_y \frac{1}{m} U_1 \tag{5.68}$$

We have to design u_y for asymptotic tracking of $y-$ subsystem. Let the error variables be given by :

$$z_5 = x_9 - y_d \qquad z_6 = x_{10} - \alpha_3 - \dot{y}_d \tag{5.69}$$

where y_d is the reference position and α_3 is the virtual control variable. Then,

$$\dot{z}_5 = \dot{x}_9 - \dot{y}_d = x_{10} - \dot{y}_d = z_6 + \alpha_3 \tag{5.70}$$

Let the Lyapunov function for the first subsystem be given by :

$$V_5 = \frac{1}{2} z_5^2 \tag{5.71}$$

Then,

$$\dot{V}_5 = z_5 \dot{z}_5 = z_5(z_6 + \alpha_3) \tag{5.72}$$

Choose $\alpha_3 = -c_5 z_5$. Then,

$$\dot{V}_5 = z_5 z_6 - c_5 z_5^2 \tag{5.73}$$

The time derivative of α_3 is given by :

$$\dot{\alpha}_3 = -c_5 \dot{z}_5 = -c_5 x_{10} + c_5 \dot{y}_d \tag{5.74}$$

Consider the following Lyapunov function candidate :

$$V_6 = V_5 + \frac{1}{2} z_6^2 \tag{5.75}$$

Then, the time derivative of the above Lyapunov function candidate along the system trajectories become :

$$\begin{aligned} \dot{V}_6 &= z_5 z_6 - c_5 z_5^2 + z_6(\dot{x}_{10} - \dot{\alpha}_3 - \ddot{y}_d) \\ &= z_5 z_6 - c_5 z_5^2 + z_6(\frac{u_y}{m} U_1 + c_5 x_{10} - c_5 \dot{y}_d - \ddot{y}_d) \end{aligned} \tag{5.76}$$

Choose

$$u_y = \frac{m}{U_1}(-c_5 x_{10} + c_5 \dot{y}_d + \ddot{y}_d - c_6 z_6 - z_5) \tag{5.77}$$

then $\dot{V}_6$ becomes :

$$\dot{V}_6 = -c_5 z_5^2 - c_6 z_6^2 < 0 \tag{5.78}$$

Therefore, the $y-$ subsystem becomes asymptotically stable and $y \to y_d$ as $t \to \infty$.

5.5.5 $X-$ subsystem

The $X-$ subsystem is :

$$\dot{x}_7 = x_8 \qquad \dot{x}_8 = u_x \frac{1}{m} U_1 \tag{5.79}$$

Again we have to design u_x for asymptotic tracking of $x-$ subsystem. Let the error variables be given by :

$$z_7 = x_7 - x_d \qquad z_8 = x_8 - \alpha_4 - \dot{x}_d \tag{5.80}$$

where x_d is the reference position and α_4 is the virtual control variable. Then,

$$\dot{z}_7 = \dot{x}_7 - \dot{x}_d = x_8 - \dot{x}_d = z_8 + \alpha_4 \tag{5.81}$$

Let the Lyapunov function for the first subsystem be given by :

$$V_7 = \frac{1}{2} z_7^2 \tag{5.82}$$

The time derivative is given by :

$$\dot{V}_7 = z_7 \dot{z}_7 = z_7 (z_8 + \alpha_4) \tag{5.83}$$

Let us choose $\alpha_4 = -c_7 z_7$. Then,

$$\dot{V}_5 = z_7 z_8 - c_7 z_7^2 \tag{5.84}$$

Also,

$$\dot{\alpha}_4 = -c_7 \dot{z}_7 = -c_7 x_8 + c_7 \dot{x}_d \tag{5.85}$$

Consider the following Lyapunov function candidate to design the control input :

$$V_8 = V_7 + \frac{1}{2} z_8^2 \tag{5.86}$$

Then, the time derivative of the above Lyapunov function becomes :

$$\begin{aligned}\dot{V}_8 &= z_7 z_8 - c_7 z_7^2 + z_8(\dot{x}_8 - \dot{\alpha}_4 - \ddot{x}_d) \\ &= z_7 z_8 - c_7 z_7^2 + z_8(\frac{u_x}{m} U_1 + c_7 x_8 - c_7 \dot{x}_d - \ddot{x}_d)\end{aligned} \tag{5.87}$$

Let us choose

$$u_x = \frac{m}{U_1}(-c_7 x_8 + c_7 \dot{x}_d + \ddot{x}_d - c_8 z_8 - z_7) \tag{5.88}$$

then $\dot{V}_8$ becomes :

$$\dot{V}_8 = -c_7 z_7^2 - c_8 z_8^2 < 0 \tag{5.89}$$

Therefore, the $x-$ subsystem becomes asymptotically stable and $x \to x_d$ as $t \to \infty$.

5.5.6 $\phi-$ Subsystem

The $\phi-$ subsystem is given by :

$$\dot{x}_1 = x_2 \qquad \dot{x}_2 = a x_4 x_6 + \frac{l}{I_x} U_2 \tag{5.90}$$

The error variables are defined as :

$$z_9 = x_1 - \phi_d \qquad z_{10} = x_2 - \alpha_5 - \dot{\phi}_d \tag{5.91}$$

where ϕ_d is the reference roll angle and α_5 is the virtual control variable. Then,

$$\dot{z}_9 = \dot{x}_1 - \dot{\phi}_d = x_2 - \dot{\psi}_d = z_{10} + \alpha_5 \tag{5.92}$$

Let the Lyapunov function for the first subsystem be given by :

$$V_9 = \frac{1}{2} z_9^2 \tag{5.93}$$

Then,

$$\dot{V}_9 = z_9 \dot{z}_9 = z_9(z_{10} + \alpha_5) \tag{5.94}$$

Let us choose $\alpha_5 = -c_9 z_9$. Then,

$$\dot{V}_9 = z_9 z_{10} - c_9 z_9^2 \tag{5.95}$$

Let us calculate the time derivative of α_5 :

$$\dot{\alpha}_5 = -c_9\dot{z}_9 = -c_9x_2 + c_9\dot{\phi}_d \tag{5.96}$$

Consider the following Lyapunov function candidate for the whole subsystem :

$$V_{10} = V_9 + \frac{1}{2}z_{10}^2 \tag{5.97}$$

Then, its time derivative becomes :

$$\begin{aligned}\dot{V}_{10} &= z_9z_{10} - c_9z_9^2 + z_{10}(\dot{x}_2 - \dot{\alpha}_5 - \ddot{\phi}_d) \\ &= z_9z_{10} - c_9z_9^2 + z_{10}(ax_4x_6 + c_9x_2 - c_9\dot{\phi}_d + \frac{l}{I_x}U_2 - \ddot{\phi}_d)\end{aligned} \tag{5.98}$$

If we choose

$$U_2 = \frac{I_x}{l}(-ax_4x_6 - c_9x_2 + c_9\dot{\phi}_d + \ddot{\phi}_d - z_9 - c_{10}z_{10}) \tag{5.99}$$

then $\dot{V}_{10}$ is :

$$\dot{V}_{10} = -c_9z_9^2 - c_{10}z_{10}^2 < 0 \tag{5.100}$$

Therefore, $\phi \to \phi_d$ as $t \to \infty$.

5.5.7 $\theta-$ Subsystem

The $\theta-$ subsystem is :

$$\dot{x}_3 = x_4 \qquad \dot{x}_4 = bx_2x_6 + \frac{l}{I_y}U_3 \tag{5.101}$$

The error variables are :

$$z_{11} = x_3 - \theta_d \qquad z_{12} = x_4 - \alpha_6 - \dot{\theta}_d \tag{5.102}$$

where θ_d is the reference pitch angle and α_6 is the virtual control variable. Then,

$$\dot{z}_{11} = \dot{x}_3 - \dot{\theta}_d = x_4 - \dot{\theta}_d = z_{12} + \alpha_6 \tag{5.103}$$

Let the Lyapunov function for the first subsystem be given by :

$$V_{11} = \frac{1}{2} z_{11}^2 \tag{5.104}$$

Its time derivative is given by :

$$\dot{V}_{11} = z_{11}\dot{z}_{11} = z_{11}(z_{12} + \alpha_6) \tag{5.105}$$

Choose $\alpha_6 = -c_{11}z_{11}$. Then,

$$\dot{V}_{11} = z_{11}z_{12} - c_{11}z_{11}^2 \tag{5.106}$$

Also,

$$\dot{\alpha}_6 = -c_{11}\dot{z}_{11} = -c_{11}x_4 + c_{11}\dot{\theta}_d \tag{5.107}$$

Consider the following Lyapunov function candidate :

$$V_{12} = V_{11} + \frac{1}{2} z_{12}^2 \tag{5.108}$$

Then, its time derivative become :

$$\begin{aligned} \dot{V}_{12} &= z_{11}z_{12} - c_{11}z_{11}^2 + z_{12}(\dot{x}_4 - \dot{\alpha}_6 - \ddot{\theta}_d) \\ &= z_{11}z_{12} - c_{11}z_{11}^2 + z_{12}(bx_2x_6 + c_{11}x_4 - c_{11}\dot{\theta}_d + \frac{l}{I_y}U_3 - \ddot{\theta}_d) \end{aligned} \tag{5.109}$$

Let us choose

$$U_3 = \frac{I_y}{l}(-bx_2x_6 - c_{11}x_4 + c_{11}\dot{\theta}_d + \ddot{\theta}_d - z_{11} - c_{12}z_{12}) \tag{5.110}$$

Then $\dot{V}_{12}$ becomes :

$$\dot{V}_{12} = -c_{11}z_{11}^2 - c_{12}z_{12}^2 < 0 \tag{5.111}$$

Therefore, the $\theta-$ subsystem becomes asymptotically stable and $\theta \to \theta_d$ as $t \to \infty$.

5.6 Numerical Simulations

A numerical simulation was performed to test the validity of the proposed controller augmented with the state predictor. The simulation was done in MATLAB/SIMULINK

Table 5.1: Parameters used in simulation

Parameter	**Values**	**Units**	**Parameter**	**Values**	**Units**
g	9.81	m/s^2	I_x	4.1 $\times 10^{-3}$	kg m^2
m	0.468	kg	I_y	4.1 $\times 10^{-3}$	kg m^2
$c_i\{i \ \ even\}$	2	-	I_z	8.8 $\times 10^{-3}$	kg m^2
$k_i\{i \ \ odd\}$	4	-	$c_i\{i \ \ odd\}$	5	-
$k_i\{i \ \ even\}$	2	-	l	0.225	-

with an integration step size of 0.001 sec. The input, as well as the state delay, was taken to be $\tau_b = \tau_f = 0.1$ sec. Therefore, $\tau = 0.2$ sec. A table of parameters used in the simulation is shown in Table. 5.1. The state predictor was initialized with the same initial condition as that of the system. The initial condition for the system was taken to be $[\phi(0); \theta(0); \psi(0); x(0); y(0); z(0)] = [\pi/4, \pi/4, \pi/4, 0, 0, 0]$ and $[\dot{\phi}(0); \dot{\theta}(0); \dot{\psi}(0); \dot{x}(0); \dot{y}(0); \dot{z}(0)] = [0, 0, 0, 0, 0, 0]$. The desired trajectory was specified to be

$$x_d = y_d = z_d = 2m \ \text{ and } \ \psi_d = \pi/4, \phi_d = 0, \theta_d = 0$$
$$\dot{x}_d = \dot{y}_d = \dot{z}_d = 0 \ \text{ and } \ \dot{\psi}_d = \dot{\phi}_d = \dot{\theta}_d = 0$$

It can be observed from Fig.5.2 that the trajectory tracking performance is quite good, and the final trajectory converges to the desired trajectory within 10 sec. The predicted values of the state are also shown in Fig. 5.3, and it can be observed that the predicted values converge to the desired value within 10 sec, and error in prediction goes to zero in less than 10 sec. The transient performances of both the controller and the predictor are also satisfactory. For example, both the controller and the predictor's peak overshoots are within 20% while the settling times are within 10 sec. The rise time is also within 5 sec. These can be varied with predictor and controller gains. This shows the satisfactory performance of both the controller and the predictor in terms of transient response. The control inputs and the virtual input are plotted in Fig.5.4, which is seen to be continuous, finite, and bounded and hence realizable in practice. Since there is no change in ψ_d and $\psi(0)$, the control input $U_4 = 0$ all the time, it can be concluded that the state predictor successfully predicts the future values of the state. Hence, the controller can steer the quadrotor to the desired position and orientation successfully. The control laws proposed in the literature cannot stabilize a quadrotor in the presence of input and state delays. Hence, the proposed method of predictor and controller is superior to the controllers present in the literature.

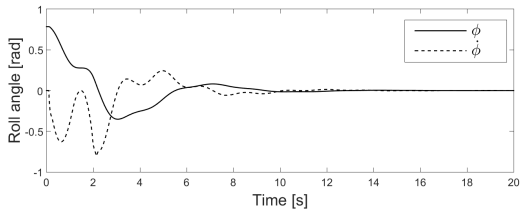

(a)

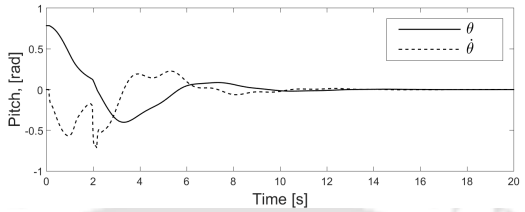

(b)

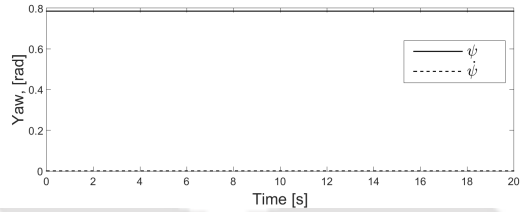

(c)

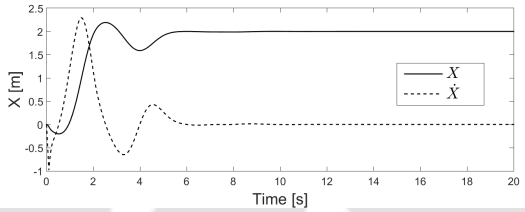

(d)

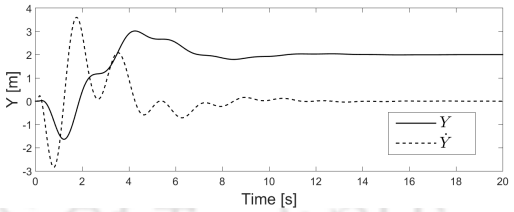

(e)

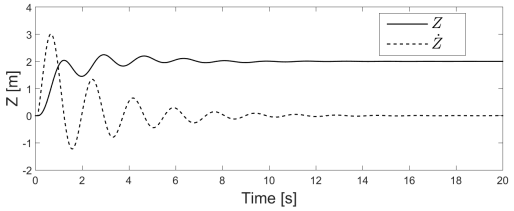

(f)

Figure 5.2: Outputs (a) Roll,$\phi[rad]$; (b) Pitch, $\theta[rad]$; (c) Yaw, $\psi[rad]$;(d) X [m] ; (e) Y [m] ; (f) Z [m].

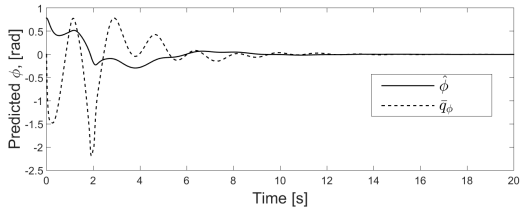

(a)

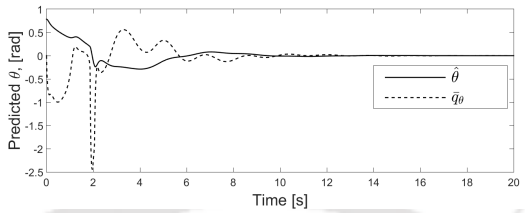

(b)

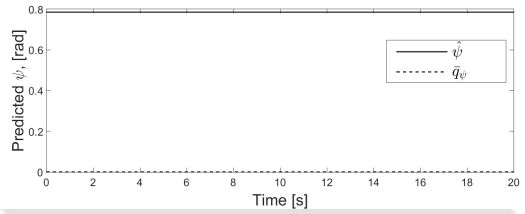

(c)

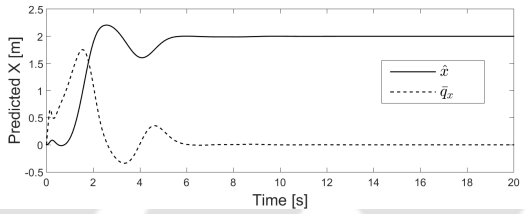

(d)

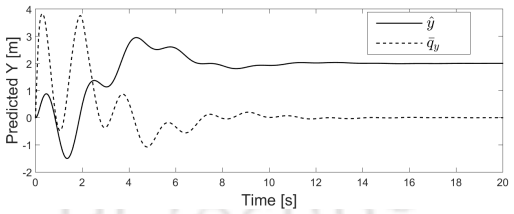

(e)

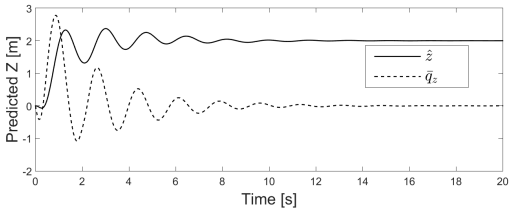

(f)

Figure 5.3: Predicted states $(a)\phi[rad]; (b)\theta[rad]; (c)\psi[rad]$; (d) X[m] ; (e) Y[m] ; (f) Z[m].

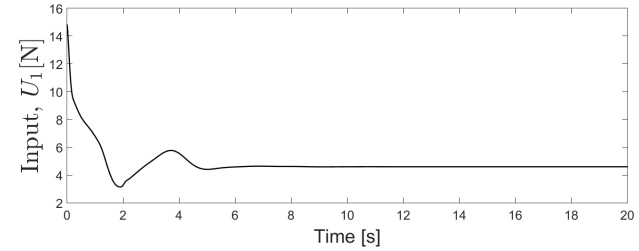

(a)

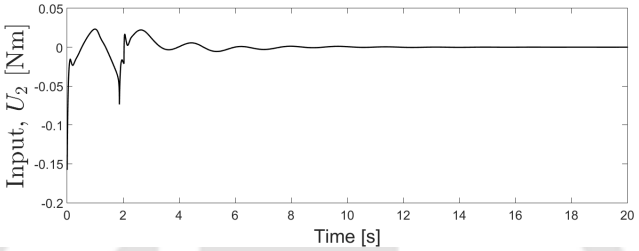

(b)

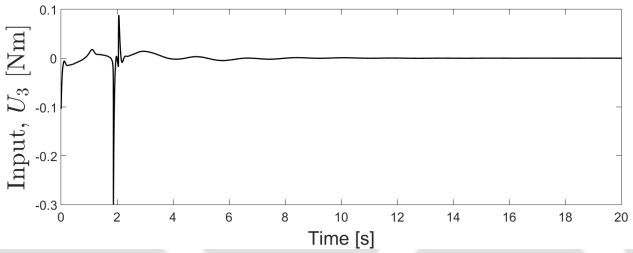

(c)

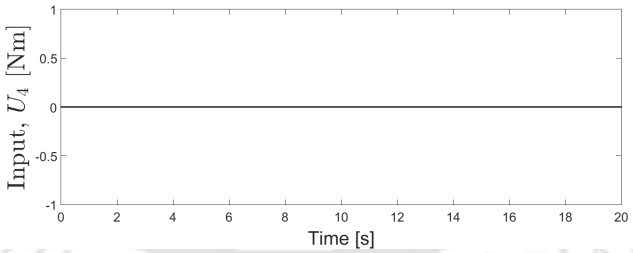

(d)

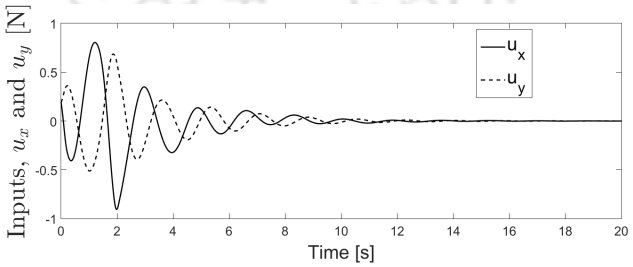

(e)

Figure 5.4: *Inputs*$(a)U_1; (b)U_2; (c)U_3; (d)U_4; (e)u_x, u_y$

5.6.1 Discussion of Results

As shown in the numerical simulations, the controller predictor pair can steer a quadrotor from origin to a desired position and orientation even in the presence of state and input delay. One can observe from Fig.5.1 that the controller and predictor pair are located at a remote location, and the quadrotor is equipped with a local controller to control its motor speed only. The approach results in the remote steering of a quadrotor from an initial configuration to a final configuration. In the simulation, we have taken the forward and backward transmission delay to be 0.1 sec, but the approach is valid for asymmetric time delay also, i.e., different delays in forward and backward transmission. We have taken a small time delay for demonstration purposes, but the same asymptotic tracking is achieved even in the presence of a long time delay. For example, a delay of 1 sec also results in asymptotic tracking performance. One can extend the backstepping controller presented to handle the external disturbances and parametric uncertainty. For instance, one can implement an adaptive backstepping controller to handle the uncertainties. The controller predictor pair architecture is scalable and can be easily extended to multi-agent systems. One can operate multiple quadrotors with this architecture by employing a centralized controller predictor pair, as shown in Fig.5.1. The central controller will calculate each quadrotor's desired control command and send it to the respective quadrotor via the wireless network. The local controller in the quadrotor will implement such a command. One can even control other robotic devices such as robotic manipulators, wheeled mobile robots, inverted pendulum with this architecture. The results demonstrate a method for the teleoperation of such robotic devices.

5.6.2 Comparison to existing literature

Almost all the controllers proposed for tracking control of a quadrotor do not consider input time delay or state delay. Since time delay results in instability of the system, the controllers proposed in the literature become unstable in the presence of time delay, whereas the proposed controller is not only stable but asymptotically stable. The literature [62, 63] consider input as well as state delay as a disturbance to the system, and the authors design a robust compensating term to take care of delays. Compared to this approach, the proposed design is superior because of the following reasons:

1. The mentioned literature does not consider network delay as such. Their approach is valid only for the small-time delay, but the proposed approach is valid for the large delay. In fact, the proposed predictor controller pair is able to perform satisfactorily even when the delay is 1 sec, while the controller proposed in the mentioned literature becomes unstable in the presence of a delay of 1 sec.

2. The mentioned literature has designed a controller only for attitude dynamics, whereas the author has designed the control law for both attitude and translational dynamics. Therefore the proposed approach is valid for trajectory tracking control of a quadrotor in three-dimensional space.
3. Moreover, the proposed approach is simple and intuitive and can be easily scaled to multi-agent systems.

5.7 Conclusion

A state predictor controller pair is developed to control a quadrotor in the presence of network-induced state and input time delay. To the best of the authors' knowledge, this study is the first to explicitly compensate for both states and input time delay in a quadrotor system. The state predictor is shown to be asymptotically stable and hence is able to estimate the future values of the states. The output of the predictor is used while implementing the controller developed in this chapter. The controller is also shown to be asymptotically stable. Through simulations, it is observed that the quadrotor's satisfactory steering is obtained with a controller augmented with the predictor in the presence of state and input delay. The future work will deal with controller design even in the presence of packet loss experienced while operating over a TCP network. Moreover, we have not considered parametric uncertainty in the estimator as well as controller design. The effect of parametric uncertainly will also be considered in future work.

Chapter 6

Robust Attitude Stabilization of a Quadrotor with Input Time Delay

In the last chapter, a predictor-controller method was presented to tackle time delays. But the presented method was developed in local coordinates and hence suffered from the singularity. Therefore, to remove this shortcoming, a predictor feedback control for attitude stabilization of quadrotors with input time delay has been presented in this chapter by representing the attitude using rotation matrices to avoid the singularities and ambiguities associated with Euler angles and quaternions. The closed-loop system is shown to be asymptotically stable with respect to a norm defined in the text. The norm has been defined in terms of states and past control efforts and hence explicitly results in Lyapunov Krasovskii functional for the system. A cascade of PDE-ODE system and the concept of transport delay has been used in the proof.

6.1 Introduction

Engineering systems inherently suffer from the state as well as input time delays due to the finite propagation speed of electrical signals. Quadrotors also suffer from such phenomena, but not much literature has been devoted to study and tackle these. In [59], a robust attitude controller was designed for multiple input multiple output uncertain quadrotors considering parametric uncertainties, external disturbances, and input time delays. A similar robust controller considering parametric uncertainties, unmodeled uncertainties, and input, as well as state delays, is designed in [62] [63].

The contributions of this chapter are mentioned below. Firstly, the chapter proposes a stabilizing controller for quadrotors with input time delay using rotation matrices for attitude dynamics. There are very few references in literature compensating input delay in a quadrotor, and this chapter is an attempt to bridge that gap. Predictor feed-

back has been developed to compensate for the input time delay in rotation dynamics of the quadrotor. The method does not make any approximations on input delay, which is prevalent in the current literature on input delay compensation. The predictor-based method has the advantage of yielding an expression for Lyapunov Krasovskii functional in designing the controller, and one needs not to have to assume such a functional beforehand. The closed-loop system's asymptotic stability is proved based on a norm defined with respect to current states and past control efforts.

The chapter is organized as follows. Section 6.2 of the chapter presents the problem formulation and various configuration errors. Some definitions used in this chapter are given in section 6.3. Section 6.4 presents the proposed controller along with the proof. Numerical simulation results are given in section 6.5. The controller's robustness property is presented in section 6.6, along with numerical simulation results in section 6.7.

6.2 Problem Formulation

6.2.1 Dynamic Model

The attitude dynamics of a quadrotor with input delay is represented below:

$$\begin{aligned} \dot{R} &= R\hat{\Omega} \\ I\dot{\Omega} &= -\Omega \times I\Omega + U(t-D) \end{aligned} \tag{6.1}$$

$R \in SO(3)$: Rotation matrix from body reference frame to inertial reference frame.
Ω : angular velocity of rigid body w.r.t inertial frame.
$\hat{(\cdot)}$: map from $\mathbb{R}^3$ to $\mathfrak{so}(3)$, space of skew symmetric matrices i.e. if $\Omega = [b_1 \quad b_2 \quad b_3]^T$, then

$$\hat{\Omega} = \begin{bmatrix} 0 & -b_3 & b_2 \\ b_3 & 0 & -b_1 \\ -b_2 & b_1 & 0 \end{bmatrix}$$

I : Moment of Inertia.
τ : external torque input in the body frame.
D : known input delay.

6.2.2 Configuration Error

The various configuration errors can be recalled from section 3.3.1 with suitable substitutions for stabilization problem i.e. substitute $\Omega_d = 0$, $R_d = I_3$ and $K = I_3$.

6.3 Some Definitions

6.3.1 Forward Completeness

A system

$$\dot{x} = f(x, u) \tag{6.2}$$

with a locally Lipschitz vector field $f : \mathbb{R}^n \times \mathbb{R} \to \mathbb{R}^n$ is said to be forward complete if, for every initial condition $x(0) = \zeta$ and every measurable locally essentially bounded input signal $u : \mathbb{R}_+ \to \mathbb{R}$, the corresponding solution is defined for all $t \geq 0$ i.e., the maximal interval of existence of solutions is $T_{max} = +\infty$.

Theorem 6.3.1. *[105] System* (6.2) *is forward complete if and only if there exist a nonnegative-valued, radially unbounded, smooth function* $V : \mathbb{R}^n \to \mathbb{R}_+$ *and a class-*$\mathcal{K}_\infty$ *function* σ *such that*

$$\frac{\partial V(x)}{\partial x} f(x, u) \leq V(x) + \sigma(|u|)$$

6.3.2 Norms for PDE state variables

Since the PDE state variable $u(x, t)$ is a function of two arguments, x and t, taking a norm in one of the variables, for example, in x, makes the norm a function of the other variable i.e.

$$||u(t)||_{L_2[0,D]} = \Big(\int_0^D u^2(x, t) \Big)^{\frac{1}{2}}$$

or

$$||u(t)||_{L_\infty[0,D]} = \sup_{x \in [0,D]} |u(x, t)|$$

6.4 Controller Design

Following propositions are the contributions of this chapter.

Proposition 6.1. *The controller given below asymptotically stabilizes system* (6.1) *for D=0.*

$$\kappa(\Omega) = -e_R - k_\Omega \Omega + \Omega \times I\Omega$$

Proof Please refer [54, 46] for proof.

The delay in the system (6.1) can be modeled by the following first-order hyperbolic PDE, also referred to as the "transport PDE" :

$$u_t(x,t) = u_x(x,t)$$
$$u(D,t) = U(t)$$

The solution to this equation is

$$u(x,t) = U(t + x - D),$$

and therefore the output

$$u(0,t) = U(t - D)$$

gives the delayed input. The system (6.1) can be modeled by the following ODE-PDE cascade known as plant system

$$I\dot{\Omega} = -\Omega \times I\Omega + u(0,t)$$
$$u_t(x,t) = u_x(x,t)$$
$$u(D,t) = U(t) \tag{6.3}$$

Let us define the following direct and inverse backstepping transformation

$$w(x,t) = u(x,t) - \kappa(p(x,t)) \tag{6.4}$$
$$u(x,t) = w(x,t) + \kappa(\pi(x,t)) \tag{6.5}$$

Then the plant system (6.3) can also be represented by the following ODE-PDE cascade known as target system :

$$\begin{aligned} I\dot{\Omega} &= -e_R - k_\Omega \Omega + w(0,t) \\ w_t(x,t) &= w_x(x,t) \\ w(D,t) &= 0 \end{aligned} \tag{6.6}$$

The predictor variables are represented by the following differential equations with appropriate initial conditions given below :

$$\begin{aligned} \dot{R} &= R\widehat{p(x,t)} \\ Ip_x(x,t) &= -p(x,t) \times Ip(x,t) + u(x,t) \\ p(0,t) &= \Omega(t) \end{aligned} \tag{6.7}$$

and

$$\begin{aligned} \dot{R} &= R\widehat{\pi(x,t)} \\ I\pi_x(x,t) &= -e_R - k_\pi \pi(x,t) + w(x,t) \\ \pi(0,t) &= \Omega(t) \end{aligned} \tag{6.8}$$

The p-system (6.7) and the π-system (6.8) are used to generate the plant-predictor and the target predictor in the following manner :

$$\begin{aligned} P(t) &= p(D,t), \\ \Pi(t) &= \pi(D,t). \end{aligned}$$

Proposition 6.2.

$$\begin{aligned} p_t(x,t) &= p_x(x,t), \\ \pi_t(x,t) &= \pi_x(x,t). \end{aligned}$$

Proof This can be proved by noting that $u(x,t)$ and $w(x,t)$ are functions of only one variable, $x+t$, and therefore so are $p(x,t)$ and $\pi(x,t)$ based on the ODEs (6.7) and (6.8). This implies that

$$\begin{aligned} p_t(x,t) &= p_x(x,t), \\ \pi_t(x,t) &= \pi_x(x,t). \end{aligned}$$

Proposition 6.3. *The plant system* (6.7) *is forward complete*

Proof Let us consider the following nonnegative-valued, radially unbounded, smooth function

$$J = \frac{1}{2}p(x,t)^T I p(x,t) + \Psi$$

Then,

$$\frac{1}{2}\lambda_{min}(I)||p||^2 + h_1||e_R||^2 \leq J \leq \frac{1}{2}\lambda_{max}(I)||p||^2 + h_2||e_R||^2$$

and

$$\begin{aligned}\dot{J} &= p^T u + e_R^T p \\ &\leq ||p||^2 + \frac{1}{2}||e_R||^2 + \frac{1}{2}||u||^2 \leq \frac{1}{min(\frac{1}{2}\lambda_{min}(I), h_1)}J + \frac{1}{2}||u||^2 \\ &= J(p(x,t)) + \sigma(||u||)\end{aligned}$$

Hence from section 6.3.1 system (6.7) is forward complete.

Proposition 6.4. *The target system* (6.8) *is input to state stable.*

Proof Let us consider the following Lyapunov function

$$L = \pi(x,t)^T I \pi(x,t) + \Psi + cIe_R^T\pi(x,t) \tag{6.9}$$

Then,

$$\lambda_{min}(\mathcal{W}_1)||z_R||^2 \leq L \leq \lambda_{max}(\mathcal{W}_2)||z_R||^2$$

where

$$\mathcal{W}_1 = \begin{bmatrix} \frac{1}{2}\lambda_{min}(I) & \frac{c}{2}\lambda_{min}(I) \\ \frac{c}{2}\lambda_{min}(I) & h_1 \end{bmatrix} \mathcal{W}_2 = \begin{bmatrix} \frac{1}{2}\lambda_{max}(I) & \frac{c}{2}\lambda_{max}(I) \\ \frac{c}{2}\lambda_{max}(I) & h_2 \end{bmatrix}$$

and $z_R = [||e_R|| \;\; ||\pi||]$. The time derivative of (6.9) is

$$\begin{aligned}\dot{L} &\leq -k_\pi||\pi||^2 + \pi^T w - c||e_R||^2 - ck_\pi e_R^T\pi + ce_R^T w + \frac{3c}{\sqrt{2}}||\pi||^2 \\ &\leq -\lambda_{min}(A)||z_R||^2 + \frac{1+c}{2}||w||^2 \\ &\leq -\lambda_{min}(A)||z_R||^2 \;\; \forall \;\; ||z_R|| \geq \sqrt{\frac{1+c}{2\lambda_{min}(A)}}||w||\end{aligned}$$

$$A = \begin{bmatrix} \frac{1}{2}c & \frac{ck_\pi}{2} \\ \frac{ck_\pi}{2} & k_\pi - \frac{1}{2} - \frac{3c}{\sqrt{2}} \end{bmatrix}$$

Hence system (6.8) is input-to-state stable.

Proposition 6.5. *Consider the closed loop system*

$$\begin{aligned} I\dot{\Omega} &= -\Omega \times I\Omega + U(t-D) \\ U(t) &= -e_R - k_\Omega P(t) + P(t) \times IP(t) \\ P(t) &= \int_{t-D}^{t} (-P(\theta) \times IP(\theta) + U(\theta))d\theta + \Omega(t), \quad t \geq 0 \\ P(\theta) &= \int_{-D}^{\theta} (-P(\sigma) \times IP(\sigma) + U(\sigma))d\sigma + \Omega(0), \ t \in [-D, 0] \end{aligned}$$

with an initial condition $\Omega_0 = \Omega(0)$ *and* $U_0(\theta) = U(\theta)$, $\theta \in [-D, 0]$. *Then there exists a function* $\beta \in \mathcal{KL}$ *such that*

$$\begin{aligned} &||e_R(t)||^2 + ||\Omega(t)||^2 + \int_{t-D}^{t} ||U(\theta)||^2 d\theta \leq \\ &\beta(||e_R(0)||^2 + ||\Omega(0)||^2 + \int_{-D}^{0} ||U(\theta)||^2 d\theta, t) \end{aligned}$$

Proof The proof will be completed in four steps :

Step 1 :

Since the plant system is forward complete, from Proposition 6.3 we can write

$$\dot{J}(p(x,t)) \leq J(p(x,t)) + \frac{1}{2}||u(x,t)||^2$$

Therefore,

$$\begin{aligned} J(p(x,t)) &\leq e^x J(p(0,t)) + \frac{1}{2}\int_0^x e^{x-\zeta}||u(\zeta,t)||^2 d\zeta \\ &= e^x J(\Omega(t)) + \frac{1}{2}\int_0^x e^{x-\zeta}||u(\zeta,t)||^2 d\zeta \\ &= e^x J(\Omega(t)) + \frac{1}{2}(e^x - 1)\sup_{0\leq\zeta\leq x} ||u(\zeta,t)||^2 \end{aligned}$$

From Proposition 6.3 we get

$$\frac{1}{2}\lambda_{min}(I)||p||^2 + h_1||e_R||^2 \leq e^x(\frac{1}{2}\lambda_{max}(I)||\Omega||^2 + h_2||e_R||^2) + \frac{1}{2}(e^x - 1)\sup_{0\leq\zeta\leq x}||u(\zeta,t)||^2$$

$$\implies min\left(\frac{1}{2}\lambda_{min}(I), h_1\right)(||p||^2 + ||e_R||^2) \leq$$

$$e^D(max\left(\frac{1}{2}\lambda_{max}(I), h_2\right)(||\Omega||^2 + ||e_R||^2)) + \frac{1}{2}(e^D - 1)\sup_{0\leq\zeta\leq x}||u(\zeta,t)||^2$$

Therefore, we have

$$||p(x,t)||^2 + ||e_R(x,t)||^2 \leq \rho_1(||e_R||^2 + ||\Omega(t)||^2 + \sup_{0\leq\zeta\leq x}||u(\zeta,t)||)$$

for some $\rho_1 \in \mathcal{K}_\infty$. Defining the L_2 norm in x as

$$||l(t)||_{L_2[0,D]} = \left(\int_0^D ||l(x,t)||^2 dx\right)^{\frac{1}{2}}$$

we can write

$$(||p(t)|| + ||e_R(t)||)_{L_2[0,D]} \leq \rho_1(||e_R(t)||^2 + ||\Omega(t)||^2 + ||u(t)||_{L_2[0,D]})$$

From Proposition 6.1

$$||\kappa(p)|| \leq ||e_R|| + k_p||p|| + \lambda_{max}(I)||p||^2 = \rho_2(||p||)$$

for $\rho_2 \in \mathcal{K}_\infty$. Considering (6.7) with (6.4) as output map we can conclude :

$$||\Omega(t)||^2 + ||e_R(t)||^2 + ||w(t)||_{L_2[0,D]} \leq \rho_3(||e_R||^2 + ||\Omega(t)||^2 + ||u(t)||_{L_2[0,D]})$$

for some $\rho_3 \in \mathcal{K}_\infty$.

Step 2 :

Since the target system is input-to-state stable we get from proposition 6.4

$$||\pi(x,t||) \leq \beta_1(||\pi(0,t)||, t) + \gamma_1\left(\sup_{0\leq\zeta\leq x}||w(x,t)||\right)$$

$$||\pi(x,t||) \leq \beta_1(||\Omega(t)||, t) + \gamma_1\left(\sup_{0\leq\zeta\leq x}||w(x,t)||\right)$$

for some class $\mathcal{KL}$ function β_1 and class $\mathcal{K}$ function γ_1. Similar to step 1 taking a L_2-norm on both sides we get :

$$(||\pi(t)|| + ||e_R(t)||)_{L_2[0,D]} \leq \beta_1(||e_R(t)||^2 + ||\Omega(t)||^2, 0) + \gamma_1(||w(t)||_{L_2[0,D]})$$

Considering (6.8) with (6.5) as output map we can conclude :

$$||\Omega(t)||^2 + ||e_R(t)||^2 + ||u(t)||_{L_2[0,D]} \leq \rho_4(||e_R||^2 + ||\Omega(t)||^2 + ||w(t)||_{L_2[0,D]})$$

Step 3 :

Let us consider the target system (6.6) and prove its exponential stability. Let us consider the following Lyapunov function for that purpose :

$$V(t) = \frac{1}{2}\Omega^T I\Omega + \Psi + cI\Omega^T e_R + (c+1)\int_0^D e^{(c+1)x}||w(t,x)||^2$$

V is bounded by

$$min(\lambda_{min}(\mathcal{W}_3), (c+1))(||z_R||^2 + \int_0^D e^{(c+1)x}||w(t,x)||^2) \leq V(t) \leq$$
$$max(\lambda_{max}(\mathcal{W}_4)|, c+1)(||z_R||^2 + \int_0^D e^{(c+1)x}||w(t,x)||^2)$$

where

$$\mathcal{W}_3 = \begin{bmatrix} h_1 & \frac{c\lambda_{min}(I)}{2} \\ \frac{c\lambda_{min}(I)}{2} & \frac{\lambda_{min}(I)}{2} \end{bmatrix} \quad \mathcal{W}_4 = \begin{bmatrix} h_2 & \frac{c\lambda_{max}(I)}{2} \\ \frac{c\lambda_{max}(I)}{2} & \frac{\lambda_{max}(I)}{2} \end{bmatrix}$$

Then its time derivative is given by :

$$\begin{aligned}
\dot{V} &= -k_\Omega||\Omega||^2 + \Omega^T w(0,t) - c||e_R||^2 - ck_\Omega e_R^T\Omega + ce_R^T w(0,t) \\
&+ cI\Omega_T\dot{e}_R + (c+1)\int_0^D e^{(c+1)x}w(t,x)^T w_t(x,t)dx \\
&\leq -\frac{c}{2}||e_R||^2 - (k_\Omega - \frac{1}{2} - \frac{3}{\sqrt{2}}c\lambda_{max}(I))||\Omega||^2 \\
&+ \frac{c+1}{2}||w(0,t)||^2 + ck_\Omega||e_R||||\Omega|| + (c+1)\int_0^D e^{(c+1)x}w(t,x)^T w_x(x,t)dx \\
&\leq -\frac{c}{2}||e_R||^2 - (k_\Omega - \frac{1}{2} - \frac{3}{\sqrt{2}}c\lambda_{max}(I))||\Omega||^2 \\
&+ \frac{c+1}{2}||w(0,t)||^2 + ck_\Omega||e_R||||\Omega|| + \frac{c+1}{2}\int_0^D e^{(c+1)x}d||w(t,x)||^2 \\
&\leq -\lambda_{min}(B)||z||^2 - (c+1)\int_0^D e^{(c+1)x}||w(t,x)||^2
\end{aligned}$$

where in the last step integration by parts has been applied and $z = [||e_R||\ \ ||\Omega||]$ with

$$B = \begin{bmatrix} \frac{c}{2} & \frac{ck_\Omega}{2} \\ \frac{ck_\Omega}{2} & k_\Omega - \frac{1}{2} - \frac{3}{\sqrt{2}}c\lambda_{max}(I) \end{bmatrix}$$

Therefore

$$\dot{V} \leq -\mu V$$

where

$$\mu = \frac{min(\lambda_{min}(B), c+1)}{max(\lambda_{max}(\mathcal{W}_4), c+1)}$$

Hence there exists a class-$\mathcal{KL}$ function β_2 such that

$$V(t) \leq \beta_2(V(0), t), \quad \forall t \geq 0.$$

Also there exists a function $\beta_4 \in \mathcal{KL}$ such that

$$||e_R(t)||^2 + ||\Omega(t)||^2 + ||w(t)||_{L_\infty[0,D]} \leq \beta_4(||e_R(0)||^2 + ||\Omega(0)||^2 + ||w(0)||_{L_\infty[0,D]}, t).$$

Step 4 :
From steps 1,2 and 3 one obtains the following result

$$||e_R(t)||^2 + ||\Omega(t)||^2 + ||u(t)||_{L_2[0,D]} \leq \rho_4(\beta_4(\rho_3(||e_R(0)||^2 + ||\Omega(0)||^2 + ||u(0)||_{L_2[0,D]}), t)).$$

Then there exists a function $\beta_5 \in \mathcal{KL}$ such that :

$$||e_R(t)||^2 + ||\Omega(t)||^2 + ||u(t)||_{L_2[0,D]} \leq \beta_5(||e_R(0)||^2 + ||\Omega(0)||^2 + ||u(0)||_{L_2[0,D]}, t).$$

or

$$||e_R(t)||^2 + ||\Omega(t)||^2 + \int_{t-D}^{t} ||U(\theta)||^2 d\theta \leq \beta(||e_R(0)||^2 + ||\Omega(0)||^2 + \int_{-D}^{0} ||U(\theta)||^2 d\theta, t)$$

6.5 Numerical Simulations I

Numerical simulations are carried out for the system whose moment of inertia is mentioned below.

$$I_{xx} = 0.082kg/m^2, I_{yy} = 0.0845kg/m^2, I_{zz} = 0.1377kg/m^2$$

The initial conditions for simulation are assumed to be

$$\Omega(0) = [0.2; 0.1; 0.5], \quad \dot{\Omega}(0) = [0; 0; 0],$$

$$R(0) = \begin{bmatrix} 0 & 0 & 1 \\ 0 & 1 & 0 \\ -1 & 0 & 0 \end{bmatrix}$$

The proposed control law is simulated in MATLAB for the quadrotor attitude dynamics with the initial conditions mentioned above. The stabilization performance of the control law is shown in Figs.6.1-6.3 for delay D=0.1 sec. It is observed that the quadrotor stabilizes to $(R, \Omega) = (I, 0)$ within 5 sec. The control law proposed in [46, 54] fails to stabilize the quadrotor in the presence of an input delay of 0.1 sec while the proposed controller is able to stabilize the quadrotor. Similar stabilization results are obtained with input delay of 0.05 sec, 0.2 sec, and 0.3 sec, but the simulation results are not given due to repetition. We can observe that the stabilization results are valid for long input delay as well as small input delay. The results are even robust to variations in the inertia matrix and can be demonstrated by repeating the simulation for a small deviation in the inertia matrix.

6.6 Robustness to Delay Mismatch

Since the exact delay is difficult to be known, we consider the scenario where there is a small deviation in the delay. We will prove the exponential stability of the predictor feedback even in the presence of a small deviation in the known delay. In the presence of delay mismatch, the original system is given by :

$$\begin{aligned} \dot{R} &= R\hat{\Omega} \\ I\dot{\Omega} &= -\Omega \times I\Omega + U(t - D_0 - \Delta D) \end{aligned} \tag{6.10}$$

where D_0 is the nominal delay which is known and ΔD is the delay mismatch. We use the same ODE-PDE method of modeling plant and target system. The plant system is

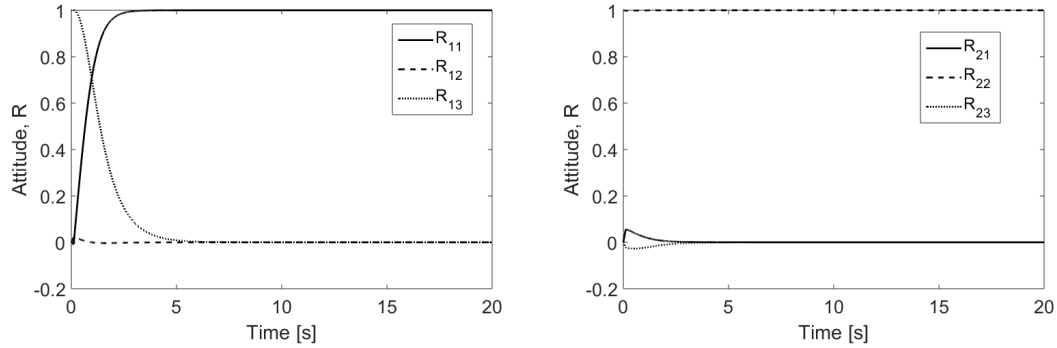

(a) (b)

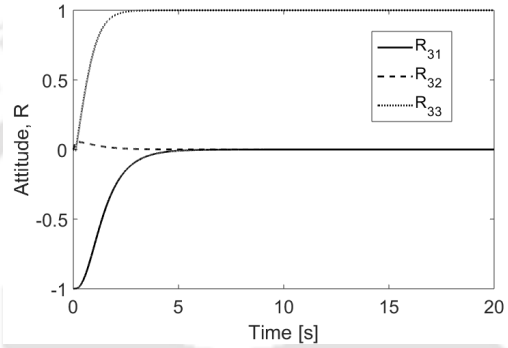

(c)

Figure 6.1: Attitude Tracking.

modeled as :

$$\begin{aligned} I\dot{\Omega} &= -\Omega \times I\Omega + u(0,t) \\ u_t(x,t) &= u_x(x,t) \\ u(D_0 + \Delta D, t) &= U(t) \end{aligned} \tag{6.11}$$

where the domain of the spatial variable of the PDE is defined as:

$$x \in (\min\{0, \Delta D\}, D_0 + \Delta D) \tag{6.12}$$

Also

$$u(x,t) = U(t + x - D_0 - \Delta D) \tag{6.13}$$

such that

$$u(0,t) = U(t - D_0 - \Delta D) \tag{6.14}$$

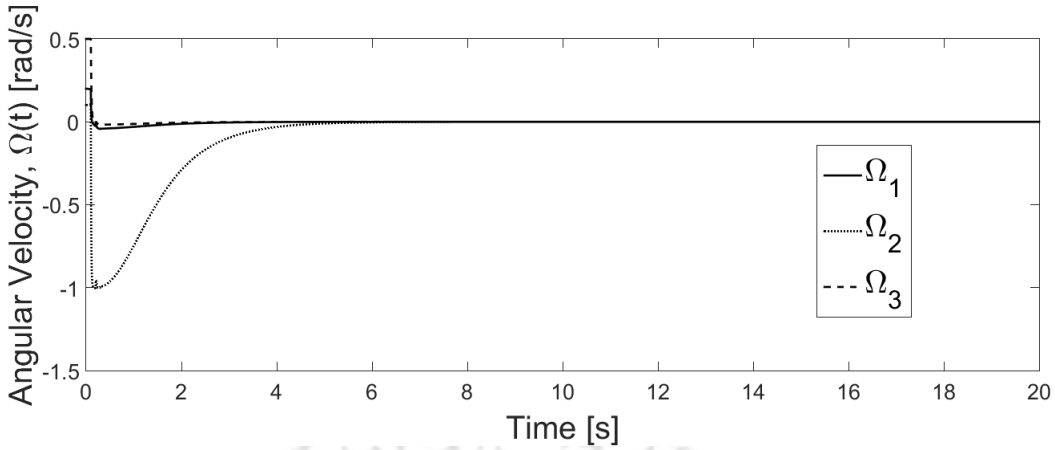

Figure 6.2: Angular Velocity stabilization

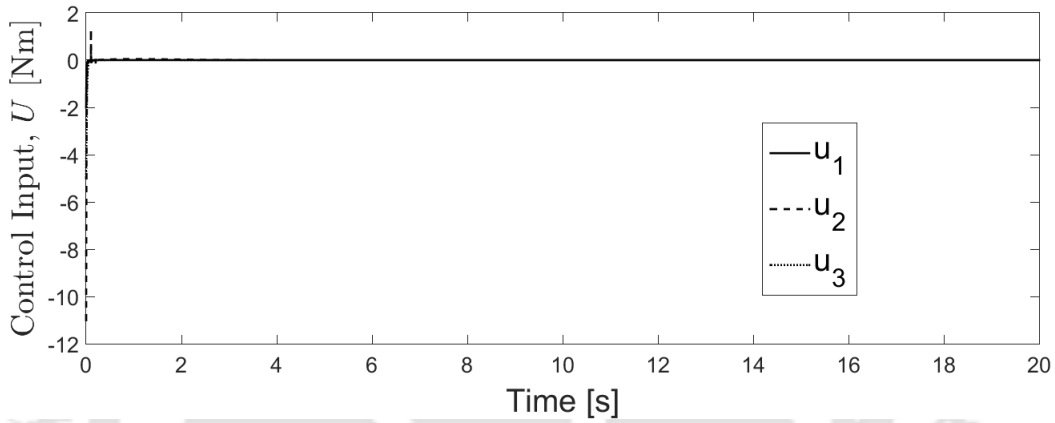

Figure 6.3: Control input

The target system is given by :

$$\begin{aligned} I\dot{\Omega} &= -e_R - k_\Omega \Omega + w(0,t) \\ w_t(x,t) &= w_x(x,t) \\ w(D_0 + \Delta D, t) &= 0 \end{aligned} \tag{6.15}$$

Proposition 6.6. *For $\delta > 0$ such that*

$$\Delta D \in (-\delta, \delta) \tag{6.16}$$

the system (6.10) *with the control law in proposition 4.3 with $D = D_0$ is exponentially stable i.e. there exists a function $\beta_1 \in \mathcal{KL}$ such that*

$$||e_R(t)||^2 + ||\Omega(t)||^2 + \int_{t-\bar{D}}^{t} ||U(\theta)||^2 d\theta \leq \beta_1(||e_R(0)||^2 + ||\Omega(0)||^2 + \int_{-\bar{D}}^{0} ||U(\theta)||^2 d\theta, t)$$

where

$$\bar{D} = D_0 + max\{0, \Delta D\} \tag{6.17}$$

6.7 Numerical Simulations II

Numerical simulations were carried out with the same parameters and initial conditions as in section 6.5. The proposed control law is simulated in MATLAB for the quadrotor attitude dynamics. The stabilization performance of the control law is shown in Figs.6.5-6.6 for nominal delay $D_0 = 0.1$ sec and delay mismatch $\Delta D = 0.01$ sec. It is observed that the quadrotor stabilizes to $(R, \Omega) = (I, 0)$ within 5 sec even in the presence of delay mismatch. The control input also settles down to zero as expected after 2 sec which is quite fast. Thus we can conclude that the proposed control law is robust to mismatch in delay.

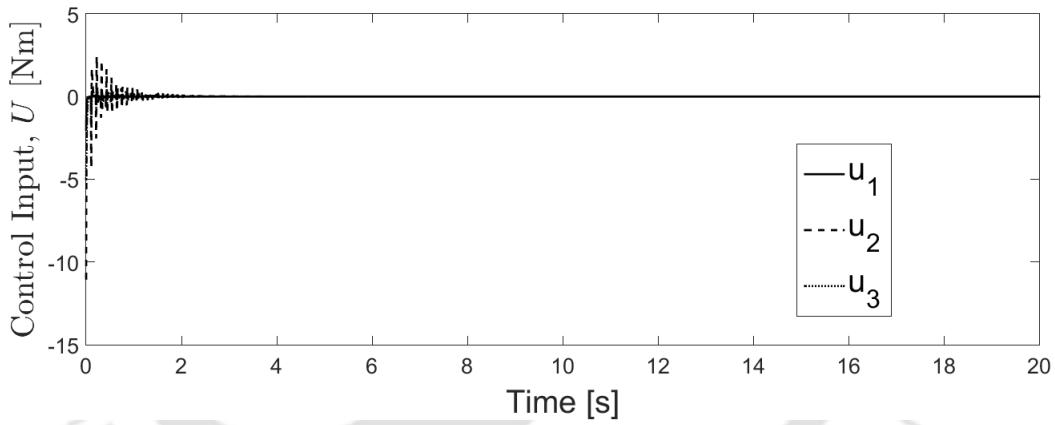

Figure 6.4: Control input - Case II

6.8 Conclusion

A nonlinear geometric finite-time controller is proposed for attitude stabilization of quadrotors where the attitude is represented using rotation matrices. The predictor method proposed in this chapter is able to stabilize the quadrotor in the presence of input delay, while the methods proposed in the current literature are not able to stabilize the quadrotors in the presence of input delay. The proposed method works for a wide variation in input delay and is even robust to delay mismatch.

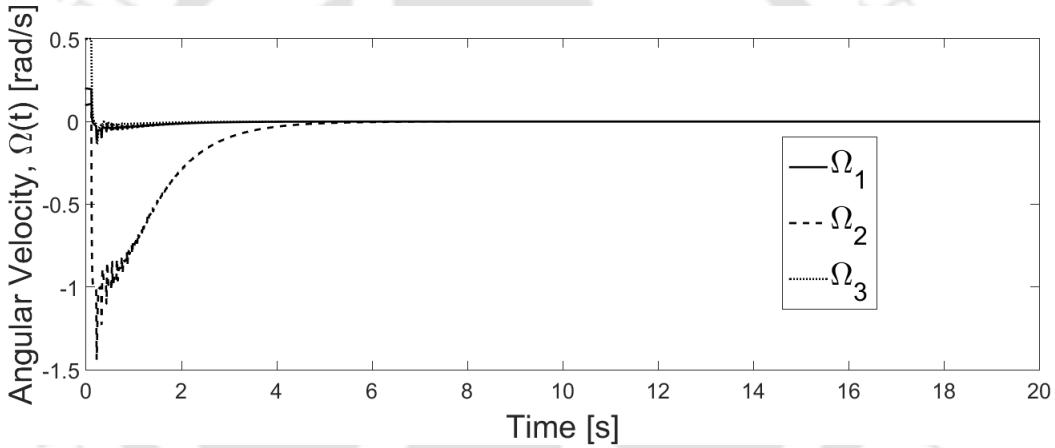

Figure 6.5: Angular Velocity stabilization - Case II

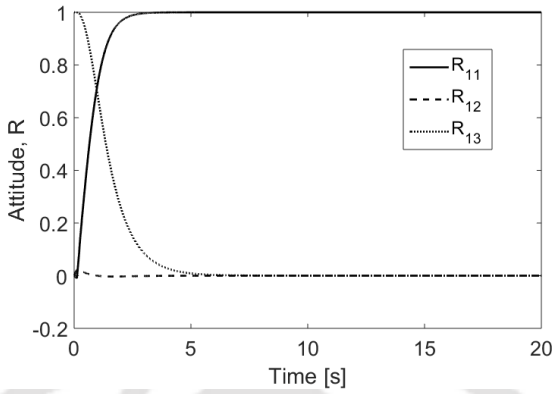

(a)

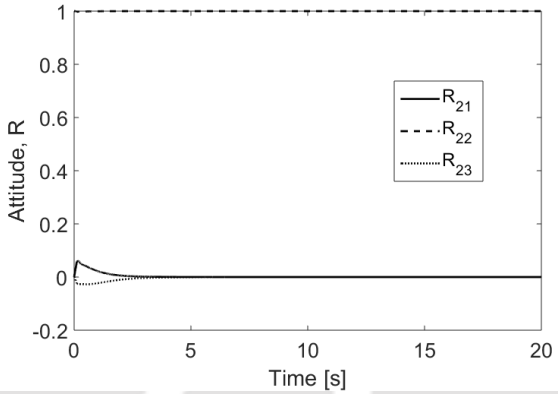

(b)

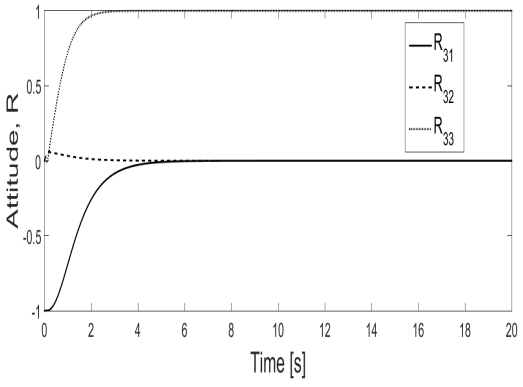

(c)

Figure 6.6: Attitude Tracking - Case II.

Chapter 7

Geometric Control of a Quadrotor with Finite-Time Convergence and Improved Transients

The previous chapters presented geometric control of quadrotors with either exponential or asymptotic convergence. Improving upon the convergence properties of the earlier methods, a finite-time geometric control of a quadrotor has been presented in this chapter by representing the attitude using rotation matrices to avoid the singularities and ambiguities associated with Euler angles and quaternions. A composite error function is designed, and it is proved mathematically that the closed-loop attitude and the translational dynamics are finite-time stable. The coordinate invariant approach is another unique feature of the proposed method as opposed to the literature. Numerical simulations have been provided at the end to show the effectiveness of the proposed method. Simulation results demonstrate the better transient performance of the proposed control method than the control law presented in the literature.

7.1 Introduction

Due to the advantages of finite-time controllers such as faster convergence rate, higher tracking precision, better disturbance rejection properties, and robustness against uncertainties [74, 51], such a controller is more desirable. But the finite-time controllers proposed in the current literature are discontinuous in nature; therefore, continuous finite-time controllers are more desirable due to ease of implementation on actuators. Moreover, the continuous feedback stabilization in finite time does not excite unmodeled high-frequency dynamics as compared to discontinuous feedback. A continuous finite-time controller based on homogeneity [75, 76] was developed for robot manipulators in [77]. A

continuous finite-time stabilizing feedback law was developed for the double translational, and rotational double integrator in [78]. A finite-time attitude stabilizing result based on a homogeneous method was presented in [79]. Similarly, a finite time attitude tracking control law for single and multiple spacecraft was developed in [80], but the attitude was represented using Modified Rodriguez Parameters (MRPs). To deal with the external disturbances, a finite disturbance observer-based finite-time attitude tracking control of a rigid spacecraft was developed in [81]. In [82], a multivariable finite-time attitude tracking law based on a homogeneous method was presented. As an improvement to the method mentioned above, an adaptive variant of the controller was developed in [83].

The contributions of this chapter are mentioned below. Firstly, the chapter presents a nonlinear geometric controller for a quadrotor using rotation matrices for attitude dynamics. The second novelty of this chapter is the utilization of left tracking errors while developing the tracking controller. The third contribution of this chapter is that the developed control law guarantees the convergence of the attitude as well as the translational motion to the equilibrium configuration in finite time, while most of the existing literature develops only finite time attitude tracking control law. Moreover, a finite time control law has been developed for trajectory tracking for an underactuated aerial vehicle on the nonlinear manifold $SE(3)$. A composite error function has been constructed, and rigorous mathematical proof has been given to show the controller's finite-time stabilizing property. Lastly, the proposed control law is continuous and chattering free, while most of the robust control laws proposed in the literature are discontinuous and hence possess chattering. Due to the continuous and chattering free nature, the proposed control law can be implemented in a physical system without excessive wear and tear. Moreover, the proposed controller is simpler and intuitive. The control law is also robust to bounded external disturbances, and one does not need a robust control strategy if the bound on the disturbances satisfies the inequality derived in section 6. The simulation results show improved convergence time and less peak overshoot as compared to exponentially stabilizing control law developed in the literature.

Section 7.2 of the chapter explains the dynamic model used in developing the controller. Section 7.3 lists some important theorem and lemma used in the subsequent development. Section 7.4 explains the development of the finite-time geometric controller along with the proofs. An analysis of robustness to bounded disturbances is presented in section 7.5. Numerical simulation and comparison results have been presented in section 7.6.

7.2 Some Definitions

Theorem 7.2.1. *([51]) Let us consider the following differential equations*

$$\dot{x} = f(x(t)) \tag{7.1}$$

Let us denote by $\psi^x(\cdot)$ the unique solution of (7.1) satisfying $\psi(0,x) = 0$. The origin is said to be a finite-time stable equilibrium of (7.1) if there exists an open neighborhood $\mathcal{N} \subseteq \mathcal{D}$ of the origin and a function $T : \mathcal{N}/\{0\} \to (0,\infty)$, called the settling-time function, such that the following statements hold:

(i) Finite-time convergence: For every $x \in \mathcal{N}/\{0\}$, ψ^x is defined on $[0, T(x))$, $\psi^x(t) \in \mathcal{N}/\{0\}$ for all $t \in [0, T(x))$, and $lim_{t\to T(x)}\psi^x(t) = 0$.
(ii) Lyapunov stability: For every open neighborhood $\mathcal{U}_\epsilon$ of 0 there exists an open subset $\mathcal{U}_\delta$ of $\mathcal{N}$ containing 0 such that, for every $x \in \mathcal{U}_\delta/\{0\}$, $\psi^x(t) \in \mathcal{U}_\epsilon$ for all $t \in [0, T(x))$.

The origin is said to be a globally finite-time stable equilibrium if it is a finite-time stable equilibrium with $\mathcal{D} = \mathcal{N} = \mathbb{R}^n$.

Theorem 7.2.2. *([51]) Let us consider the following differential equations*

$$\dot{x} = f(x(t)) \tag{7.2}$$

If there exists a continuous function $V : \mathcal{D} \to \mathbb{R}$ with V being positive definite and if there exists real numbers $c > 0$ and $\alpha \in (0,1)$. Also in an open neighborhood $\mathcal{V} \subseteq \mathcal{D}$ if the following is valid

$$\dot{V}(x) + c(V(x))^\alpha \leq 0 \ , \quad x \in \mathcal{V}\backslash\{0\}$$

Then the finite-time-stability of the origin of (7.2) is inferred. Moreover if T is the settling-time function, then

$$T(x) \leq \frac{1}{c(1-\alpha)} V(x)^{1-\alpha}$$

If $\mathcal{D} = \mathbb{R}^n$, V is proper, and $\dot{V} < 0$ on $\mathbb{R}^n\backslash\{0\}$, then globally finite-time-stability of the origin of (7.2) can be inferred.

Lemma 7.2.3. *([108]) For $x \in \mathbb{R}^n$, and $p \in (0,1]$, following inequality is valid : $(|x_1| + \cdots + |x_n|)^p \leq |x_1|^p + \cdots + |x_n|^p \leq n^{1-p}(|x_1| + \cdots + |x_n|)^p$.*

Lemma 7.2.4. *([109]) If P is a symmetric matrix and $x^T y > 0$, the bound on $x^T P y$ can be written as :*

$$\lambda_{min}(P)x^T y \leq x^T P y \leq \lambda_{max}(P)x^T y,$$

7.3 Controller Design

The reader may refer to Section 2.4 to recall the dynamic model and section 3.3.1 for various configuration errors before proceeding. Following propositions are the contributions of this chapter.

Proposition 7.1. *The attitude dynamics* (3.2) *driven by control law* (7.3) *renders the closed loop attitude error dynamics $\{e_R, e_\Omega\}$ locally finite-time stable :*

$$\begin{aligned}\tau =& - R_d^T e_R - K_l l||l||^{\alpha-1} + I\dot{\Omega}_d + \Omega \times I\Omega + I\hat{\Omega}_d R_d^T e_R||e_R||^{\alpha-1} \\ & - IR_d^T E e_\Omega ||e_R||^{\alpha-1} - (\alpha-1)IR_d^T e_R^T E e_\Omega \frac{e_R}{||e_R||^{3-\alpha}}\end{aligned} \tag{7.3}$$

where,

$$l = e_\Omega + R_d^T e_R ||e_R||^{\alpha-1}, \ \alpha \in (0,1) \tag{7.4}$$

and K_l is a gain matrix.

Proof. Define the composite error function as :

$$l = e_\Omega + R_d^T e_R ||e_R||^{\alpha-1} \tag{7.5}$$

for $\alpha \in (0,1)$ Let the Lyapunov function for the attitude dynamics be :

$$V_R = \frac{1}{2} l^T I l + \Psi = \frac{1}{2} l^T I l + \frac{1}{2}\text{tr}(K(I - RR_d^T)) \tag{7.6}$$

Then

$$\begin{aligned}I\dot{l} =& I\dot{e}_\Omega + I\frac{d}{dt}R_d^T e_R||e_R||^{\alpha-1} \\ =& I(\dot{\Omega} - \dot{\Omega}_d) + I\frac{d}{dt}R_d^T e_R||e_R||^{\alpha-1} \\ =& -\Omega \times I\Omega + \tau - I\dot{\Omega}_d + I\frac{d}{dt}R_d^T e_R||e_R||^{\alpha-1} \\ =& -R_d^T e_R - K_l l||l||^{\alpha-1}\end{aligned} \tag{7.7}$$

The time derivative of Lyapunov function Eqn.(7.6) is given by :

$$\begin{aligned}\dot{V}_R &= l^T I\dot{l} - \frac{1}{2}(K\dot{R}R_d^T + KR\dot{R}_d^T) \\ &= -K_l l^T ||l||^{\alpha-1} - l^T R_d^T e_R - \frac{1}{2}\text{tr}(KRe_\Omega^\dagger R_d^T) \\ &= -K_l ||l||^{\alpha+1} - (e_\Omega + R_d^T e_R ||e_R||^{\alpha-1})^T R_d e_R - \frac{1}{2}\text{tr}(KR\hat{e}_\Omega R_d^T) \end{aligned} \tag{7.8}$$

From the identity $A\hat{x}A^T = \widehat{Ax}$, we can write :

$$\dot{V}_R = -K_l ||l||^{\alpha+1} - (e_\Omega + R_d^T e_R ||e_R||^{\alpha-1})^T R_d e_R - \frac{1}{2}\text{tr}(KRR_d^T \widehat{(R_d e_\Omega)})$$

From the equality $-\frac{1}{2}\text{tr}(\hat{x}\hat{y}) = x \cdot y$, we can write :

$$\dot{V}_R = -K_l ||l||^{\alpha+1} - ||e_R||^{\alpha+1} \leq -min(K_l, 1)(||l||^{\alpha+1} + ||e_R||^{\alpha+1}) \tag{7.9}$$

From Lemma 7.2.3, we can write :

$$\dot{V}_R \leq -min(K_l, 1)(||l||^2 + ||e_R||^2)^{\frac{\alpha+1}{2}} \tag{7.10}$$

Since

$$V_R = \frac{1}{2} l^T I l + \Psi$$

we have,

$$\frac{1}{2}\lambda_{min}(I)||l||^2 + h_1||e_R||^2 \leq V_R \leq \frac{1}{2}\lambda_{max}(I)||l||^2 + h_2||e_R||^2$$

Therefore,

$$V_R \geq min(\frac{1}{2}\lambda_{min}(I), h_1)(||l||^2 + ||e_R||^2) \tag{7.11}$$

From (7.10) and (7.11), we can write :

$$\dot{V}_R \leq -\frac{min(K_l, 1)}{min(\frac{1}{2}\lambda_{min}(I), h_1)} V^{\frac{\alpha+1}{2}} \tag{7.12}$$

or,

$$\dot{V}_R \leq -cV^\beta \tag{7.13}$$

where,

$$c = \frac{min(K_l, 1)}{min(\frac{1}{2}\lambda_{min}(I), h_1)} \text{ and } \beta = \frac{\alpha + 1}{2} \in (0, 1) \tag{7.14}$$

Therefore, from Theorem 7.2.2, the attitude error dynamics is finite time stable. The settling time, t_R for the rotational motion is given by

$$t_R = \frac{1}{c(1-\alpha)} V_R^{1-\alpha}(0)$$

The above proposition shows that the attitude error vector converges to zero in finite time. But this does not mean that $R \to R_d$ in finite time. Due to the nonlinear structure of $SO(3)$ there exists three additional critical points of Ψ namely $\{R_d\ exp(\pi \hat{s})\}$ for $s \in \{e_1, e_2, e_3\}$ where $e_R = 0$. This cannot be avoided for any continuous control systems on $SO(3)$ [9]. But it can be shown that those three additional equilibrium points are unstable by using linearization. These points have both stable and unstable manifolds, also known as saddle equilibria [110]. It has an almost-global stabilization property because the stable manifolds' union to these undesirable equilibria has a lower dimension than the tangent bundle of the configuration space. □

One should note that the control law (7.3) has singularity at $||e_R|| = 0$. This singularity issue can be avoided by replacing $||e_R||$ by $(||e_R|| + \epsilon)$ where ϵ is a small number. For our purposes, we have chosen $\epsilon = 0.001$. For large errors, this small number can be neglected, thereby retaining the finite-time convergence property. For small errors, the denominator will never approach zero, but $e_R, e_\Omega \to 0$, thereby the concerning terms in the expression will converge to 0. Therefore the modified control law τ becomes :

$$\begin{aligned}\tau = &- R_d^T e_R - K_l l(||l|| + \epsilon)^{\alpha-1} + I\dot{\Omega}_d + \Omega \times I\Omega + I\hat{\Omega}_d R_d^T e_R(||e_R|| + \epsilon)^{\alpha-1} \\ &- IR_d^T E e_\Omega(||e_R|| + \epsilon)^{\alpha-1} - (\alpha - 1) IR_d^T e_R^T E e_\Omega \frac{e_R}{(||e_R|| + \epsilon)^{3-\alpha}}\end{aligned} \tag{7.15}$$

The above-modified control law has been tested in simulation, and the results are the same as that of control law when $\epsilon = 0$. Therefore the singularity issue can be avoided using this approach.

Proposition 7.2. *The complete dynamics* (3.2), (3.1) *driven by control law* (7.3), (7.16) *renders the closed loop error dynamics* $\{e_R, e_\Omega, e_x, e_v\}$ *locally finite-time stable :*

$$f_c^d = -K_x e_x - K_p p||p||^{\alpha-1} + m(\dot{v}_d + g e_3) - m e_v ||e_x||^{\alpha-1} - m(\alpha - 1) e_x^T e_v \frac{e_x}{||e_x||^{3-\alpha}} \tag{7.16}$$

where $K_x, K_p \in \mathbb{R}^{3\times3}$ *are positive definite gain matrices and*

$$p = e_v + e_x||e_x||^{\alpha-1},\ \alpha \in (0,1)$$

It is assumed that

$$\left|\left| - K_x e_x - K_p p||p||^{\alpha-1} - m e_v||e_x||^{\alpha-1} - m(\alpha-1)e_x^T e_v \frac{e_x}{||e_x||^{3-\alpha}}\right|\right| \leq f_{cM} \tag{7.17}$$

such that

$$||f_c^d|| \leq f_{cM} + f_M^d \leq f_M$$

where

$$f_M^d = \sup_{t\geq t_0}(||mge_3 + m\dot{v}_d)$$

and f_M *is given physical meaning in the proof below. Hence the Lyapunov analysis is valid in the set*

$$\{\{e_x, e_v\} \in \mathbb{R}^3 \times \mathbb{R}^3 : Eq.(7.17) holds\}$$

Proof. Define the composite error function as :

$$p = e_v + e_x||e_x||^{\alpha-1} \tag{7.18}$$

for $\alpha \in (0,1)$ Let the Lyapunov function for the translation dynamics be :

$$V_T = \frac{1}{2}p^T m p + \frac{1}{2}e_x^T K_x e_x \tag{7.19}$$

In this chapter following control law and torque is proposed to be applied to the quadrotor :

$$f_b = ||f_c^d||e_3 \tag{7.20}$$

The choice of control f_b always results in positive thrust to the quadrotor, whereas in [46] the total thrust becomes negative when the angle between the vertical body axis and the desired thrust becomes greater than 90°. For a standard VTOL vehicle, it is required

that $f_b^T e_3 > 0$. Then the time derivative of V_T is

$$\dot{V}_T = p^T m\dot{p} + e_x^T K_x e_v \tag{7.21}$$

We can find $m\dot{p}$ as

$$\begin{aligned} m\dot{p} &= m\dot{e}_v + m\frac{d}{dt}e_x||e_x||^{\alpha-1} \\ &= m\dot{v} - m\dot{v}_d + m\frac{d}{dt}e_x||e_x||^{\alpha-1} \\ &= -mge_3 + Rf_b - m\dot{v}_d + m\frac{d}{dt}e_x||e_x||^{\alpha-1} \\ &= -mge_3 + Rf_b + f_c^d - f_c^d - m\dot{v}_d + m\frac{d}{dt}e_x||e_x||^{\alpha-1} \\ &= -K_x e_x - K_p p||p||^{\alpha-1} + \Delta f \end{aligned} \tag{7.22}$$

Combining Eqns.(7.21) and (7.22) :

$$\begin{aligned} \dot{V}_T &= p^T(-K_x e_x - K_p p||p||^{\alpha-1} + \Delta f) + e_x^T K_x e_v \\ &= -p^T K_x e_x - K_p p^T p||p||^{\alpha-1} + p^T\Delta f + e_x^T K_x e_v \\ &= -(e_v + e_x||e_x||^{\alpha-1})^T K_x e_x - K_p||p||^{\alpha+1} + p^T\Delta f + e_x^T K_x e_v \\ &= -K_x||e_x||^{\alpha+1} - K_p||p||^{\alpha+1} + p^T\Delta f \end{aligned} \tag{7.23}$$

where, $\Delta f = Rf_b - f_c^d$. From (3.15), the norm of Δf can be written as :

$$||\Delta f|| < \sqrt{2h_2}||e_R||f_M$$

Therefore, eqn.(7.23) becomes :

$$\dot{V}_T \leq -K_x||e_x||^{\alpha+1} - K_p||p||^{\alpha+1} + \sqrt{2h_2}||p||||e_R||f_M \tag{7.24}$$

The complete error dynamics can be proved to be finite-time stable by taking $V = V_T + V_R$ as the Lyapunov function candidate for the complete dynamics. Therefore, letting $z = [||e_R||\ \ ||l||\ \ ||e_x||\ \ ||p||]^T$, we can write

$$\begin{aligned} &\frac{1}{2}\lambda_{min}(I)||l||^2 + h_1||e_R||^2 + \frac{1}{2}m||p||^2 + \frac{1}{2}\lambda_{min}(K_x)||e_x||^2 \leq \\ &V \leq \frac{1}{2}\lambda_{max}(I)||l||^2 + h_2||e_R||^2 + \frac{1}{2}m||p||^2 + \frac{1}{2}\lambda_{max}(K_x)||e_x||^2 \end{aligned} \tag{7.25}$$

The bound on V can be further written as :

$$V \geq min(\frac{1}{2}\lambda_{min}(I), h_1, \frac{1}{2}m, \frac{1}{2}\lambda_{min}(K_x))(||l||^2 + ||e_R||^2 + ||p||^2 + ||e_x||^2) \tag{7.26}$$

From (7.9) and (7.24), the time derivative of V can be written as :

$$\dot{V} \leq -K_l||l||^{\alpha+1} - ||e_R||^{\alpha+1} - K_x||e_x||^{\alpha+1} - K_p||p||^{\alpha+1} + \sqrt{2h_2}||p||||e_R||f_M \tag{7.27}$$

Since $||e_R|| \leq 1$, we have, $||e_R|| \leq ||e_R||^\alpha$ for $\alpha \in (0,1)$ and therefore, Eq.(7.27) can be modified as :

$$\begin{aligned}\dot{V} &\leq -K_l||l||^{\alpha+1} - ||e_R||^{\alpha+1} - K_x||e_x||^{\alpha+1} - K_p||p||^{\alpha+1} + \sqrt{2h_2}||p||||e_R||^\alpha f_M \\ &\leq -K_l||l||^{\alpha+1} - ||e_R||^{\alpha+1} - K_x||e_x||^{\alpha+1} - K_p||p||^{\alpha+1} + \sqrt{2h_2}||p||||e_R||^\alpha f_M \\ &+ \sqrt{2h_2}||p||^\alpha||e_R||f_M \end{aligned} \tag{7.28}$$

Let $z_\alpha = [||e_R||^\alpha \;\; ||l||^\alpha \;\; ||e_x||^\alpha \;\; ||p||^\alpha]^T$, then (7.28) is

$$\dot{V} \leq -z_\alpha^T P z \tag{7.29}$$

where

$$P = \begin{bmatrix} 1 & 0 & 0 & \sqrt{2h_2}f_M \\ 0 & K_l & 0 & 0 \\ 0 & 0 & K_x & 0 \\ \sqrt{2h_2}f_M & 0 & 0 & K_p \end{bmatrix}$$

□

From Lemma 7.2.4, inequality (7.29) can be further written as :

$$\dot{V} \leq -\lambda_{min}(P)z_\alpha^T z \tag{7.30}$$

Here P is chosen to be a positive definite matrix. Eq.(7.30) becomes :

$$\dot{V} \leq -\lambda_{min}(P)(||e_R||^{\alpha+1} + ||l||^{\alpha+1} + ||e_x||^{\alpha+1} + ||p||^{\alpha+1}) \tag{7.31}$$

From Lemma 7.2.3 inequality (7.31) becomes :

$$\dot{V} \leq -\lambda_{min}(P)(||e_R||^2 + ||l||^2 + ||e_x||^2 + ||p||^2)^{\frac{\alpha+1}{2}} \tag{7.32}$$

From Eq.(7.26), (7.32) is written as :

$$\dot{V} \leq -\frac{\lambda_{min}(P)}{min(\frac{1}{2}\lambda_{min}(I), h_1, \frac{1}{2}m, \frac{1}{2}\lambda_{min}(K_x))} V^{\frac{\alpha+1}{2}} = -cV^{\beta} \tag{7.33}$$

where

$$c = \frac{\lambda_{min}(P)}{min(\frac{1}{2}\lambda_{min}(I), h_1, \frac{1}{2}m, \frac{1}{2}\lambda_{min}(K_x))}$$
$$\beta = \frac{\alpha+1}{2} \in (0,1)$$

Hence from Theorem 7.2.2, the complete closed-loop error dynamics is finite-time stable. The settling time, t_S for the complete motion is given by

$$t_S = \frac{1}{c(1-\alpha)} V(0)^{1-\alpha}$$

Again the control law (7.16) has singularity at $||e_x|| = 0$. Similar to previous method, this issue can be avoided by replacing $||e_x||$ by $(||e_x|| + \epsilon)$ where ϵ is a small number, where $\epsilon = 0.001$. The reason for adding ϵ can be understood in the same fashion as before. Therefore the modified control law f_c^d becomes :

$$\begin{aligned} f_c^d = &-K_x e_x - K_p p(||p|| + \epsilon)^{\alpha-1} + m(\dot{v}_d + g e_3) \\ &- m e_v (||e_x|| + \epsilon)^{\alpha-1} - m(\alpha-1) e_x^T e_v \frac{e_x}{(||e_x|| + \epsilon)^{3-\alpha}} \end{aligned} \tag{7.34}$$

Therefore the singularity issue can be avoided using this approach.

7.4 Robustness to bounded disturbances

The dynamic equation of a quadrotor while accounting for external disturbances present in rotational and translational dynamics is presented in section 3.2 but is mentioned below for completeness :

$$\dot{x} = v$$
$$\dot{R} = R\hat{\Omega}$$
$$m\dot{v} = -mge_3 + Rf_b + d_x \tag{7.35}$$
$$I\dot{\Omega} = -\Omega \times I\Omega + \tau_b + d_\Omega \tag{7.36}$$

Following assumptions are considered before showing robustness to bounded external disturbances :

Assumption 5.

The norm of the disturbance vector in translational dynamics is bounded by a known constant i.e. $||d_x|| \leq d_{xmax}$.

Assumption 6.

The norm of the disturbance vector in attitude dynamics is bounded by a known constant i.e. $||d_\Omega|| \leq d_{\Omega max}$.

Proposition 7.3. *If the disturbance in the attitude dynamics is bounded as in Assumption 6 and* (7.37)*, then the finite-time control law* (7.3) *for the attitude dynamics makes the attitude error dynamics converge to the neighborhood of* $(e_R, e_\Omega) = (0, 0)$.

$$d_{\Omega max} \leq \frac{K_l l_{max}^{\alpha+1} + 1}{l_{max}} \tag{7.37}$$

Proof. This can be proved by taking the time derivative of the Lyapunov function V_R as in Eq.(7.6). Proceeding as before along the system dynamics (7.36), we obtain :

$$\dot{V}_R = -K_l ||l||^{\alpha+1} - ||e_R||^{\alpha+1} + l^T d_\Omega \tag{7.38}$$

From Assumptions 6 one gets :

$$\begin{aligned} \dot{V}_R &\leq -K_l l_{max}^{\alpha+1} - 1 + ||l||||d_\Omega|| \\ &\leq -K_l l_{max}^{\alpha+1} - 1 + l_{max} d_{\Omega max} \end{aligned} \tag{7.39}$$

Therefore, $\dot{V}_R$ is non-positive if

$$\dot{V}_R \leq 0 \tag{7.40}$$

which is a sufficient condition for the attitude errors to converge to the neighborhood of $(I, 0)$. The above condition can be utilized to derive the expression for the bound of disturbance vector in attitude dynamics i.e. Eqn.(7.37). □

Proposition 7.4. *If the disturbance in the attitude as well as translational dynamics is bounded as in Assumption 5-6 and* (7.37)*,* (7.41)*, then the finite-time control law* (7.3)*,* (7.16) *for the attitude dynamics and translational dynamics makes the closed loop error*

dynamics converge to the neighborhood of $(e_R, e_\Omega, e_x, e_v) = (0, 0, 0, 0)$.

$$d_{xmax} \leq \frac{\lambda_{min}(P)(l_{max}^{\alpha+1} + 1 + e_{xmax}^{\alpha+1} + p_{max}^{\alpha+1})}{p_{max}} - \frac{l_{max} d_{\Omega max}}{p_{max}} \tag{7.41}$$

Proof. This can be proved by taking the time derivative of the Lyapunov function V_T as in Eq.(7.21). Proceeding as before along the system dynamics (7.35), we obtain :

$$\dot{V}_T = -K_x ||e_x||^{\alpha+1} - K_p ||p||^{\alpha+1} + p^T \Delta f + p^T \Delta_x \tag{7.42}$$

□

For the complete dynamics take $V = V_T + V_R$ as before. From Eqns. (7.38) and (7.42) and proceeding as before we get :

$$\begin{aligned}
\dot{V} &\leq -\lambda_{min}(P)(||e_R||^{\alpha+1} + ||l||^{\alpha+1} + ||e_x||^{\alpha+1} + ||p||^{\alpha+1}) + l^T d_\Omega + p^T \Delta_x \\
&\leq -\lambda_{min}(P)(l_{max}^{\alpha+1} + 1 + e_{xmax}^{\alpha+1} + p_{max}^{\alpha+1}) + l_{max} d_{\Omega max} + p_{max} d_{xmax}
\end{aligned}$$

Therefore, $\dot{V}$ is non-positive if

$$\dot{V} \leq 0 \tag{7.43}$$

which is a sufficient condition for the errors to converge to the neighborhood of $(e_R, e_\Omega, e_x, e_v) = (0, 0, 0, 0)$. The above condition can be utilized to derive the expression for the bound of disturbance vector in translational dynamics i.e. Eqn.(7.41).

7.5 Numerical Simulations

The simulation results have been divided into three sections. The first section demonstrates the tracking performance of the proposed controller. From the simulation diagrams, it can be observed that the tracking performance is quite good. The second section presents the comparison result with the existing exponentially stabilizing controller in the literature. It is shown that the proposed method results in faster convergence to the desired trajectory. It is shown through comparison Table 7.2 and 7.3 that the peak overshoot and the settling time of the proposed controller are significantly less as compared to the other controller. The third section demonstrates the robustness property of the proposed controller. It is shown that better position tracking is obtained with the finite-time control law than the exponentially converging control law in the presence of bounded external disturbances. The detailed results are discussed below, in which both

Table 7.1: Parameters used in simulation

Parameter	Values	Units	Parameter	Values	Units
g	9.81	m/s^2	I_{xx}	0.082	kg m^2
m	1.0	kg	I_{yy}	0.0845	kg m^2
K_x	$2I_3$	-	I_{zz}	0.1377	kg m^2
K_p	$2I_3$	-	K_l	$2I_3$	-
K	I_3	-	α	0.8	-

qualitative and quantitative results are presented. The comparison has been made in terms of RMS error in trajectory tracking.

7.5.1 Trajectory Tracking

In order to illustrate the theoretical results, numerical simulations were carried out for the system whose parameters are shown in Table.7.1. The reference trajectory is given by

$$x_d(t) = [2\cos\left[\frac{\pi t}{10}\right]; 2\sin\left[\frac{\pi t}{10}\right]; \frac{t}{2}] \text{ and } b_{1d}(t) = \frac{\dot{x}_d(t)}{||\dot{x}_d(t)||}$$

The initial conditions for simulation are assumed to be

$$[x(0), y(0), z(0)] = [0, 0, 0], [\dot{x}(0), \dot{y}(0), \dot{z}(0)] = [0, 0, 0] \text{ and}$$
$$R(0) = I_3.$$

The proposed control law is simulated in MATLAB/SIMULINK for the quadrotor dynamics with the trajectory and initial conditions mentioned above. The trajectory tracking performance of the control law is shown in Fig.7.1. It is observed that the finite-time control law tracks the reference trajectory quite well. The settling time is small, and the peak overshoot is also small. These parameters have been quantified in the next section.

7.5.2 Comparison Result

The proposed control law is also compared with the control law proposed in [54] where a geometric controller with exponential convergence is developed for a quadrotor. The various comparative simulation results are shown in Figs. 7.2-7.3. It is observed from various comparative figures that the proposed method results in faster convergence to the desired trajectory with less peak overshoot, except in the case of angular velocity errors. One can observe the tracking error performance in Fig.7.2 while velocity error

performance is shown in Fig.7.4. The attitude error and angular velocity error performances are shown in Fig.7.5-7.6. The time taken by the errors to converge within a range of 0.02m for each control law is illustrated in Table 7.2. One can infer that the convergence in the proposed control law's case is very fast and is almost $\frac{1}{5}$ in some cases compared to the exponentially stable controller. A comparison of peak overshoot due to both control efforts is illustrated in Table 7.3. It can be inferred from the table that the peak overshoot in the case of the proposed control law is small as compared to the approach in [54]. The torque inputs shown in Fig.7.7 in both the cases are very similar, and hence the finite-time control law is guaranteeing faster convergence at the same control input. The control input in the body z-axis in the case of the proposed method converges to the desired value within 5 sec while it takes almost 20 sec for similar convergence in case of [54]. The configuration error function converges to zero very fast, as shown in Fig.7.3-b within 2 sec in the case of the proposed control method. Very similar results were obtained by comparing the proposed control law with the control law developed in [46] and is not mentioned here for the sake of repetition. In [46] a geometric control law is developed for a quadrotor but with the right tracking error function. Similar convergence times were also obtained in this case also. From the simulation results, it can be inferred that the control inputs are bounded and continuous, unlike many control laws in literature where they are discontinuous, and hence the problem of chattering may occur. The proposed control law is continuous and can be applied to practical actuators.

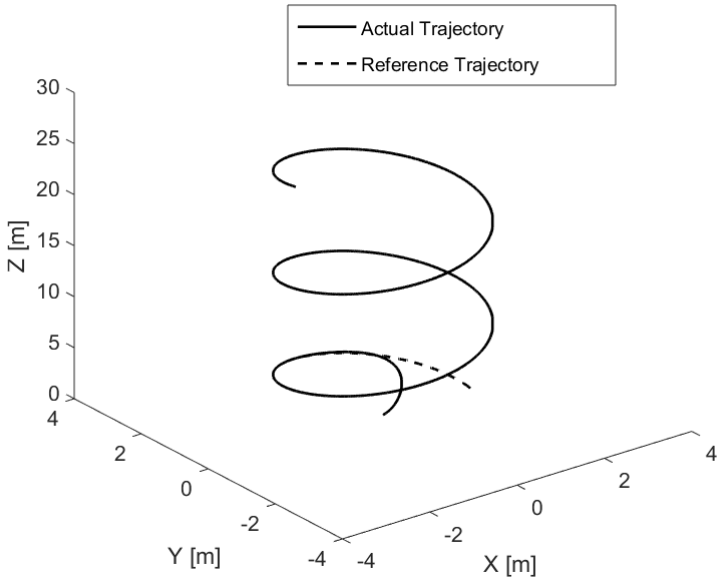

Figure 7.1: Trajectory tracking in 3D

Table 7.2: Convergence time for the parameters by each control law in sec[s]

Parameter	Invernizzi and Lovera	Proposed method
e_x	25	5
e_y	25	5
e_z	25	5
e_{vx}	25	6
e_{vy}	25	6
e_{vz}	26	6
$e_r(1)$	9	4
$e_r(2)$	6	3
$e_r(3)$	4	3
$e_\Omega(1)$	4	5
$e_\Omega(2)$	4	4
$e_\Omega(3)$	4	3
Ψ	3.5	2

Table 7.3: Peak overshoot for parameters in both approaches in metres [m]

Parameter	Invernizzi and Lovera	Proposed method
e_x	0.6	0.01
e_y	-0.8	-0.5
e_z	-0.45	-0.22
e_{vx}	0.82	0.85
e_{vy}	0.35	0.25
e_{vz}	0.2	0.1
$e_r(1)$	0.01	0.01
$e_r(2)$	0.01	0.01
$e_r(3)$	0.01	0.01
$e_\Omega(1)$	0.035	0.075
$e_\Omega(2)$	0.1	0.25
$e_\Omega(3)$	0.2	0.25

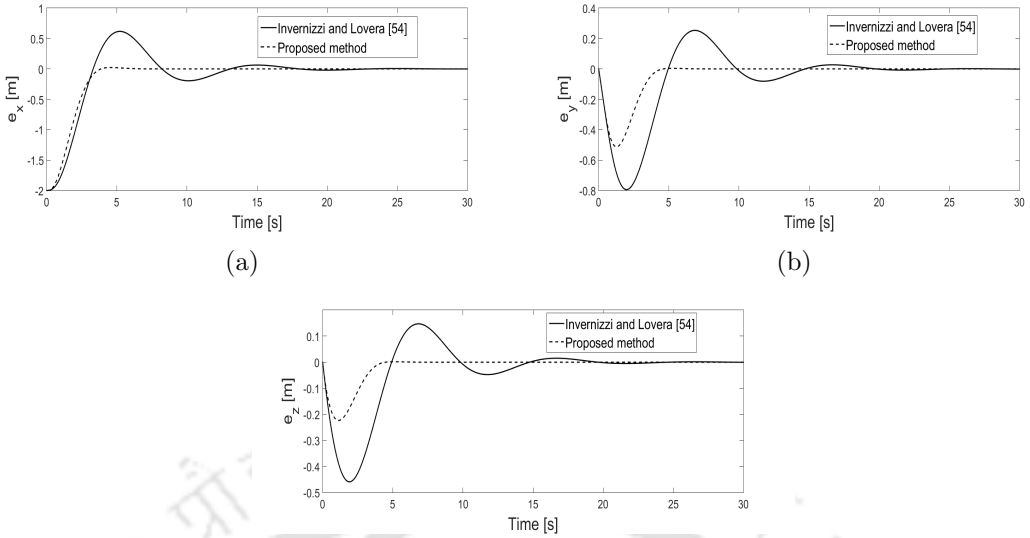

(a) (b)

(c)

Figure 7.2: Tracking Error in (a) X [m]; (b) Y [m];(c) Z [m].

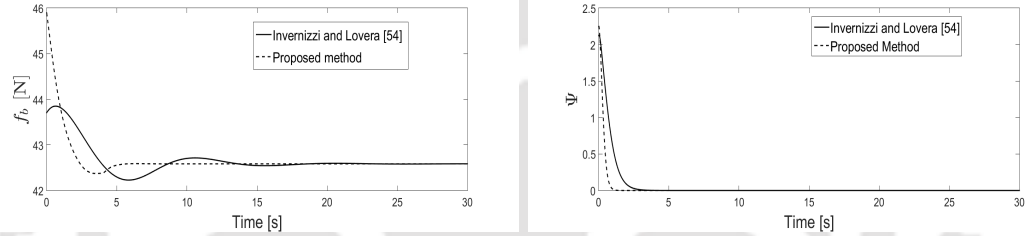

(a) (b)

Figure 7.3: (a) Force along body Z-axis [N]; (b) Configuration error.

7.5.3 Robustness to disturbances

The external disturbances generated in the simulation environment are given by

$$d_x(t) = [0.13\tan^{-1}\left(\frac{t}{2}\right); 0.2\tan^{-1}\left(\frac{t}{2}\right); 0.26\tan^{-1}\left(\frac{t}{2}\right)].$$
$$d_\Omega(t) = [0.13\tan^{-1}\left(\frac{t}{2}\right); 0.2\tan^{-1}\left(\frac{t}{2}\right); 0.26\tan^{-1}\left(\frac{t}{2}\right)].$$

The position tracking performance is shown in Fig 7.7-d. It is observed from Fig. 7.7-d that better position tracking is obtained with the finite-time control law than the exponentially converging control law. The RMS error in position tracking in the case of exponentially converging control law is found to be $[2.9028; 2.8644; 0.6898]m$ while RMS error in position tracking with the finite-time control law is found to be $[0.3621; 0.1880; 0.0849]m$ which is a substantial improvement. The transient performance and the dynamic response of the finite-time control law are also significantly improved compared to the one

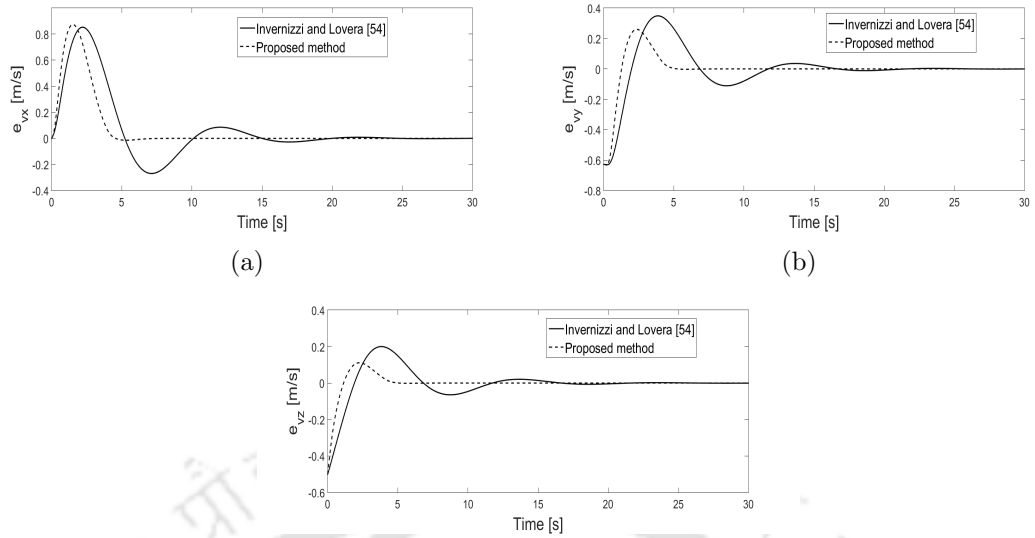

(a) (b)

(c)

Figure 7.4: Velocity Error in (a) X [m/s]; (b) Y [m/s];(c) Z [m/s].

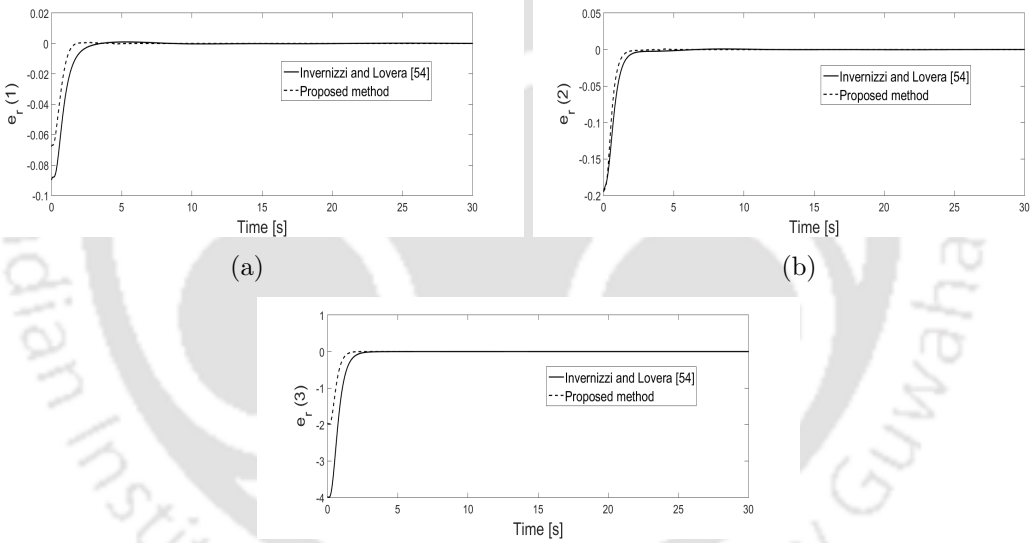

(a) (b)

(c)

Figure 7.5: Attitude Error in (a) Roll [rad]; (b) Pitch [rad];(c) Yaw [rad].

with exponentially converging control law.

7.6 Conclusion

A nonlinear geometric finite-time controller is proposed for quadrotors for their attitude as well as translational dynamics. A composite error is constructed based on which finite-time control law is formulated for both rotational and translational dynamics. The theoretical proof shows that the proposed control law results in a finite-time

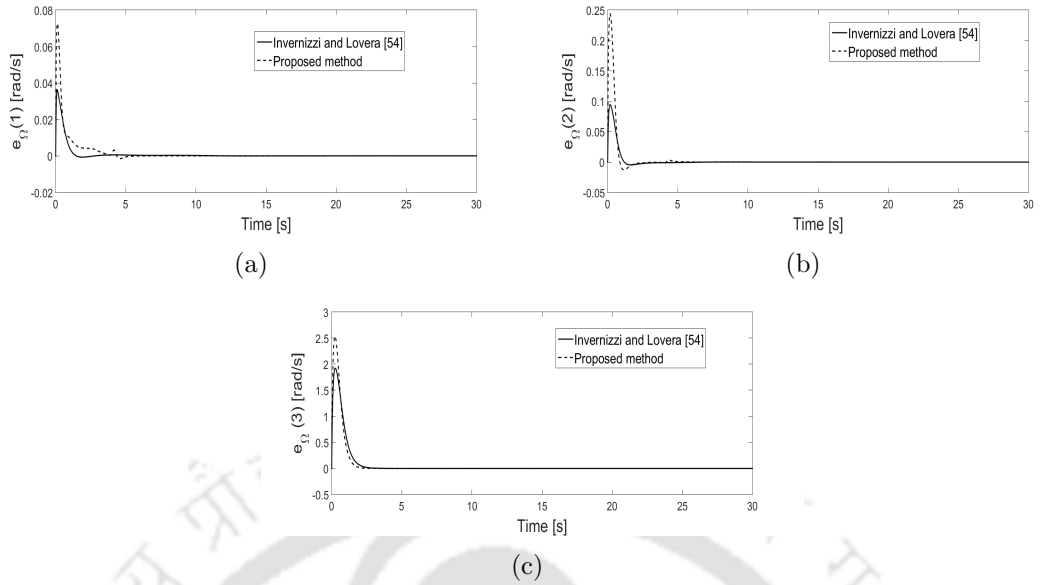

Figure 7.6: Angular Velocity Error in (a) Roll [rad/s]; (b) Pitch [rad/s];(c) Yaw [rad/s].

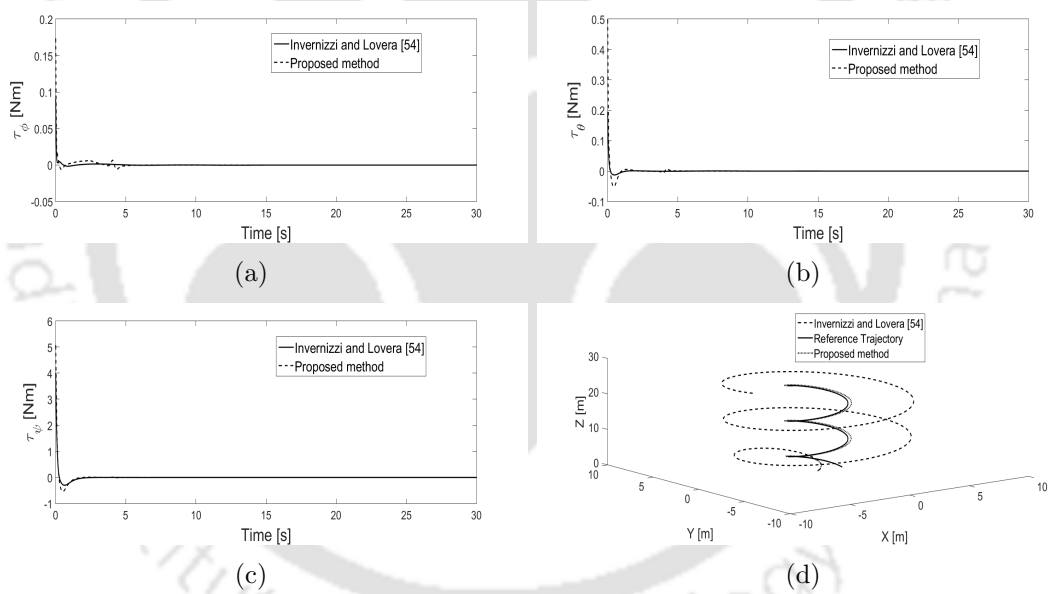

Figure 7.7: Torque input in (a) Roll [Nm]; (b) Pitch [Nm];(c) Yaw [Nm]; (d) Tracking performance in the presence of bounded disturbances

stable closed-loop system. Simulation results show better tracking performance and faster convergence to the desired trajectory as compared to other exponentially converging control laws in the literature. The control law is also intrinsic, i.e., coordinate invariant. Hence the proposed method not only gives a finite-time stable closed-loop system but also improved transients. The simulation results also show that the proposed control law is extremely robust to bounded external disturbances and results in very little RMS error as compared to exponentially converging control law. A comparison table has been pro-

vided to demonstrate the proposed control law's better performance compared to other control laws. Future work includes the implementation of the above finite-time control law on a real-time hardware prototype. It is planned to implement this control law on an open-source Pixhawk board based on PX4 firmware.

Chapter 8

Conclusions and Future Works

8.1 Conclusions

In this thesis report, several globally valid algorithms for the control of quadrotors in the presence of disturbance and time-delays are presented. The second chapter presents a globally valid model of a quadrotor on $SE(3)$ using variational principles.

In the third chapter, a nonlinear disturbance observer-based controller was designed for a quadrotor. The proposed disturbance observer-based controller's main advantage is that the bound on the disturbance is not assumed to be known. The controller is also shown to have a simpler structure. The theoretical proof shows that the proposed controller is locally input to state stable with respect to the derivative of the disturbances if the disturbance, as well as its derivatives, are bounded, and hence the tracking errors are also bounded. The simulation results and the experimental results show the proposed controller's effectiveness in the presence of disturbances and modeling inaccuracies.

In the fourth chapter, a nonlinear geometric adaptive controller was proposed for quadrotors when the center of gravity's location is different from the geometric center. The theoretical proof shows that the proposed control law along with coordinate invariant adaptive laws is stable. Simulation results show better tracking performance when the offset is explicitly compensated as compared to when it is not explicitly compensated. It can be observed that beyond a certain threshold in offset between the center of gravity and geometric center, if the system dynamics is not compensated explicitly with the proposed method, then the system becomes unstable. Hence, the proposed method gives a tracking controller and stable adaptive control laws, which have been verified through numerical simulations.

In the fifth work, a state predictor controller pair was developed to control a quadrotor in the presence of network-induced state and input time delay. To the best of the authors' knowledge, this study is the first to explicitly compensate for both states and

input time delay in a quadrotor system. The state predictor was shown to be asymptotically stable and hence was able to estimate the states' future values. The output of the predictor is used while implementing the controller developed in this chapter. The controller is also shown to be asymptotically stable. Through simulations, it is observed that the quadrotor's satisfactory steering is obtained with a controller augmented with the predictor in the presence of state and input delay.

In the sixth chapter, a predictor feedback control for attitude stabilization of quadrotors with input time delay has been proposed by representing the attitude using rotation matrices to avoid the singularities and sign ambiguities associated with Euler angles and quaternions, respectively. The closed-loop system is shown to be asymptotically stable with respect to a norm defined in the text. The norm has been defined in terms of states and past control efforts and hence explicitly results in Lyapunov Krasovskii functional for the system. A cascade of PDE-ODE system and the concept of transport delay has been used in the proof. The control law is also shown to be robust in the presence of external disturbances as well as delay mismatch.

In the seventh chapter, a nonlinear geometric finite-time controller was proposed for quadrotors for their attitude as well as translational dynamics. A composite error was constructed based on which finite-time control law was formulated for both rotational and translational dynamics. The theoretical proof shows that the proposed control law results in a finite-time stable closed-loop system. Simulation results show better tracking performance and faster convergence to the desired trajectory as compared to other exponentially converging control laws in the literature. Hence the proposed method not only gives a finite-time stable closed-loop system but also improved transients. The simulation results also show that the proposed control law is extremely robust to bounded external disturbances and results in very little RMS error as compared to exponentially converging control law. A comparison table has been provided to demonstrate the proposed control law's better performance compared to other control laws.

8.2 Future Works

The future work will mainly focus on the following scenario :

- The future work will deal with controller design even in the presence of packet loss experienced while operating over a TCP network. This is a very practical scenario since the network is never perfect, and packet loss is inevitable.

- Moreover, we have not considered parametric uncertainty in the estimator as well as controller design. The effect of parametric uncertainly will also be considered in

future work. In fact, globally valid control law in the presence of input and state delay considering external disturbance is being developed presently.

- The proposed algorithm can be easily extended to multi-agent quadrotor systems. For example, one can work on consensus or formation control of multiple quadrotors. This work is presently being looked into.
- The experimental verification of the proposed method in this thesis is another area to be looked into. This will demonstrate the effectiveness of the proposed method in a real-life scenario.
- Geometric optimal control of multiple quadrotors is another promising area where one can develop globally valid control law on $SE(3)$ minimizing a performance index. Since a quadrotor consumes a lot of energy, one can choose to minimize control input to reduce energy consumption. One can also choose to minimize the time required in tracking a trajectory.

Appendix A

SUPPLEMENTARY MATERIALS

A.1 Hardware Setup

The specifications of the hardware set up are given below :

1. PIXHAWK FMU 2.4.8 with PX4 Firmware
2. 30A Electronic Speed Controllers (ESC)
3. A2212/13T 1000KV BLDC Motors
4. GPS Module with Compass
5. 3000 mAh 3 cell 11.1 V 30 C Li-ion batteries
6. 433 MHz Telemetry Module
7. Buzzer
8. 10 × 4.5 propellers
9. FS-CT6B Transmitter
10. Raspberry Pi 3.0 motherboard

The hardware setup, assembled in the lab, is shown in Fig.A.1.

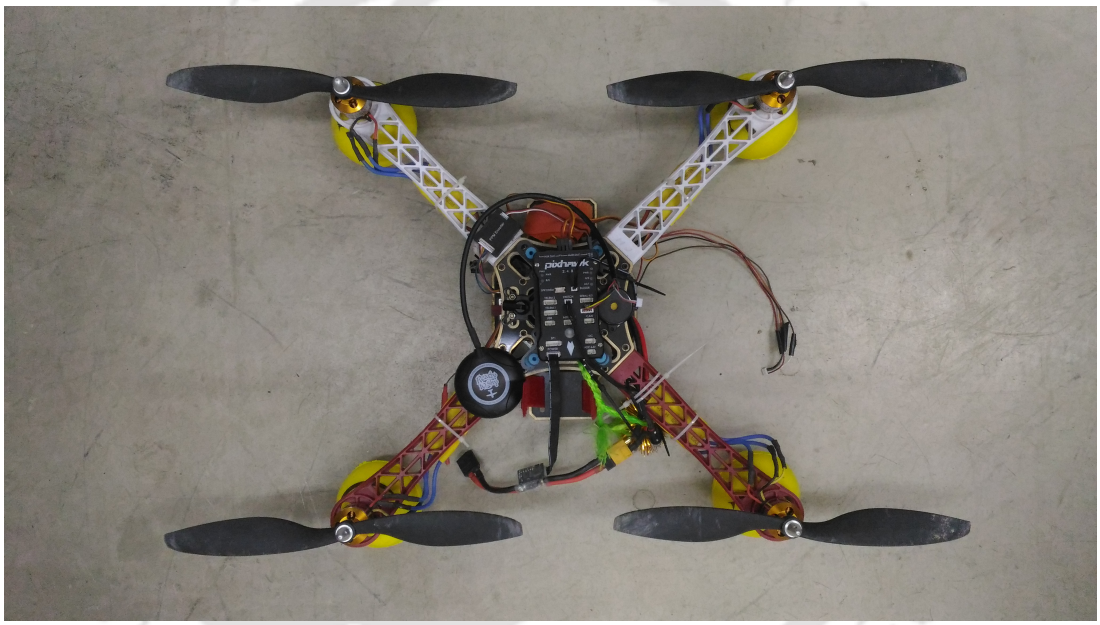

Figure A.1: Quadrotor setup assembled in the Lab

List of Publications

CONFERENCES

[1] M. Sharma and I. Kar, "Geometric modeling and attitude stabilization of quadcopters," in 12th Asian Control Conference, Japan, 61-66, 2019.

[2] M. Sharma and I. Kar, "Geometric Tracking Control of a Quadrotor on SE (3) using left tracking error function," in ACODS, 53 (1), 301-306, 2020, IIT Madras.

[3] M. Sharma and I. Kar, "Finite Time Disturbance Observer Based Geometric Control of Quadrotors," in ACODS, 53 (1), 295-300, 2020, IIT Madras.

[4] M. Sharma and I. Kar, "Attitude Stabilization of a Quadrotor with Input Time Delay," in IFAC WC, 53(2), 9360-9365, 2020, Germany.

JOURNALS

[1] M. Sharma and I. Kar, "Nonlinear Disturbance observer based geometric control of quadrotors," Asian Journal of Control, 23(4), 1936-1951, 2021.
DOI : https://doi.org/10.1002/asjc.2318

[2] M. Sharma and I. Kar, "Adaptive geometric control of quadrotors with dynamic offset between center of gravity and geometric center," Asian Journal of Control, 23(4), 1923-1935, 2021. DOI : https://doi.org/10.1002/asjc.2327

[3] M. Sharma and I. Kar, 'Control of a quadrotor with network induced time delay," ISA Transactions, 111, 132-143, 2021, DOI : https://doi.org/10.1016/j.isatra.2020.11.008

[4] M. Sharma and I. Kar, 'Geometric control of quadrotor with finite-time convergence and improved transients," International Journal of Systems Science, 52 (7), 1396-

1413,2021, DOI : https://doi.org/10.1080/00207721.2020.1857880

Bibliography

[1] Mikrokopter, 2006. [Online]. Available: http://www.mikrokopter.de/

[2] Microdrone-bulgaria. [Online]. Available: http://www.microdrones-bulgaria.com/

[3] Dragonfly-innovations, 1998. [Online]. Available: http://www.draganfly.com/

[4] Quanser-3-DOF-Hover. [Online]. Available: https://www.quanser.com/products/3-dof-hover/

[5] I. Kroo and F. Prinz, in *Mesicopter Project*, 1999. [Online]. Available: https://nplab.stanford.edu/publications/mesicopter-meso-scale-flight-vehicle

[6] J. Borenstein, in *Hoverbot Project*, 1992. [Online]. Available: Univ. of Michigan,http://www-personal.umich.edu/ johannb/hoverbot.htm

[7] F. Bullo and A. D. Lewis, *Geometric control of mechanical systems: modeling, analysis, and design for simple mechanical control systems*. Springer Science & Business Media, 2004, vol. 49.

[8] A. Tewari, *Atmospheric and Space Flight Dynamics*. Springer, 2007.

[9] S. P. Bhat and D. S. Bernstein, "A topological obstruction to global asymptotic stabilization of rotational motion and the unwinding phenomenon," in *Proceedings of the 1998 American Control Conference. ACC (IEEE Cat. No.98CH36207)*, vol. 5, Jun 1998, pp. 2785–2789 vol.5.

[10] S. Bouabdallah, A. Noth, and R. Siegwart, "PID vs LQ control techniques applied to an indoor micro quadrotor," in *2004 IEEE/RSJ International Conference on Intelligent Robots and Systems (IROS) (IEEE Cat. No.04CH37566)*, vol. 3, Sept 2004, pp. 2451–2456 vol.3.

[11] G. M. Hoffmann, H. Huang, S. L. Waslander, and C. J. Tomlin, "Quadrotor helicopter flight dynamics and control: Theory and experiment," in *AIAA Guidance, Navigation and Control Conference and Exhibit*, August 2007.

[12] V. Mistler, A. Benallegue, and N. K. M'Sirdi, "Exact linearization and noninteracting control of a 4 rotors helicopter via dynamic feedback," in *Proceedings 10th IEEE International Workshop on Robot and Human Interactive Communication. ROMAN 2001 (Cat. No.01TH8591)*, 2001, pp. 586–593.

[13] T. J. Koo and S. Sastry, "Output tracking control design of a helicopter model based on approximate linearization," in *Proceedings of the 37th IEEE Conference on Decision and Control (Cat. No.98CH36171)*, vol. 4, Dec 1998, pp. 3635–3640 vol.4.

[14] A. Das, K. Subbarao, and F. Lewis, "Dynamic inversion with zero-dynamics stabilisation for quadrotor control," *IET Control Theory Applications*, vol. 3, no. 3, pp. 303–314, March 2009.

[15] E. Altug, J. P. Ostrowski, and R. Mahony, "Control of a quadrotor helicopter using visual feedback," in *Proceedings 2002 IEEE International Conference on Robotics and Automation (Cat. No.02CH37292)*, vol. 1, 2002, pp. 72–77 vol.1.

[16] E. Altug, J. P. Ostrowski, and C. J. Taylor, "Quadrotor control using dual camera visual feedback," in *2003 IEEE International Conference on Robotics and Automation (Cat. No.03CH37422)*, vol. 3, Sept 2003, pp. 4294–4299 vol.3.

[17] S. Bouabdallah, P. Murrieri, and R. Siegwart, "Design and control of an indoor micro quadrotor," in *Robotics and Automation, 2004. Proceedings. ICRA '04. 2004 IEEE International Conference on*, vol. 5, April 2004, pp. 4393–4398 Vol.5.

[18] A. Tayebi and S. McGilvray, "Attitude stabilization of a four-rotor aerial robot," in *2004 43rd IEEE Conference on Decision and Control (CDC) (IEEE Cat. No.04CH37601)*, vol. 2, Dec 2004, pp. 1216–1221 Vol.2.

[19] A. R. Teel, "Global stabilization and restricted tracking for multiple integrators with bounded controls," *Systems & Control Letters*, vol. 18, no. 3, pp. 165 – 171, 1992.

[20] P. Castillo, A. Dzul, and R. Lozano, "Real-time stabilization and tracking of a four-rotor mini rotorcraft," *IEEE Transactions on Control Systems Technology*, vol. 12, no. 4, pp. 510–516, July 2004.

[21] T. Hamel, R. Mahony, R. Lozano, and J. Ostrowski, "Dynamic modelling and configuration stabilization for an X4-Flyer." *IFAC Proceedings Volumes*, vol. 35, no. 1, pp. 217 – 222, 2002, 15th IFAC World Congress.

[22] A. Roza and M. Maggiore, "Path following controller for a quadrotor helicopter," in *2012 American Control Conference (ACC)*, June 2012, pp. 4655–4660.

[23] S. Bouabdallah and R. Siegwart, "Backstepping and Sliding-mode techniques applied to an indoor micro quadrotor," in *Proceedings of the 2005 IEEE International Conference on Robotics and Automation*, April 2005, pp. 2247–2252.

[24] T. Madani and A. Benallegue, "Control of a quadrotor mini-helicopter via full state backstepping technique," in *Proceedings of the 45th IEEE Conference on Decision and Control*, Dec 2006, pp. 1515–1520.

[25] R. Xu and U. Ozguner, "Sliding mode control of a quadrotor helicopter," in *Proceedings of the 45th IEEE Conference on Decision and Control*, Dec 2006, pp. 4957–4962.

[26] Z. Zuo, "Trajectory tracking control design with command-filtered compensation for a quadrotor," *IET Control Theory Applications*, vol. 4, no. 11, pp. 2343–2355, November 2010.

[27] J. Hu and H. Zhang, "Immersion and invariance based command-filtered adaptive backstepping control of VTOL vehicles," *Automatica*, vol. 49, no. 7, pp. 2160 – 2167, 2013.

[28] A. Astolfi, D. Karagiannis, and R. Ortega, *Nonlinear and Adaptive Control with Applications*, 1st ed. Springer Publishing Company, Incorporated, 2008.

[29] G. V. Raffo, M. G. Ortega, and F. R. Rubio, "Backstepping/nonlinear $\mathcal{H}_\infty$ control for path tracking of a quadrotor unmanned aerial vehicle," in *2008 American Control Conference*, June 2008, pp. 3356–3361.

[30] A. J. van der Schaft, "L_2-gain analysis of nonlinear systems and nonlinear state-feedback $\mathcal{H}_\infty$ control," *IEEE Transactions on Automatic Control*, vol. 37, no. 6, pp. 770–784, June 1992.

[31] M. Chen and M. Huzmezan, *A Combined MBPC/2 DOF $\mathcal{H}_\infty$ Controller for a Quad Rotor UAV*. [Online]. Available: https://arc.aiaa.org/doi/abs/10.2514/6.2003-5520

[32] G. V. Raffo, M. G. Ortega, and F. R. Rubio, "Path tracking of a UAV via an underactuated control strategy," *European Journal of Control*, vol. 17, no. 2, pp. 194 – 213, 2011. [Online]. Available: http://www.sciencedirect.com/science/article/pii/S0947358011705878

[33] ——, "An integral predictive/nonlinear $\mathcal{H}_\infty$ control structure for a quadrotor helicopter," *Automatica*, vol. 46, no. 1, pp. 29 – 39, 2010. [Online]. Available: http://www.sciencedirect.com/science/article/pii/S0005109809004798

[34] N. Fethalla, M. Saad, H. Michalska, and J. Ghommam, "Robust observer-based backstepping controller for a quadrotor UAV," in *2017 IEEE 30th Canadian Conference on Electrical and Computer Engineering (CCECE)*, April 2017, pp. 1–4.

[35] L. Besnard, Y. B. Shtessel, and B. Landrum, "Control of a quadrotor vehicle using sliding mode disturbance observer," in *2007 American Control Conference*, July 2007, pp. 5230–5235.

[36] T. Madani and A. Benallegue, "Sliding mode observer and backstepping control for a quadrotor unmanned aerial vehicles," in *2007 American Control Conference*, July 2007, pp. 5887–5892.

[37] A. Benallegue, A. Mokhtari, and L. Fridman, "Feedback linearization and high order sliding mode observer for a quadrotor UAV," in *International Workshop on Variable Structure Systems, 2006. VSS'06.*, June 2006, pp. 365–372.

[38] A. Mokhtari and A. Benallegue, "Dynamic feedback controller of Euler angles and wind parameters estimation for a quadrotor unmanned aerial vehicle," in *Robotics and Automation, 2004. Proceedings. ICRA '04. 2004 IEEE International Conference on*, vol. 3, April 2004, pp. 2359–2366 Vol.3.

[39] C. Hancer, K. T. Oner, E. Sirimoglu, E. Cetinsoy, and M. Unel, "Robust position control of a tilt-wing quadrotor," in *49th IEEE Conference on Decision and Control (CDC)*, Dec 2010, pp. 4908–4913.

[40] H. Huang, G. M. Hoffmann, S. L. Waslander, and C. J. Tomlin, "Aerodynamics and control of autonomous quadrotor helicopters in aggressive maneuvering," in *2009 IEEE International Conference on Robotics and Automation*, May 2009, pp. 3277–3282.

[41] C. Nicol, C. J. B. Macnab, and A. Ramirez-Serrano, "Robust neural network control of a quadrotor helicopter," in *2008 Canadian Conference on Electrical and Computer Engineering*, May 2008, pp. 001 233–001 238.

[42] M. Santos, V. López, and F. Morata, "Intelligent fuzzy controller of a quadrotor," in *2010 IEEE International Conference on Intelligent Systems and Knowledge Engineering*, Nov 2010, pp. 141–146.

[43] T. Dierks and S. Jagannathan, "Output feedback control of a quadrotor UAV using neural networks," *IEEE Transactions on Neural Networks*, vol. 21, no. 1, pp. 50–66, Jan 2010.

[44] H. Boudjedir, Y. Fouad, O. Bouhali, and N. Rizoug, "Adaptive neural network for a quadrotor unmanned aerial vehicle," *International Journal in Foundations of Computer Science & Technology (IJFCST)*, vol. 2, pp. 1–13, 07 2012.

[45] A. Das, F. Lewis, and K. Subbarao, *Dynamic Neural Network-Based Robust Backstepping Control approach for Quadrotors*. [Online]. Available: https://arc.aiaa.org/doi/abs/10.2514/6.2008-6780

[46] T. Lee, M. Leoky, and N. H. McClamroch, "Geometric tracking control of a quadrotor UAV on SE(3)," in *49th IEEE Conference on Decision and Control (CDC)*, Dec 2010, pp. 5420–5425.

[47] T. Lee, M. Leok, and N. H. McClamroch, "Nonlinear robust tracking control of a quadrotor UAV on SE(3)," in *2012 American Control Conference (ACC)*, June 2012, pp. 4649–4654.

[48] T. Lee, "Robust adaptive attitude tracking on SO(3) with an application to a quadrotor UAV," *IEEE Transactions on Control Systems Technology*, vol. 21, no. 5, pp. 1924–1930, Sept 2013.

[49] F. Goodarzi, D. Lee, and T. Lee, "Geometric nonlinear PID control of a quadrotor uav on SE(3)," in *2013 European Control Conference (ECC)*, July 2013, pp. 3845–3850.

[50] R. R. Warier, A. K. Sanyal, S. Sukumar, and S. P. Viswanathan, "Feedback tracking control schemes for a class of underactuated vehicles in SE(3)," in *2017 American Control Conference (ACC)*, May 2017, pp. 899–904.

[51] S. P. Bhat and D. S. Bernstein, "Finite-time stability of continuous autonomous systems," *SIAM Journal on Control and Optimization*, vol. 38, no. 3, pp. 751–766, 2000.

[52] S. P. Viswanathan, A. K. Sanyal, and R. R. Warier, "Finite-time stable tracking control for a class of underactuated aerial vehicles in SE(3)," in *2017 American Control Conference (ACC)*, May 2017, pp. 3926–3931.

[53] N. Nordkvist and A. K. Sanyal, "A Lie group variational integrator for rigid body motion in SE(3) with applications to underwater vehicle dynamics," in *49th IEEE Conference on Decision and Control (CDC)*, Dec 2010, pp. 5414–5419.

[54] D. Invernizzi and M. Lovera, "Geometric tracking control of a quadcopter tiltrotor UAV," *IFAC-PapersOnLine*, vol. 50, no. 1, pp. 11 565 – 11 570, 2017, 20th IFAC World Congress.

[55] T. Lee, "Global exponential attitude tracking controls on SO(3)," *IEEE Transactions on Automatic Control*, vol. 60, no. 10, pp. 2837–2842, Oct 2015.

[56] T. Lee, D. E. Chang, and Y. Eun, "Attitude control strategies overcoming the topological obstruction on SO(3)," in *2017 American Control Conference (ACC)*, May 2017, pp. 2225–2230.

[57] P. Castillo, P. Albertos, P. Garcia, and R. Lozano, "Simple real-time attitude stabilization of a quad-rotor aircraft with bounded signals," in *Proceedings of the 45th IEEE Conference on Decision and Control*, Dec 2006, pp. 1533–1538.

[58] N. Cao and A. F. Lynch, "Inner-outer loop control for quadrotor UAVs with input and state constraints," *IEEE Transactions on Control Systems Technology*, vol. 24, no. 5, pp. 1797–1804, Sept 2016.

[59] H. Liu, D. Liu, and Z. Zuo, "Robust attitude control for uncertain quadrotors with input time delays," in *2016 European Control Conference (ECC)*, June 2016, pp. 2312–2315.

[60] H. Liu, Y. Bai, G. Lu, and Y. Zhong, "Robust attitude control of uncertain quadrotors," *IET Control Theory Applications*, vol. 7, no. 11, pp. 1583–1589, July 2013.

[61] H. Liu, X. Wang, and Y. Zhong, "Quaternion-based robust attitude control for uncertain robotic quadrotors," *IEEE Transactions on Industrial Informatics*, vol. 11, no. 2, pp. 406–415, April 2015.

[62] H. Liu, D. Li, and Y. Zhong, "Robust attitude stabilization controller design for quadrotor systems with multiple uncertainties and delays," in *2016 American Control Conference (ACC)*, July 2016, pp. 2241–2245.

[63] H. Liu, J. Xi, and Y. Zhong, "Robust attitude stabilization for nonlinear quadrotor systems with uncertainties and delays," *IEEE Transactions on Industrial Electronics*, vol. 64, no. 7, pp. 5585–5594, July 2017.

[64] P. F. Hokayem and M. W. Spong, "Bilateral teleoperation: An historical survey," *Automatica*, vol. 42, no. 12, pp. 2035 – 2057, 2006. [Online]. Available: http://www.sciencedirect.com/science/article/pii/S0005109806002871

[65] T. Oguchi and H. Nijmeijer, "Control of nonlinear systems with time-delay using state predictor based on synchronization." *ENOC-2005, Eindhoven, Netherlands, 7-12 August 2005*, pp. 1150–1156, 2005.

[66] A. Alvarez-Aguirre, H. Nijmeijer, T. Oguchi, and K. Kojima, "Remote control of a mobile robot subject to a communication delay," in *Proceedings of the 7th International Conference on Informatics in Control, Automation and Robotics - Volume 2: ICINCO,*, INSTICC. SciTePress, 2010, pp. 55–62.

[67] K. Kojima, T. Oguchi, A. Alvarez-Aguirre, and H. Nijmeijer, "Predictor-based tracking control of a mobile robot with time-delays," *IFAC Proceedings Volumes*, vol. 43, no. 14, pp. 167 – 172, 2010, 8th IFAC Symposium on Nonlinear Control Systems. [Online]. Available: http://www.sciencedirect.com/science/article/pii/S1474667015369603

[68] S. Al Issa, M. Sharma, and I. Kar, "Event-triggered backstepping control scheme for networked mobile robots," in *Proceedings of the Advances in Robotics 2019*, ser. AIR 2019. New York, NY, USA: Association for Computing Machinery, 2019. [Online]. Available: https://doi.org/10.1145/3352593.3352606

[69] N. Sharma, S. Bhasin, Q. Wang, and W. E. Dixon, "Predictor-based control for an uncertain Euler-Lagrange system with input delay," *Automatica*, vol. 47, no. 11, pp. 2332 – 2342, 2011. [Online]. Available: http://www.sciencedirect.com/science/article/pii/S0005109811003487

[70] J. Ghommam and F. Mnif, "Predictor-based control for an inverted pendulum subject to networked time delay," *ISA Transactions*, vol. 67, pp. 306 – 316, 2017. [Online]. Available: http://www.sciencedirect.com/science/article/pii/S0019057817301180

[71] H. Liu, D. Liu, and Z. Zuo, "Robust attitude control for uncertain quadrotors with input time delays," in *2016 European Control Conference (ECC)*, June 2016, pp. 2312–2315.

[72] Z.-G. Liu and Y.-Q. Wu, "Universal strategies to explicit adaptive control of nonlinear time-delay systems with different structures," *Automatica*, vol. 89, pp. 151 – 159, 2018. [Online]. Available: http://www.sciencedirect.com/science/article/pii/S0005109817305642

[73] Z. Liu, L. Xue, W. Sun, and Z. Sun, "Robust output feedback tracking control for a class of high-order time-delay nonlinear systems with input dead-zone and disturbances," *Nonlinear Dynamics*, vol. 97, pp. 921 – 935, 2019.

[74] S. P. Bhat and D. S. Bernstein, "Finite-time stability of homogeneous systems," in *Proceedings of the 1997 American Control Conference (Cat. No.97CH36041)*, vol. 4, June 1997, pp. 2513–2514 vol.4.

[75] S. P. Bhat and D. S. Bernstein, "Geometric homogeneity with applications to finite-time stability," *Mathematics of Control, Signals and Systems*, vol. 17, no. 2, pp. 101–127, Jun 2005.

[76] S. P. Bhat and D. S. Bernstein, "Finite-time stability of homogeneous systems," in *Proceedings of the 1997 American Control Conference (Cat. No.97CH36041)*, vol. 4, June 1997, pp. 2513–2514 vol.4.

[77] Y. Hong, Y. Xu, and J. Huang, "Finite-time control for robot manipulators," *Systems & Control Letters*, vol. 46, no. 4, pp. 243 – 253, 2002.

[78] S. P. Bhat and D. S. Bernstein, "Continuous finite-time stabilization of the translational and rotational double integrators," *IEEE Transactions on Automatic Control*, vol. 43, no. 5, pp. 678–682, May 1998.

[79] H. Du and S. Li, "Finite-time attitude stabilization for a rigid spacecraft using homogeneous method," *IFAC Proceedings Volumes*, vol. 44, no. 1, pp. 2620 – 2625, 2011, 18th IFAC World Congress.

[80] H. Du, S. Li, and C. Qian, "Finite-time attitude tracking control of spacecraft with application to attitude synchronization," *IEEE Transactions on Automatic Control*, vol. 56, no. 11, pp. 2711–2717, Nov 2011.

[81] Q. Lan, C. Qian, and S. Li, "Finite-Time Disturbance Observer Design and Attitude Tracking Control of a Rigid Spacecraft," *Journal of Dynamic Systems, Measurement, and Control*, vol. 139, no. 6, 04 2017.

[82] B. Tian, L. Liu, H. Lu, Z. Zuo, Q. Zong, and Y. Zhang, "Multivariable finite time attitude control for quadrotor UAV: Theory and experimentation," *IEEE Transactions on Industrial Electronics*, vol. 65, no. 3, pp. 2567–2577, March 2018.

[83] B. Tian, J. Cui, H. Lu, Z. Zuo, and Q. Zong, "Adaptive finite-time attitude tracking of quadrotors with experiments and comparisons," *IEEE Transactions on Industrial Electronics*, vol. 66, no. 12, pp. 9428–9438, Dec 2019.

[84] A. K. Sanyal, J. Bohn, and A. M. Bloch, "Almost global finite time stabilization of rigid body attitude dynamics," in *52nd IEEE Conference on Decision and Control*, Dec 2013, pp. 3261–3266.

[85] J. Bohn and A. K. Sanyal, "Almost global finite-time stabilization of rigid body attitude dynamics using rotation matrices," *International Journal of Robust and Nonlinear Control*, vol. 26, no. 9, pp. 2008–2022, 2016.

[86] S. P. Viswanathan, A. K. Sanyal, and M. Izadi, *Integrated Guidance and Nonlinear Feedback Control of Underactuated Unmanned Aerial Vehicles in SE(3).*

[87] H. Du, G. Wen, Y. Cheng, and J. Lu, "Design and implementation of bounded finite-time control algorithm for speed regulation of permanent magnet synchronous motor," *IEEE Transactions on Industrial Electronics*, vol. PP, pp. 1–1, 02 2020.

[88] H. Du, C. Jiang, G. Wen, W. Zhu, and Y. Cheng, "Current sharing control for parallel DC-DC buck converters based on finite-time control technique," *IEEE Transactions on Industrial Informatics*, vol. 15, no. 4, pp. 2186–2198, 2019.

[89] D. Mellinger and V. Kumar, "Minimum snap trajectory generation and control for quadrotors," in *2011 IEEE International Conference on Robotics and Automation*, May 2011, pp. 2520–2525.

[90] K. Nonami, F. Kendoul, S. Suzuki, W. Wang, and D. Nakazawa, *Autonomous Flying Robots-Unmanned Aerial Vehicles and Micro Aerial Vehicles.* Springer Japan, 2010.

[91] R. M. Murray, Z. Li, S. S. Sastry, and S. S. Sastry, *A mathematical introduction to robotic manipulation.* CRC press, 1994.

[92] D. Holm, T. Schmah, and C. Stoica, *Geometric Mechanics and Symmetry: From Finite to Infinite Dimensions*, 01 2009.

[93] R. Zhang, Q. Quan, and K. . Cai, "Attitude control of a quadrotor aircraft subject to a class of time-varying disturbances," *IET Control Theory Applications*, vol. 5, no. 9, pp. 1140–1146, June 2011.

[94] S. Li, J. Yang, W.-H. Chen, and X. Chen, *Disturbance Observer-Based Control: Methods and Applications*, 1st ed. Boca Raton, FL, USA: CRC Press, Inc., 2014.

[95] W.-H. Chen and L. Guo, "Analysis of disturbance observer based control for nonlinear systems under disturbances with bounded variation," in *In Proceedings of UKACC 2004*, 2004.

[96] H. Khalil, *Nonlinear Systems*, ser. Pearson Education. Prentice Hall, 2002.

[97] M. Krstic, P. V. Kokotovic, and I. Kanellakopoulos, *Nonlinear and Adaptive Control Design*, 1st ed. New York, NY, USA: John Wiley & Sons, Inc., 1995.

[98] A. Mironchenko, "Local input-to-state stability: Characterizations and counterexamples," *Systems & Control Letters*, vol. 87, pp. 23 – 28, 2016.

[99] Pixhawk. [Online]. Available: https://pixhawk.org/

[100] I. Palunko and R. Fierro, "Adaptive control of a quadrotor with dynamic changes in the center of gravity," *IFAC Proceedings Volumes*, vol. 44, no. 1, pp. 2626 – 2631, 2011, 18th IFAC World Congress.

[101] G. Antonelli, F. Arrichiello, S. Chiaverini, and P. R. Giordano, "Adaptive trajectory tracking for quadrotor mavs in presence of parameter uncertainties and external disturbances," in *2013 IEEE/ASME International Conference on Advanced Intelligent Mechatronics*, July 2013, pp. 1337–1342.

[102] G. Antonelli, E. Cataldi, F. Arrichiello, P. R. Giordano, S. Chiaverini, and A. Franchi, "Adaptive trajectory tracking for quadrotor mavs in presence of parameter uncertainties and external disturbances," *IEEE Transactions on Control Systems Technology*, vol. 26, no. 1, pp. 248–254, Jan 2018.

[103] T. I. Fossen *et al.*, *Guidance and control of ocean vehicles*, vol. 199, no. 4.

[104] J. Huang, C. Wen, W. Wang, and Z.-P. Jiang, "Adaptive stabilization and tracking control of a nonholonomic mobile robot with input saturation and disturbance," *Systems & Control Letters*, vol. 62, no. 3, pp. 234 – 241, 2013.

[105] M. Krstic, *Delay Compensation for Nonlinear, Adaptive, and PDE Systems*. Birkhauser Basel, 2009.

[106] M. Wu, Y. He, and J. She, *Stability Analysis and Robust Control of Time-Delay Systems*, 2010.

[107] K. Gu, V. Kharitonov, and J. Chen, "Stability of time-delay systems," 2003.

[108] G. Hardy, K. M. R. Collection, J. Littlewood, G. Pólya, D. Littlewood, and G. Pólya, *Inequalities*, ser. Cambridge Mathematical Library. Cambridge University Press, 1952.

[109] K. Garg and D. Panagou, "New results on finite-time stability: Geometric conditions and finite-time controllers," in *Proceedings of the 2018 American Control Conference*, 06 2018, pp. 442–447.

[110] T. Lee, M. Leok, and N. H. McClamroch, "Stable manifolds of saddle equilibria for pendulum dynamics on S^2 and SO(3)," in *2011 50th IEEE Conference on Decision and Control and European Control Conference*. IEEE, 2011, pp. 3915–3921.